

AD-A036 575

SOLAR SAN DIEGO CALIF

F/G 11/6

TITANIUM BRAZE SYSTEM FOR HIGH TEMPERATURE APPLICATIONS.(U)

AUG 76 C E SMELTZER, A N HAMMER

F33615-74-C-5118

UNCLASSIFIED

RDR-1786-6

AFML-TR-76-145

NL

1 OF 2

AD
A036575



ADA036575

AFML-TR-76-145

(12)

2

TITANIUM BRAZE SYSTEM FOR HIGH TEMPERATURE APPLICATIONS

*SOLAR DIVISION INTERNATIONAL HARVESTER
2200 PACIFIC HIGHWAY
SAN DIEGO, CA 92138*

AUGUST 1976

TECHNICAL REPORT AFML-TR-76-145
FINAL REPORT FOR PERIOD MAY 7, 1974 - APRIL 30, 1976



Approved for public release; distribution unlimited

AIR FORCE MATERIALS LABORATORY
AIR FORCE WRIGHT AERONAUTICAL LABORATORIES
AIR FORCE SYSTEMS COMMAND
WRIGHT-PATTERSON AIR FORCE BASE, OHIO 45433

NOTICE

When Government drawings, specifications, or other data are used for any purpose other than in connection with a definitely related Government procurement operation, the United States Government thereby incurs no responsibility nor any obligation whatsoever; and the fact that the government may have formulated, furnished, or in any way supplied the said drawings, specifications, or other data, is not to be regarded by implication or otherwise as in any manner licensing the holder or any other person or corporation, or conveying any rights or permission to manufacture, use, or sell any patented invention that may in any way be related thereto.

This report has been reviewed by the Information Office (IO) and is releasable to the National Technical Information Service (NTIS). At NTIS, it will be available to the general public, including foreign nations.

This technical report has been reviewed and is approved for publication.

Donald W. Becker

Donald W. Becker
Project Engineer

Martin V. Hunt

Martin H. Horowitz
Supervisor

FOR THE COMMANDER

Nathan G. Tupper

Nathan G. Tupper
Acting Chief, Structural Metals Branch

Martin A. Foreman
Supervisor

Assigned to _____
White Section ☐
Buff Section ☐

For
and

MAINTENANCE
JUSTIFICATION

BY _____
DESTRUCTION/AVAILABILITY CODE

Doc. _____

A

Copies of this report should not be returned unless return is required by security considerations, contractual obligations, or notice on a specific document.

Unclassified

SECURITY CLASSIFICATION OF THIS PAGE (When Data Entered)

REPORT DOCUMENTATION PAGE		READ INSTRUCTIONS BEFORE COMPLETING FORM
1. REPORT NUMBER AFML-TR-76-145	2. GOVT ACCESSION NO.	3. RECIPIENT'S CATALOG NUMBER
4. TITLE (and Subtitle) Titanium Braze System for High Temperature Applications		5. TYPE OF REPORT & PERIOD COVERED Final <i>technical rept.</i> 7 May 1974 - 30 Apr 1976
7. AUTHOR(s) C. E. Smeltzer A. N. Hammer		6. PERFORMING ORG. REPORT NUMBER RDR-1786-16
9. PERFORMING ORGANIZATION NAME AND ADDRESS Solar Division International Harvester Co. P.O. Box 80966 San Diego, CA 92138		8. CONTRACT OR GRANT NUMBER(s) F33615-74-C-5118 <i>new</i>
11. CONTROLLING OFFICE NAME AND ADDRESS Air Force Materials Lab Air Force Systems Command, USAF Wright-Patterson Air Force Base, Ohio 45433		10. PROGRAM ELEMENT, PROJECT, TASK AREA & WORK UNIT NUMBERS Project No. 7351
14. MONITORING AGENCY NAME & ADDRESS (if different from Controlling Office)		12. REPORT DATE August 1976
		13. NUMBER OF PAGES 159 <i>150 p.</i>
		15. SECURITY CLASS. (of this report) Unclassified
		15a. DECLASSIFICATION/DOWNGRADING SCHEDULE
16. DISTRIBUTION STATEMENT (of this Report) Approved for Public Release; Distribution Unlimited		
17. DISTRIBUTION STATEMENT (of the abstract entered in Block 20, if different from Report)		
18. SUPPLEMENTARY NOTES		
19. KEY WORDS (Continue on reverse side if necessary and identify by block number) Titanium joining, braze alloys, high temperature joining, braze development		
20. ABSTRACT (Continue on reverse side if necessary and identify by block number) This report describes the design rationale and development of special, high-temperature braze systems for joining titanium and titanium alloys, suitable for long term aerospace application to 800°F. Candidate braze alloy designs were substrate-compatible, low-melting (1650-1750°F) compositions within the metallurgically similar Ti-, Zr-, Ti-Zr, Ti-V, and Zr-V-Ti (base) systems. Best results were obtained with the Ti-Zr system. Desired hypoeutectic structure and melt-solidification behavior were achieved wherever possible through controlled		

DD FORM 1 JAN 73 1473 EDITION OF 1 NOV 65 IS OBSOLETE

Unclassified

SECURITY CLASSIFICATION OF THIS PAGE (When Data Entered)

SPG

Unclassified

SECURITY CLASSIFICATION OF THIS PAGE(When Data Entered)

reduction of major melting-point depressants and/or Zr/Ti ratios, backing-off from eutectic alloying levels. Principal alloying objectives were (a) braze strength, toughness and ductility properties (RT-800°F) comparable to the high-melting Ti-15Cu-15Ni baseline braze alloy, (b) conventional brazing characteristics superior to the baseline braze, particularly brazing capability 1750°F to avoid "beta embrittlement" of the substrate (Ti-6Al-4V) and (c) intrinsic long-term resistance to structural damage from aqueous salt spray, 800°F air oxidation, and 800°F hot-salt corrosion. Over 350 different braze alloy designs were evaluated through various screening tests. The two braze alloy designs which best met program objectives are designated AC5-16 (Ti-27.2Zr-15.0Ni-7.0Cu) and AC1-20 (Ti-28.8Zr-28.0Cu). These new braze alloys exhibited tensile shear strengths (RT-800°F), long-term stress-rupture performance (800°F) and levels of RT toughness (gaged by high-strain-rate ingot comminution test) closely approaching the baseline braze. Both alloys showed marked superiority to the baseline braze in terms of energy required to initiate and propagate braze-line peel (RT; slow-strain-rate peel); assumed primarily due to the absence of beta-embrittlement phenomena (BAZ). Environmental conditioning in 100°F salt spray and 800°F moving air (with and without hot-salt accretion) had no significant effect on brazement properties or structure. Some form of post-braze thermal treatment was indicated to optimize braze toughness and elevated-temperature shear strengths. The principal substrate alloy employed was Ti-6Al-4V; some comparison tests were conducted with Beta-C substrate alloy.

Unclassified

SECURITY CLASSIFICATION OF THIS PAGE(When Data Entered)

PREFACE

This Final Technical Report documents work performed by the Research Department, Solar Division International Harvester Company, San Diego, California under USAF Contract F33615-74-C-5118, Project No. 7351, for the period of 4 May 1974 through 30 April 1976.

The program was administered by the Structural Metals Branch, Air Force Materials Laboratory, Air Force Systems Command, United States Air Force, Wright-Patterson Air Force Base, Ohio; under the (initial) technical direction of Capt. R. P. Oates, Project Engineer, Air Force Materials Laboratory. Sgt. D. K. Haggard, AFML, was the Air Force Project Engineer assigned subsequently to this program. The final (AFML/LLS) program monitor was Mr. D. Becker, Metals and Ceramics Division.

Mr. C. E. Smeltzer was the Principal Investigator (Solar Research Department) under the general technical direction of Mr. J. F. Nachman, Program Manager. Also contributing to the work reported herein was Mr. A. N. Hammer (Solar Research Department). The results are published for information only and do not necessarily represent the recommendations, conclusions or approval of the Air Force. Contractor identification of this report is RDR 1786-6, and the submittal date was May 1976.

TABLE OF CONTENTS

<u>Section</u>	<u>Page</u>
I INTRODUCTION AND PROGRAM SCOPE	1
II ALLOYING APPROACH AND RATIONALE	9
Base Selection	11
Braze Toughness	13
Melting-Point Depression	14
General Alloying Approach	17
Alloying Guidelines	18
III EXPERIMENTAL MATERIALS AND PROCEDURES	21
IV EXPERIMENTAL RESULTS AND DISCUSSION	31
Braze Alloy Design and Screening (Phase I)	31
Single-Phase Alloy Designs	32
Hypoeutectic Alloy Designs	37
Advanced Screening Tests	49
General Comments, End of Phase I	72
Braze Optimization Studies (Phase II)	72
Braze Design Problems and Possible Solutions	73
Post-Braze Thermal Treatments	77
Rare-Earth-Metal Scavenging	103
General Comments, End of Phase II	113
Braze Characterization (Phase III)	114
Double-Lap Peel-Energy Tests (RT)	115
Single-Lap Stress-Rupture Tests (800°F)	120
Single-Lap Tensile Shear Tests (Environmental Conditioning)	123
General Comments, End of Phase III	126
REFERENCES	129
APPENDIX	133

LIST OF ILLUSTRATIONS

<u>Figure</u>		<u>Page</u>
1	Flow Chart of Program Organization	5
2	T-Joint Specimen	7
3	Finished Single-Lap Shear Test Specimen	7
4	Typical Double-Lap Joint Specimen for Braze Peel Test	8
5	Schematic of Four-Point Bending Flexure Beam	8
6	Controlled Atmosphere Arc Melter	22
7	Schematic Diagram of the Laboratory Brazing Furnace	25
8	Pre-Brazed Shear Specimen Blanks	28
9	Portion of Ti-Zr-V Ternary Diagram	33
10	Portion of Ti-Zr-Cu Ternary Diagram	39
11	Microstructure of Ti-21.0Zr-30.0Cu Brazement (AC1-2); T-Joint Intercept and Fillet Region	41
12	Microstructure of Ti-40.0Zr-20.0Cu Brazement (A2-3); T-Joint Intercept and Fillet Region	41
13	Portion of (50Ti/50Zr)-Ni-Cu Quaternary Diagram (Pseudo-Ternary)	43
14	Portion of Ti-Zr-(75Cu/25Mn) Quaternary Diagram (Pseudo-Ternary)	46
15	Lap-Shear Specimen Brazement, Made With Ti-15Cu-15Ni Alloy (Baseline)	48
16	Microstructure of Ti-15.0Cu-15.0Ni Brazement: T-Joint Intercept and Fillet Region	48
17	Cross-Section of T-Joint Brazement Remote From Unmelted Residue (Ti-15Cu-15Ni Braze Alloy)	49
18	Typical Lap-Shear Specimen Brazements Made With No. AC5-16 Experimental Braze (1750°F)	53

LIST OF ILLUSTRATIONS (Contd)

<u>Figure</u>		<u>Page</u>
19	Microstructures of Braze Fillet Region; Single-Lap Shear Specimen Brazement, Braze Alloy AC5-21	57
20	Microstructure of Single-Lap Shear Specimen Brazement (Faying Surface Regions); Braze Alloy AC5-7	58
21	Variation in Shear Stress Parameters With Ingot Comminution Resistance (ICR)	61
22	Average Shear Strength Levels of Candidate Braze Alloys (Phase I, Screening Tests)	66
23	Steel Mortar and Pestle Used to Determine ICR	73
24	Primary Comminution Crack Surfaces (Edge Mounts) in As-Cast Braze Alloys	76
25	Primary Comminution Crack Surfaces (Edge Mounts) in As-Cast Braze Alloys	76
26	Primary Comminution Crack Surfaces (Edge Mounts) in As-Cast Braze Alloy	77
27	Braze Microhardness and Ingot Comminution Rating (ICR) Plotted Versus Isothermal Aging Temperature (Alloys AC6-15 and AC6-16)	80
28	Braze Microhardness and Ingot Comminution Rating (ICR) Plotted Versus Isothermal Aging Temperature (Alloys AC6-18 and AC6-21)	81
29	Braze Microhardness and Ingot Comminution Rating (ICR) Plotted Versus Isothermal Aging Temperature (Alloys AC5-2, AC5-15 and AC5-16)	82
30	Braze Microhardness and Ingot Comminution Rating (ICR) Plotted Versus Isothermal Aging Temperature (Alloys AC5-18 and AC5-21)	83
31	Braze Microhardness and Ingot Comminution Rating (ICR) Plotted Versus Isothermal Aging Temperature (Alloys AC5-2 and AC5-7)	84
32	Braze Microhardness and Ingot Comminution Rating (ICR) Plotted Versus Isothermal Aging Temperature (Alloys AC1-20 and AC1-24)	85

LIST OF ILLUSTRATIONS (Contd)

<u>Figure</u>		<u>Page</u>
33	Microstructure of Alloy AC5-16 (Ti-Zr-Ni-Cu) (As Cast Condition)	91
34	Microstructure of Alloy AC5-16 (Ti-Zr-Ni-Cu) (Isothermally Aged at 1025°F)	91
35	Microstructures of Alloy AC5-21 (Ti-Zr-Ni-Cu) (As-Cast vs. 1025°F and 1200°F Aging)	92
36	Microstructures of Alloy AC5-18 (Ti-Zr-Ni) (As-Cast vs. 1025°F Aging)	92
37	Microstructures of Alloy AC5-21 (Ti-Zr-Ni-Cu) (As-Cast vs. 1025°F and 1200°F Aging)	93
38	Microstructures of Alloy AC5-18 (Ti-Zr-Ni) (As-Cast vs. 1025°F Aging)	93
39	Microstructure of Alloy AC5-21 (Ti-Zr-Ni-Cu) (As-Cast vs. 1025°F and 1200°F Aging)	94
40	Microstructures of Alloy AC5-7 (Ti-Zr-Ni-Cu) (As-Cast vs. 1025°F Aging)	94
41	Microstructures of Alloy AC5-7 (Ti-Zr-Ni-Cu) (As-Cast vs. 1025°F Aging)	95
42	Microstructures of Alloy AC1-20 (Ti-Zr-Cu) (As-Cast vs. 1025°F and 1200°F Aging)	96
43	Microstructures of Alloy AC1-20 (Ti-Zr-Cu) (As-Cast vs. 1025°F and 1200°F Aging)	96
44	Microstructures of Alloy AC1-20 (Ti-Zr-Cu) (As-Cast vs. 1025°F and 1200°F Aging)	97
45	Microstructure of Alloy AC5-16 (Ti-Zr-Ni-Cu) Cyclic Annealed Between 1200°F and 1000°F (Schedule B)	99
46	Microstructure of Alloy AC5-16 (Ti-Zr-Ni-Cu) Beta-Solutioned at 1400°F, 1/2 Hour, FC to RT (Schedule D)	100
47	Microstructure of Alloy AC5-16 (Ti-Zr-Ni-Cu) Cyclic Annealed Between 1150°F and 1000°F (Schedule C)	101

LIST OF ILLUSTRATIONS (Contd)

<u>Figure</u>		<u>Page</u>
48	Microstructure of Alloy AC5-16 (Ti-Zr-Ni-Cu) Showing Secondary Commintion Cracks; Cyclic Annealed Between 1150°F and 1000°F (Schedule C)	101
49	Microstructure of Alloy AC5-16 (Ti-Zr-Ni-Cu) Cyclic Annealed Between 1100°F and 1000°F (Schedule A)	102
50	Microstructure of Alloy AC5-16 (Ti-Zr-Ni-Cu) Showing Secondary Commintion Crack; Cyclic Annealed Between 1100°F and 1000°F (Schedule A)	102
51	Microstructure of Alloy AC5-16 (Ti-Zr-Ni-Cu) Showing Secondary Commintion Crack; Cyclic Annealed Between 1200°F and 1000°F (Schedule B)	103
52	Free Energy of Formation of Liquid Metal (Ti-Zr)-Oxygen Solutions (1600°F); Showing Compositional Equilibria With Various Refractory Oxides	105
53	Double-Lap Peel-Energy Tests (Typical)	117
54	Double-Lap Peel-Energy Tests (Typical)	118
55	Double-Lap Peel-Energy Tests (Typical)	119

LIST OF TABLES

<u>Table</u>		<u>Page</u>
1	Braze Alloys for Ti Foil Structures	10
2	Results of Lap-Shear Tests for Solar-Developed Braze Alloys; Braze-Bonded Versus Self-Diffusion Bonded Specimens	11
3	Standard Oxidation - Reduction Potentials of Candidate Braze Bases	12
4	Binary Systems Showing Strong Melting Point Depression	15
5	Binary Systems Showing Weak-to-Moderate Melting Point Depression	16
6	High-Purity Elemental Melt Stocks	23
7	Summary of Alloying Results With the Zr-30V-20Ti Base	35
8	Summary of Alloying Results With Ti, Zr, Ti-V and Ti-Zr Bases	38
9	Promising Initial Braze Materials: Ti-Zr-Cu System	40
10	Results of Preliminary Screening Tests: The Ti-Zr-Ni-Cu System	44
11	Promising Initial Braze Alloys: Ti-Zr-Cu-Mn System	47
12	Summary of Screening Test Results (Phase I) - Single-Lap Tensile Shear Tests (RT) - Candidate Braze Alloys/As-Brazed Condition	50
13	Summary of Single-Lap Shear Tests (RT) - Baseline and Strongly Hypoeutectic Braze Alloys/As-Brazed Condition	55
14	Comparison of Nominal RT Shear Strength (a), Stress for First Cracking (b), Stress Interval [(a) Minus (b)], and Commination Resistance for Twelve Promising Alloys (Process A)	60
15	Characterization of Recommended Braze Alloy Designs (Phase I)	64

LIST OF TABLES (Contd)

<u>Table</u>		<u>Page</u>
16	Comparative Lap-Shear Strength Data	65
17	Comparative Lap-Shear Strength Data	68
18	Comparative Lap-Shear Strength Data (Beta-C Substrate Alloy)	71
19	Data From Post-Braze Isothermal Aging Study (Phase II)	75
20	Comparative RT Lap-Shear Strength Data	89
21	Ingot Comminution Ratings for Cyclic Annealed Versus As-Cast Structures	99
22	Initial Alloying Plan for Rare-Earth Scavenging	106
23	Results of Comminution Studies Upon Cerium-Modified Braze Alloys	107
24	Results of Comminution Studies Upon Lanthanum-Modified Braze Alloys	108
25	Results of Comminution Studies Upon Neodymium-Modified Braze Alloys	109
26	Results of Comminution Studies Upon Yttrium-Modified Braze Alloys	110
27	Results of Comminution Studies Upon Gadolinium-Modified Braze Alloys	111
28	Results of Comminution Studies Upon Scandium-Modified Braze Alloys	112
29	Recommended Braze Finalists	113
30	Results of Double-Lap Peel-Energy Tests (RT)	116
31	Comparative Data: 800°F Stress-Rupture Tests	122
32	Comparative Data: Tensile Shear Strength Tests (RT and 800°F)	125

SECTION I

INTRODUCTION AND PROGRAM SCOPE

The two primary incentives for titanium alloy usage (vis-a-vis steels) in both commercial and military aircraft are superior intrinsic corrosion resistance in industrial, salt-desert and maritime environments and the prospect for lighter weight, higher performance aircraft and power plants. Pertinent high-temperature brazed structures in advanced aircraft designs include lightweight titanium heat exchangers and titanium jet engine components such as stator vane assemblies, compressor wheels, hydraulic ducting, honeycomb shrouds and skins, nozzle fairings, and acoustic sandwich panels.

The actualization of many advanced concepts involving brazed titanium structures has been deferred for years by the general unavailability of all-around suitable braze materials. "Suitable" in this context means operable to 800°F, the usual maximum service temperature contemplated for titanium-base engineering alloys. The most notable deficiencies of currently available braze alloys are poor inherent salt-corrosion protection, inadequate long-term oxidation resistance and thermal stability for service to 800°F, low ductility and fracture toughness, and aggressive erosiveness. No single developmental braze alloy to date has (universally) solved these shortcomings, although such an alloy should be feasible through the application of alloying logic and metallurgical principles.

The existing commercial braze systems have limited application potential for highly stressed titanium structures operating long-term and cyclically over the elevated temperature range, 500-800°F. This is largely due to the fact that most braze alloys were developed for special (often extraneous) purposes, and none were designed to address all the shortcomings noted above. For example, the Ti-Zr-Be and Ti-Zr-Ni-Be braze alloys pioneered by Solar (Ref. 1) were developed within an AFML-sponsored program for the conventional braze-joining of thin-foil honeycomb structures, where titanium-foil erosion and resistance to salt corrosion were the overriding design considerations. However, the problem of Be toxicity has been a major deterrent to their use. The many silver-base braze alloys, still infrequently employed for titanium, were adapted to titanium from other braze technologies, primarily because of their vast commercial utilization (with steels and superalloys) and not for sound metallurgical reasons. Not surprisingly, a number of serious deficiencies have surfaced with their use. The silver alloys exhibit good brazeability and adequate initial joint strength, but

are severely time- and stress-limited because of interface embrittlement related to the TiAg intermetallic, accelerated crevice corrosion in salt-spray environment, deleterious oxidation effects in the range of 600-800° F, hot-salt stress corrosion and substrate erosion (Refs. 2, 3).

The first-generation Ti- and Ti-Zr-base braze alloys developed over the past decade by Solar, G. E., WESGO and AMI also show desired low-braze temperatures, good brazeability (conventional procedures) and high joint strengths (Refs. 4, 5, 6). More importantly, they possess markedly improved resistances to erosion, salt-spray corrosion, elevated-temperature oxidation, (and in some cases hot-salt corrosion) due to their more balanced metallurgical designs. However, levels of braze ductility and toughness leave something to be desired because of the high concentrations of brittle intermetallic phases within the braze microstructures.

A novel and unconventional type of braze system, under development by Rohr Corporation, tends to minimize embrittling effects associated with dissimilar-metal conventional brazements by drastically limiting the amount of filler (braze) metal available for intermetallic compound formation (Ref. 7). This special method, called "diffusion brazing", requires rapid inward diffusion of certain elements plated upon the titanium faying surfaces to (transiently) form miniscule quantities of low-melting titanium eutectics. Although metallurgically sound, the practical application of diffusion brazing is very often restricted by the inordinately difficult surface preparation, the ultra-precise fitup requirements, and the interface pressure controls necessary to assure the formation of a satisfactory bond.

In view of the inadequacies cited above, the subject program was contracted, with goals of designing and developing high-temperature (500-800° F) brazing systems for joining titanium and its alloys and of defining their performance characteristics and limitations. The new braze systems were to be adaptable to bonding the wide variety of faying surface joints found in aerospace applications using conventional brazing (in situ or external braze placement, 100% liquation [Ref. 8]) or diffusion brazing (minimal braze, in situ placement, total or partial liquation [Ref. 7, 8]) techniques. Conventional brazing with external placement (requiring substrate wetting and capillary flow) was employed in the subject work.

Unlike existing high-temperature braze materials, the new braze systems were to be designed to attempt combination of three important attributes:

1. High resistance to environmental reactants in service (aqueous salt spray, hot salt corrosion, air oxidation to 800° F)
2. Improved toughness and ductility levels, approaching commercial titanium substrate alloys

3. Good brazing characteristics in the desired process temperature range of 1600° to 1750°F, to enable good retention of braze strength to 800 F without adversely altering the substrate alloy properties or structures.

Corollary program objectives include the accurate definition of preferred processing and performance characteristics provided by the new braze systems. Mechanical properties and microstructural characteristics of lap-joint and T-joint brazements would be determined over the entire service temperature range (RT-800°F). Effects on the above performance characteristics of extended, simulated service environments (aqueous salt spray, hot salt coating and air oxidation) were to be closely monitored by further mechanical testing and metallography. Ultimately, the two most promising braze alloy candidates would be identified and usable quantities of each provided to the sponsor.

As to scope, the basic program was one of fundamental metallurgical alloy development. Candidate braze alloys were designed upon metallurgical principles and screened for suitability to elevated-temperature service. In Phase I, Braze Alloy Design and Screening (Fig. 1), preliminary screening and evaluation of several hundred exploratory braze alloy designs commenced with brazing parameter and microstructure studies using simple T-joint brazements (see Fig. 2). The 26 most promising braze systems were narrowed next to 12 through mechanical property (tensile shear strength) tests and environmental exposure tests upon single lap-joint brazements, per AWS Spec. C3.2-63/60.105 (Figs. 1 and 3). Phase II, Braze Optimization followed with iterative attempts to optimize brazement strength, toughness, ductility, oxidation-corrosion resistance and brazeability (viz., stated program objectives) through special alloying and heat treatment procedures listed in Figure 1. These included rare-earth and trace element alloying additions as well as post-braze heat treatments to disperse and spheroidize hard intermetallic compounds and to promote favorable matrix transformations. The three most responsive and promising braze alloys were selected finally for more thorough mechanical property and environmental testing. This final work constituted Phase III, Braze Characterization (see Fig. 1). Advanced characterization tests were programmed to include comparative tensile shear strength, fatigue strength and stress rupture strength determinations to 800°F upon single lap-joint brazements (Fig. 3); peel strength and peel energy (toughness) determinations upon double lap-joint brazements (Fig. 4), and flexure strength determinations upon four-point bending, single-lap flexure beams (Fig. 5). After complete data analysis, Solar and the sponsor agreed to define the one or two most acceptable braze systems evolved from the program.

The sponsor requested the adoption of mill annealed Ti-6Al-4V and annealed Beta C (Ti-3Al-8V-6Cr-4Mo-4Zr) alloy sheet stocks as test substrate alloys. Arrangements were made to procure sheets of these titanium alloys in the requested 0.050

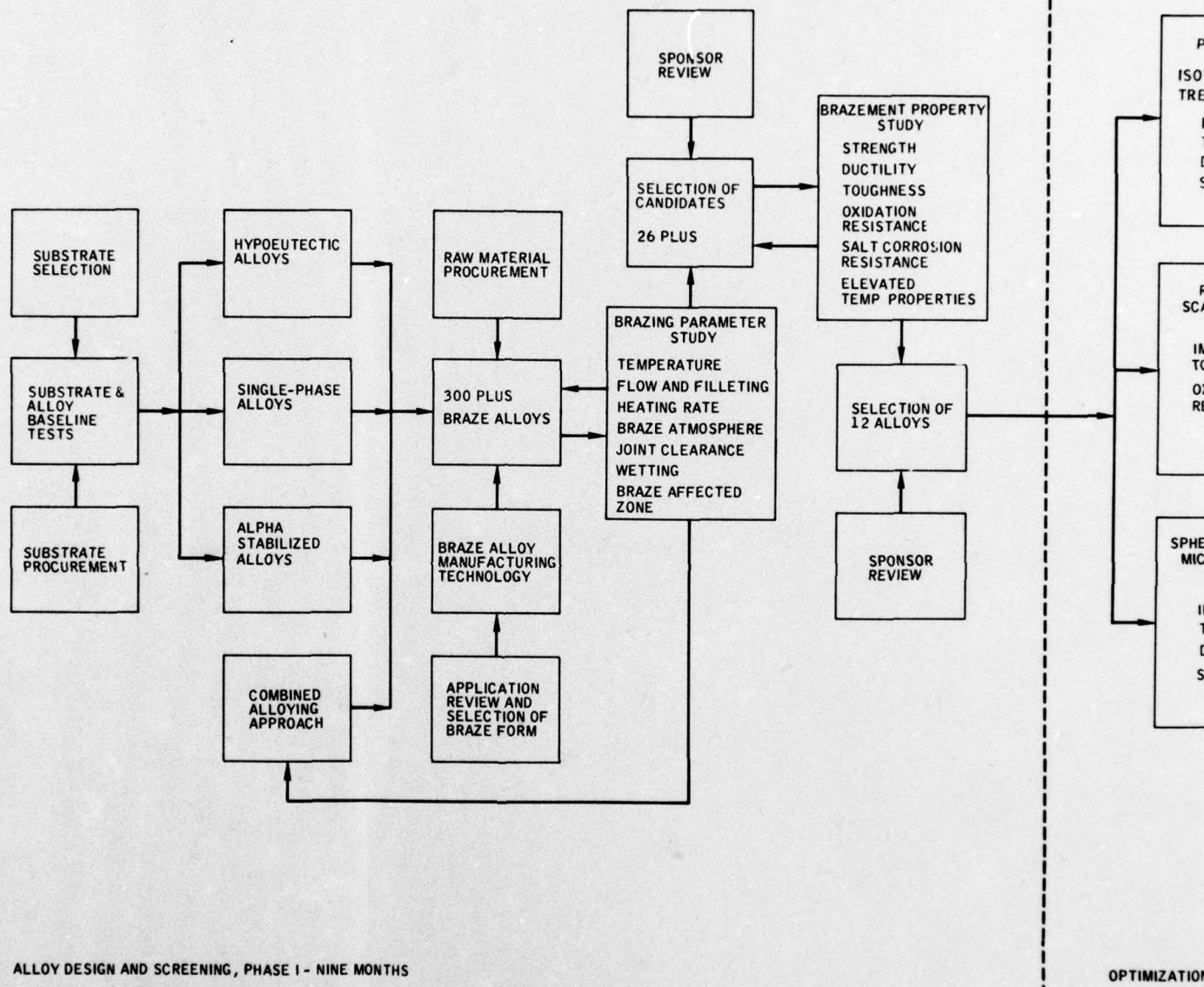
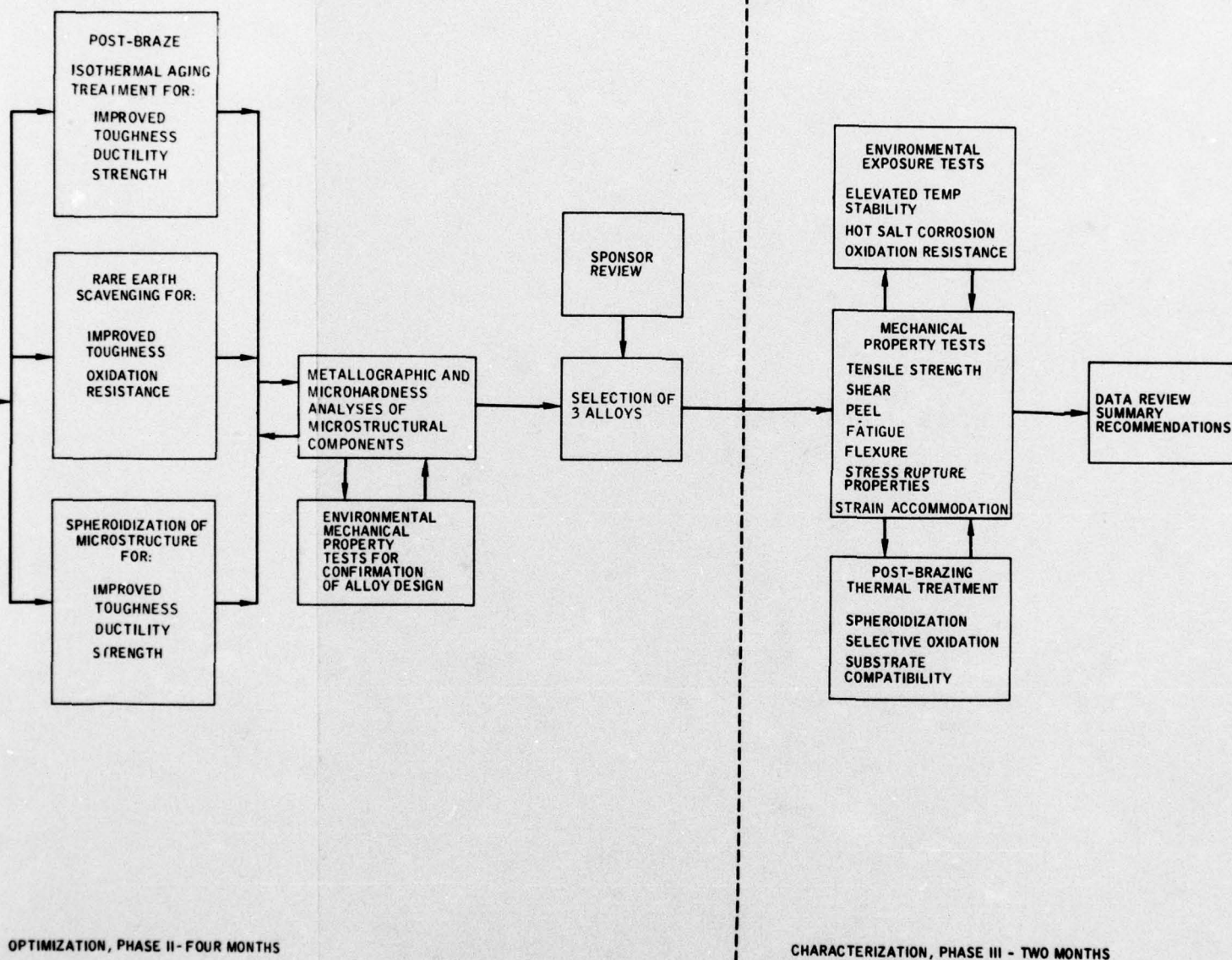
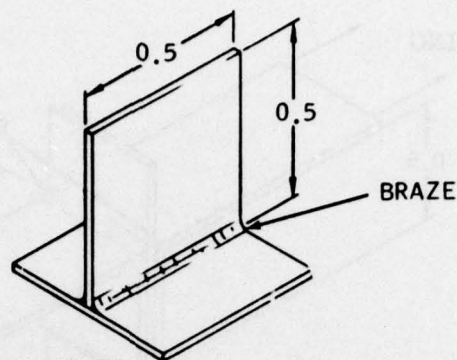


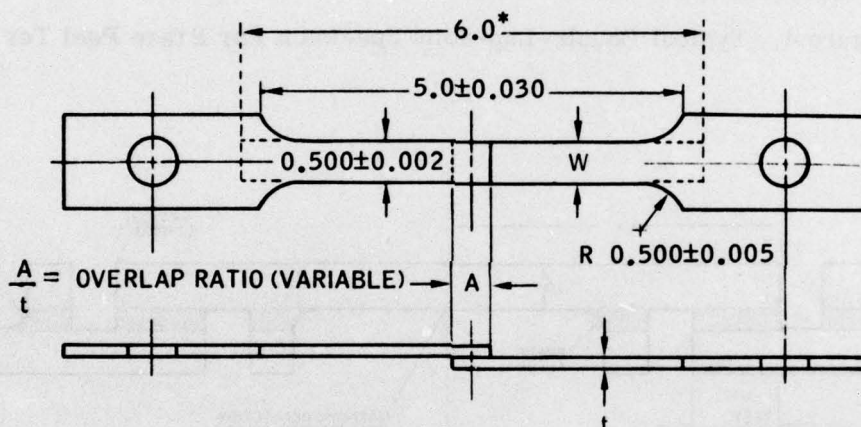
Figure 1. Flow Chart of Program Organization





ALL DIMENSIONS IN INCHES

Figure 2. T-Joint Specimen



ALL DIMENSIONS IN INCHES

(AWS SPEC. C3.2-63/60.105)

Figure 3. Finished Single-Lap Shear Test Specimen

and 0.062 inch thickness. The lean alpha-beta alloy, Ti-6Al-4V, possesses good inherent oxidation-corrosion resistance and elevated temperature strength, both due mainly to the high aluminum content. In the annealed condition, Ti-6Al-4V possesses outstanding fracture toughness among titanium alloys. (The beta transus temperature is high, ~1825°F, which should permit brazing to 1750°F without risk of beta embrittlement.) Because of these features, Ti-6Al-4V is by far the most popular high-temperature titanium alloy in aerospace and is felt to be a good program choice for braze joining, e.g., 90 percent of the titanium applications in the B-1 aircraft are assigned to Ti-6Al-4V, (Ref. 9). The sponsor also requested that the Ti-6Al-4V alloy substrate be emphasized in braze alloy screening work (Phase I, Fig. 1).

SECTION II

ALLOYING APPROACH AND RATIONALE

As the number and quality of high-temperature, creep-resistant and oxidation-resistant titanium alloys keep increasing (Ref. 11, 12, 13), the technology for effectively braze-joining aerospace structures of these alloys has not advanced perceptibly since the mid-1960's. This is regrettable because intermediate temperature (1600-1750°F) brazing and braze-assisted diffusion bonding offer the best opportunities for reliably joining titanium alloys below their various beta-transus temperatures and/or grain-coarsening temperatures, thereby avoiding the joint embrittlement frequently associated with higher temperature joining processes. Early brazing work with titanium in the 1950's and 1960's concentrated upon commercial Ag-, Au-, Cu- and Pd-base braze alloys for service up to 600-800°F, and Al-base braze alloys for lower temperature service (RT-400°F). All of these brazements constituted dissimilar metal combinations. Serious problems of joint embrittlement and joint deterioration were related to the formation of hard, continuous intermetallic reaction films at the joint interfaces. The combination of insulating or barrier films and dissimilar metals also promoted accelerated interface (crevice) corrosion, noted even during short-term service. In the mid-to-late sixties, several series of intermediate-temperature melting Ti- and Ti-Zr-base braze alloys were developed (at Solar, Northrop, General Electric, WESGO) with closely matched surface emf's and good metallurgical compatibility with most titanium structural alloys (Ref. 4, 5, 6, 8). (The braze alloy development work at Solar was sponsored by the Air Force under AFML Contract No. AF33(615)-3137, Ref. 1.) The metallurgical and thermodynamic (quasi-) equilibria between similar braze and substrate fostered by these more logically designed braze alloys ostensibly solved the aforementioned joint stability problems. Intermetallics did not normally form at interface zones. The potential for long-term, inherent resistance to stress-corrosion and crevice-corrosion cracking (even in severe salt spray environments) was confirmed (Ref. 1). Former problems of substrate erosion and beta-embrittlement also were resolved, even for titanium foil structures, with proper temperature and time cycle controls. However, these first-generation Ti- and Ti-Zr-base braze alloys are not perfect. (See Table 1 for typical Solar braze compositions.) Some critical concern has been expressed about the friability and marginal ductility of these braze materials, due apparently to the appreciable volume percentages (~25-45%) of hard, high-modulus intermetallic compounds developed within the various eutectic structures. Although the subject intermetallics are in metallurgical equilibrium with the ductile metallic Ti- and Ti-Zr-base terminal solid solutions, the associated

Table 1
BRAZE ALLOYS FOR TI FOIL STRUCTURES

Alloy No.	Braze Alloy Designation	Nominal Composition, Wt %									Minimum Flow Temperature (°F)
		Ti	Zr	Ni	Be	Al	Co	Si	Cu	Ag	
1	RM8	Bal	43.0	12.0	2.00						1625
2	RM12	Bal	45.0	8.0	2.00						1660
3	RM43	Bal	20.0	12.0	5.00						1680
4	RM33	Bal	40.5	7.2	1.80	--	--	--	--	10.0	1580
5	RM32	Bal	38.7	12.6	--	--	--	--	--	10.0	1720
6	RM28	Bal	36.9	16.2	--	--	--	--	--	10.0	1620
7	RM23	Bal	--	17.2	4.00						1700
8	RM26	Bal	--	16.9	3.90	--	--	2.0			1660
9	RM40	Bal	20.0	8.0	5.00						1700
10	RM42	Bal	20.0	12.0	4.00						1700
11	RM44	Bal	18.0	7.2	4.50	--	--	--	--	10.0	1700
12	CS13-5	Bal	47.2	--	5.60						1620
13	CS217	Bal	47.5	--	5.00						1640
14	CS217C	Bal	45.1	--	4.75	5.0					1700
15	CS217E	Bal	45.1	5.0	4.75						1600
16	CS217F	Bal	45.1	--	4.75	--	5.0				1620
17	CS217G	Bal	46.6	--	4.90	--	--	2.0			1680
18	CS217I	Bal	42.9	--	4.50	--	--	--	9.6		1520

inservice potentials for high-stress concentrations and the (possible) resultant initiation of matrix cracking are obvious. Significant alloying additions of potent melting-point depressants such as beryllium, copper, silver, silicon and nickel were utilized singly and combined in the first generation of Ti- and Ti-Zr base alloys, in order to obtain melt and flow temperatures below ~1800°F. This unavoidably resulted in the typical networks of eutectic beryllide, nickelide, silicide and cupride intermetallics which generally detract from braze reliability and integrity in high-stress applications. These beryllide and nickelide intermetallics, however, frequently in the form of lamellar eutectic structures, do help provide braze shear strengths and ultimate braze-bond strengths (-320°F to +800°F) approximately two to three times greater than competing Ag-base or other noble-metal braze alloys (see Table 2 and Ref. 1).

The alloying approach and rationale leading to the current series of candidate braze systems (Phase I) adhere closely to the proven alloying concepts just discussed for the first generation braze alloys. Specific aspects of new braze alloy design are discussed below.

Table 2

**RESULTS OF LAP-SHEAR TESTS FOR SOLAR-DEVELOPED BRAZE ALLOYS;
BRAZE-BONDED VERSUS SELF-DIFFUSION BONDED SPECIMENS
(Ti-6Al-4V Foils; 2t Overlap; t = 0.010 in.)**

Candidate Braz Alloys	Average Foil Stress, ksi, for Failure of Lap Shear Specimens at Various Test Temperatures											
	-320° F			75° F			800° F					
	B	(a) or (v)	1000° F 100 Hours Exposure	Percent Change ⁽²⁾	B	(a) or (v)	1000° F 100 Hours Exposure	Percent Change ⁽²⁾	B	(a) or (v)	1000° F 100 Hours Exposure	Percent Change ⁽²⁾
CS217	102.0	(a)	106.6	+ 4.5	95.5	(a)	94.8	Nil	92.6	(a)	90.1	- 2.2
Percent Change ⁽¹⁾		(v)	129.0	+26.5		(v)	105.5	+10.5		(v)	98.0	+ 5.8
			-17.4				-10.1				- 8.1	
CS217C	112.0	(a)	99.1	-11.5	107.7	(a)	79.6	-26.1	97.2	(a)	76.3	-21.5
Percent Change ⁽¹⁾		(v)	117.0	+ 4.5		(v)	88.5	-17.8		(v)	84.3	-13.3
			-15.3				-10.0				- 9.5	
CS217F	97.4	(a)	73.2	-24.8	97.8	(a)	76.1	-22.2	77.8	(a)	71.3	- 4.5
Percent Change ⁽¹⁾		(v)	117.9	+21.0		(v)	88.0	-10.0		(v)	77.9	Nil
			-37.9				-13.5				- 4.6	
CS217G	105.1	(a)	102.9	- 2.1	100.9	(a)	87.3	-13.5	79.6	(a)	71.4	-10.3
Percent Change ⁽¹⁾		(v)	94.5	-10.1		(v)	101.6	Nil		(v)	90.0	+13.1
			+ 8.8				-14.1				-20.7	
RM8	110.8	(a)	75.5	-31.9	85.1	(a)	67.1	-21.1	80.7	(a)	64.1	-20.6
Percent Change ⁽¹⁾		(v)	109.6	Nil		(v)	62.9	-26.1		(v)	81.5	Nil
			-23.2				+ 6.7				-21.3	
RM12	106.6	(a)	93.3	-12.5	100.0	(a)	89.3	-10.7	87.7	(a)	67.3	-23.3
Percent Change ⁽¹⁾		(v)	101.3	- 5.0		(v)	79.0	-21.0		(v)	70.6	-19.5
			7.9				+13.0				- 4.7	
Self diffusion bonded Ti-6Al-4V	170.0	(a)	138.3	-18.6	123.0	(a)	148.0	+20.2	--	-	93.2	--

B - As-brazed
 (a) - As air oxidized 1000° F - 100 hours
 (v) - After 1000° F - 100 hours thermal exposure in high vacuum (10^{-5} torr)

- Percent change due to air oxidation only at 1000° F (difference between brazement strength after 1000° F - 100 hours thermal exposure in vacuum and after 1000° F - 100 hours air oxidation). + denotes an increase and - denotes a decrease in brazement strength.
- Percent change due to post-braze thermal treatment at 1000° F - 100 hours (static air environment or high vacuum)

BASE SELECTION

As a first consideration (base selection), Solar favored the retention of the proven Ti-, Ti-Zr, and Zr-Ti bases for long-term metallurgical compatibility with the titanium-alloy substrates, joint ductility and innate corrosion protection (Ref. 1). [Note the better-matched standard potentials of the Group IVb metals - Ti, Zr, Hf - versus other plausible bases such as Ni, Cu or the noble metals (Table 3).] That is, specifically, the BCC-A2 crystalline allotropic form or (β) beta-phase structure of

Table 3
STANDARD OXIDATION - REDUCTION POTENTIALS
OF CANDIDATE BRAZE BASES

Most Common Valences	Voltage (v)
$\text{Ti} = \text{Ti}^{++} + 2\text{e}^-$	+1.63
$\text{Ti} = \text{Ti}^{+4} + 4\text{e}^-$	+1.90
$\text{Zr} = \text{Zr}^{+4} + 4\text{e}^-$	+1.53
$\text{Hf} = \text{Hf}^{+4} + 4\text{e}^-$	+1.70
$\text{Be} = \text{Be}^{++} + 2\text{e}^-$	+1.85
$\text{Al} = \text{Al}^{+++} + 3\text{e}^-$	+1.66
$\text{Ni} = \text{Ni}^{++} + 2\text{e}^-$	+0.25
$\text{Cu} = \text{Cu}^{++} + 2\text{e}^-$	-0.34
$\text{Ag} = \text{Ag}^+ + \text{e}^-$	-0.80
$\text{Pd} = \text{Pd}^{++} + 2\text{e}^-$	-0.83
$\text{Au} = \text{Au}^+ + \text{e}^-$	-1.68

Ti and Ti-Zr, analogous to (and metallurgically compatible with) the ductile, isotropic and highly deformable solid-solution matrices of Beta-C and the other all-beta commercial titanium alloys (Ref. 10). This approach is termed "similar-metal braze design". Beta stabilization to retain a high proportion of the beta terminal solid solution over the entire service temperature range (RT-800°F) is preferred inasmuch as the lower temperature allotropic form (hexagonal alpha phase) is quite anisotropic with regard to deformation potential and ductility and is more susceptible to embrittlement by interstitial-solute contaminants (O, N, C). (A small amount of equilibrium alpha might prove useful as a scavenging phase or "sink" for such contaminants.) Beta stabilization without intermetallic formation can be achieved by alloying with ductile beta-structure isomorphs such as Zr and Hf (Group IVb) and/or Nb, V and Ta (Group Vb). This has led to the inclusion of candidate Ti-Zr, Ti-V, Zr-Ti, and Zr-V-Ti bases in the subject work (see section "Braze Alloy Design and Screening (Phase I)", page 31).

There are other valid reasons for selecting the Ti and Ti-Zr bases over competing systems. Of all the tough and ductile metallic bases (with potential for liquation in the desired temperature range), only titanium and zirconium are actively

self-fluxing and self-surface-gettering, normally displaying superb wetting, flow and filleting characteristics over a wide variety of difficult brazing conditions. This is normally true in both vacuum and inert-gas process environments (Ref. 1). As implied earlier, the greater opportunities for modulus matching and surface emf matching of substrate and braze (where both are Ti-base or Ti-Zr base) should enhance intrinsic strain accommodation and insensitivity to corrosive media in service. Of equal importance, the potentials for elevated-temperature braze strengths (500-800°F) are much greater for the high-melting Ti and Zr bases than for the softer, lower-m.p. and modulus, copper and noble-metal bases.

With regard to further consideration of noble-metal braze bases, the only other significant development in ductile braze alloys for titanium (in the 1965-1974 interim) has been the study of Ag-Pd-Ga and Ag-Pd-Al braze systems by WESGO and AMI, respectively, in an effort to prevent the interfacial formation of TiAg inter-metallic (Ref. 5,6). Continuous films of TiAg at the braze/substrate interface are felt to be the root cause of the poor salt-corrosion resistance and rapid oxidation attacks (500-800°F) of silver-base alloy brazements. Reportedly, both palladium and gallium establish interfacial diffusion barriers to silver, thus preventing (or postponing) the formation of TiAg films. The long-term effectiveness of this approach has yet to be demonstrated for extended 500-800°F service. Solar also is wary of Ag-base braze alloys for elevated temperature service because of the ~900°F m.p. eutectic between silver and silver oxide (Ag-Ag₂O) (Ref. 15). The Ag₂O oxide is unavoidable during normal service in air environment, and the eutectic formation can be quite rapid and structurally invasive, even during short-term excursions of overtemperature (≥900°F). Solar has experienced a number of silver-braze failures due to structural damage arising from this low-melting eutectic, and no longer recommends Ag-base braze alloys for service ≥600°F.

BRAZE TOUGHNESS

A second major consideration in braze alloy design is that of improved toughness*, including reduced vulnerability to geometric stress raisers and cast inter-metallic networks. One logical approach is the development of more strongly hypoeutectic braze structures, with higher volume proportions and continuity of the tough metallic, β -terminal-solid-solution base (as pro-eutectic matrix phase) and less eutectic (and associated intermetallic) volumes. This desirable structural modification should be accomplished ideally without appreciably raising liquidus and flow temperatures. This might possibly be achieved by backing off controlled amounts on the

* Material "toughness" in the abstract sense, meaning relative (a) insensitivity to notch effects and other high strain gradients (b) high energy requirements to initiate and propagate joint cracking.

eutectic-forming, strongly-intermetallic-forming m.p. depressants (e.g., Cu, Ni, Be) while substituting the synergistic effects of multiple, weak intermetallic forming and/or beta-isomorphous melting-point depressants. Elements with significant β -phase and α -phase solubilities would be preferred, e.g., V, Zr, Nb-Zr, Mn, Pd, Cr, Fe, Sn, Ga (see Tables 4 and 5). Multi-component alloying of this nature can become quite complex and require extensive exploratory effort. It should be remembered (hypoeutectic approach) that the spread between solidus and liquidus temperatures should ideally be maintained $\leq 50^\circ\text{F}$ to obtain uniform braze filleting and homogeneous braze microstructures along the joint line, and to avoid clumps of unmelted braze residue. (In actual fact, all of the superior braze alloys developed in Phase I work are representative of hypoeutectic alloy design.)

A good example of a notably tough, very strongly hypoeutectic braze design with wide solidus-liquidus spread is the commercial alloy, TICUNI (Ti-15Cu-15Ni) (Ref. 5). This ternary alloy exhibits minor eutectic melting at $\sim 1650^\circ\text{F}$, but on further heating still retains ~ 50 percent unmelted solids at 1850°F , and ~ 20 percent unmelted residue at 1900°F . Because of the residue problem, this alloy is usually considered unsuitable for conventional brazing with external braze placement, but is frequently used for conventional brazing with in-situ placement, where the braze flow requirement is negligible or minimal. TiCuNi was suggested as the baseline braze alloy by the sponsor, and is discussed further in "Alloy Guidelines", page 18 and "Braze Alloy Design and Screening (Phase I)", page 31.

Another logical approach to improved braze toughness is that of developing a low-melting, essentially single-phase (β) braze alloy with negligible or only minor intermetallic content. A great deal of effort was expended (Phase I) in exploring and evaluating the Zr-V-Ti system which (alone among preferred bases) has shown the potential for liquidus temperatures well below 2300°F (e.g., as low as 2230 - 2260°F) while maintaining a soft, ductile (stable β) single-phase structure. (The three beta-structure isomorphs, Ti, Zr and V, all possess individual melting temperatures well above 3000°F .) Minor fourth- and fifth-element alloying was attempted to lower the liquidus $\leq 1750^\circ\text{F}$ without excessive intermetallic formation or solidus-liquidus spread.

MELTING-POINT DEPRESSION

The third major consideration in the subject braze alloy design is attainment of 100 percent liquation and flow within the desired range of brazing temperatures (viz., 1600 - 1750°F). This objective is undoubtedly the least amenable to compromise. Without melting, there can be no brazing. Inasmuch as the preferred similar-metal bases have elemental melting temperatures well above 3000°F , alloying with strong melting point depressants becomes imperative. A review of binary equilibrium diagrams with Ti and Zr as bases (Ref. 14, 15, 16) reveals the following first eutectic or peritectic systems with liquidus temperatures depressed $\leq 2150^\circ\text{F}$. (Table 4.)

Table 4
BINARY SYSTEMS SHOWING STRONG MELTING POINT DEPRESSION

Base	Composition	Type	Invariant Temp. (°F) (100% Liquation)	First Intermetallic Formed	Maximum Solid Solubility β Phase (Wt. %)
Ti	Ti-32Fe	Eutectic	1985	FeTi	~25 (Fe)
Zr	Zr-16Fe	Eutectic	1720	Fe ₂ Zr	~4.2 (Fe)
Ti	Ti-28.5Ni	Eutectic	1740	Ti ₂ Ni	~13 (Ni)
Zr	Zr-17Ni	Eutectic	1765	Zr ₂ Ni	~2 (Ni)
Ti	Ti-27Co	Eutectic	1870	Ti ₂ Co	~11 (Co)
Zr	Zr-15Co	Eutectic	1800	Zr ₂ Co	~3 (Co)
Ti	Ti-42.5Mn	Eutectic	2150	TiMn ₂	~33 (Mn)
Zr	Zr-22.5Mn	Eutectic	2080	ZrMn ₂	~7 (Mn)
Ti	Ti-36Cu, or Ti-40Cu	Eutectic or peritectic	1850 1815	Ti ₂ Cu	~17 (Cu)
Zr	Zr-22Cu	Eutectic	1820	Zr ₂ Cu	~4 (Cu)
Ti	Ti-5.6Be	Eutectic	1887	TiBe ₂	~1.0 (Be)
Zr	Zr-5.5Be	Eutectic	1780	ZrBe ₂	≤0.3 (Be)
Ti	Ti-48Pd	Eutectic	1975	Pd ₃ Ti	~46 (Pd)
Zr	Zr-27Pd	Eutectic	1890	PdZr ₂	~12 (Pd)

Binary systems with eutectic or peritectic temperatures $\leq 2150^{\circ}\text{F}$ were arbitrarily regarded as representing strong melting-point depression, and favorable starting points for accessory alloying to further depress liquidus temperatures.

Candidate strong melting point depressants for both bases appear restricted to Ni, Co, Fe, Mn, Cu, Be and Pd, all intermetallic formers and beta stabilizers. This is admittedly an arbitrary list (based upon the 2150°F cut-off temperature), but the requirement of strong melting point depression (even with the anticipated aid of synergistic alloying effects) logically mandated starting with at least one strong melting point depressant. Possible accessory melting point depressants, which received attention, include the following (Table 5): Al, Sn, Si, Ge, Cr, V and Ga. Note that nearly all the melting point depressants listed in Tables 4 and 5 exhibit potential to form intermetallics (during melt solidification) at alloying levels significantly less than those required for maximum melting point depression. Further, many are reported to precipitate similar or less temperature-stable intermetallics or to form hard, ordered solutions at temperatures within the service range; or to

Table 5
BINARY SYSTEMS SHOWING WEAK-TO-MODERATE MELTING
POINT DEPRESSION

Base	Composition	Type	Invariant Temperature or Minimum Melting Point (°F)	First Intermetallic Formed	Maximum Solid Solubility β Phase (Wt. %)
Ti	Ti-35Al	Peritectic	2675	TiAl/Ti ₄ Al	~31 (Al)
Zr	Zr-11Al	Eutectic	2460	Zr ₃ Al/Zr ₂ Al	~9 (Al)
Ti	Ti-33Sn	Eutectic	2895	Ti ₃ Sn	~28 (Sn)
Zr	Zr-23.5Sn	Eutectic	2895	Zr ₄ Sn	~21 (Sn)
Ti	Ti-8.5Si	Eutectic	2430	Ti ₅ Si ₃	≤3 (Si)
Zr	Zr-2.9Si	Eutectic	2930	Zr ₄ Si	≤0.2 (Si)
Ti	Ti-21.5Ge	Eutectic	2570	Ti ₅ Ge	~13 (Ge)
Zr	Zr-7.7Ge	Eutectic	2800	Zr ₃ Ge	~0.4 (Ge)
Ti	Ti-47Cr	Min. m. p.	2535	TiCr ₂	~25 (Cr) (1850°F)
Zr	Zr-18Cr	Eutectic	2320	ZrCr ₂	~4.5 (Cr)
Zr	Zr-Hf	(No m. p. depression)	--	--	Unlimited (Hf)
Ti	Ti-35Hf	Min. m. p.	2980	None	Unlimited (Hf)
Ti	Ti-50Zr	Min. m. p.	2950	None	Unlimited (Zr)
Ti	Ti-30V	Min. m. p.	2950	None	Unlimited (V)
Zr	Zr-30V	Eutectic	2250	ZrV ₂	~10 (V)
Ti	Ti-39Ga	Eutectic	2735	Ti ₂ Ga	~38 (Ga)
Zr	Zr-18Ga	Eutectic	2520(?)	Zr ₃ Ga/ Zr ₅ Ga ₃	~6 (Ga)
Ti	Ti-Cb	(No m. p. depression)	--	--	Unlimited (Cb)
Zr	Zr-22Cb	Min. m. p.	3165	--	Unlimited >1800°F (Cb)

induce partial transformation of the beta terminal solid solutions to potentially embrittling transition products, such as omega-phase or orthorhombic martensite. Consequently, there exists in braze alloy design an underlying conflict between needed melting point depression and undesired, excessive intermetallic formation, matrix instability, etc. A workable compromise is frequently not feasible, so that much invention and exploration are necessary to identify the best alloying combinations.

Promising single-phase base compositions upon which to seek further m. p. depression (in addition to pure Ti and pure Zr) are represented by the minimum

melting point (beta isomorphous) alloys found in the Ti-Zr and Ti-V binary systems, viz., Ti-50Zr (2950°F) and Ti-30V (2950°F) (Ref. 14, 15, 16). Both are comprised of about 67 atomic percent titanium and are strongly beta stabilized. As it developed, the most promising braze alloy candidates evolved from the Ti-Zr minimum m.p., as base. Another promising low-melting braze base was that suggested by the identification of a marginally-ductile ternary eutectic in the system, Zr-V-Ti, with eutectic temperature ~ 2090°F, viz., Zr-28V-16Ti (Ref. 17,18). It was proposed that a single-phase or near single-phase (metastable β), hypoeutectic base with liquidus $\leq 2300^\circ\text{F}$ could be defined by minor alloy modification adjacent to the ternary eutectic, to suppress the intermetallic, ZrV_2 , or its ternary variant. This objective was met successfully during studies early in Phase I, but subsequent attempts to lower the liquidus further ($\leq 1750^\circ\text{F}$) by fourth- and fifth-element alloying were not successful (see "Experimental Results and Discussion, Braze Alloy Design and Screening (Phase I)", pp 32-37).

Striving for adequate melting-point depression proved one of the most difficult tasks in braze alloy design. Whereas similar-metal braze designs for most nickel-, iron-nickel, aluminum- and copper-base substrates safely permit brazing as near as 200°F to the substrate solidus temperature, the peculiar problems of beta-embrittlement, grain enlargement and/or interstitial contamination encountered with commercial titanium alloys mandates brazing at least 1300-1500°F below the titanium substrate solidus. (This translates to a maximum braze process temperature of 1750°F for Ti-6Al-4V and Beta-C alloys.) Meeting this requirement for 1300-1500°F depression of melting point (and flow point) in a similar-metal braze design can entail considerable compromise in braze microstructure and properties. (These compromises and efforts to obtain the best compromise, will be described in detail in the sections entitled "Braze Alloy Design and Screening (Phase I)", page 31; "Braze Optimization Studies (Phase II)", page 71; and "Braze Characterization (Phase III)", page 112.)

GENERAL ALLOYING APPROACH

The planned general approach consisted of probing and exploring for eutectic and near-eutectic low-melting troughs (liquidus $\leq 1750^\circ\text{F}$) within the binary-to-quinary systems of expressed interest. The actual systems explored are described in detail in Section IV; however, all alloys employ one of the following bases (Ti, Zr, Ti-Zr, Ti-V, Zr-Ti, or Zr-V-Ti) in conjunction with one or more of the strong m.p. depressants listed in Table 4. (With the Zr-V-Ti base alloys, the starting liquation temperatures were sufficiently low that even the weak-to-moderate m.p. depressants were evaluated singly.) When a promising low-melting trough was detected, alloy modification was then redirected toward hypoeutectic or single-phase structures. This redirection was done by either of two methods. One was to systematically decrease the level(s) of melting-point depressant(s); the other was to increase the ratio of Ti to Zr, or to V, or to (Zr + V) in the base. (In some instances, both methods were worked concurrently.) If these procedures resulted in an alloy with significantly lower hardness and/or appreciably greater resistance to comminution than the eutectic, while maintaining stated solidus-liquidus temperature objectives, then a candidate braze

alloy had been created for further study. If intermetallic compound levels were still too high and/or the liquidus temperature rose too much, synergistic alloying effects were then sought by substituting partially (for the principal m.p. depressant) with low-melting binary or ternary alloys based upon the principal depressant (See Section IV). In essence, these are iterative or trial-and-error methods for backing off on the effective amount of intermetallic forming, m.p. depressants added, without materially reducing the overall influence on solidus-liquidus depression. They are frequently successful in braze alloy design.

ALLOYING GUIDELINES

The guidelines established at the outset of the program were primarily lists of rational alloying priorities and constraints.

- Substitutional Alloying in the Terminal Solid Solution

The extent and nature of alloying was governed primarily by the quest for adequate m.p. depression, so long as compatible with the stated objectives of enhancing braze matrix toughness, ductility, and corrosion resistance, and inducing strong beta-phase stabilization. Alloying purely to augment matrix strength was subordinate to the above.

- Interstitial Solutes

Interstitial alloying elements such as Li, C, B, O and N were avoided because of extreme grain-boundary and phase-boundary mobilities and well documented adverse effects upon matrix ductility and stability.

- Low Melting Solutes

Very volatile, low-melting, m.p. depressants such as Zn, Cd, P, S, Se, As, Pb, Sb, etc. were prohibited because of the potential hazards of poisoning superalloy or iron-base alloy components in proximity to the braze.

- Beryllium

Beryllium, although a potent m.p. depressant, was not seriously considered because of well-publicized toxicity problems associated with Be vapors.

- Precious Metals

Very high priced metals such as Pt, Pd, Hf, Au and Ag were de-emphasized as alloying agents in order to keep the starting material costs from becoming prohibitive. Palladium, a promising major m.p. depressant was therefore not seriously considered (see Table 4).

- Vapor Pressures

Alloying agents with vapor pressures in the brazing temperature range (1600-1750°F) higher than manganese were not considered. Experience has shown that vapor pressures $\geq 1.0 \times 10^{-2}$ Torr frequently cause problems of reduced braze fluidity, rough fillet surfaces, braze porosity and extensive vapor deposition of the volatile species on all proximate surfaces.

- Baseline Braze Alloy

The sponsor requested that a commercial braze alloy, Ti-15Cu-15Ni, be adopted as a comparison baseline for the subject developmental braze alloys. Ti-15Cu-15Ni was reported to exhibit the highest tensile-shear strengths over the service range, RT-800°F, of all the corrosion-resistant braze materials currently available. A marked tendency for shear-strength levels to drop with decreasing temperature in the service range is felt to be an indication of marginal braze toughness. (This has been supported by the ease of RT comminution in the subject work.) The commercial designation for Ti-15Cu-15Ni is "TICUNI" (Western Gold and Platinum Company). Major drawbacks for conventional brazing are the very high liquidus temperature ($\geq 1900^\circ\text{F}$) and the wide spread between solidus and liquidus temperatures ($\geq 250^\circ\text{F}$). (Ti-15Cu-15Ni is a strongly hypoeutectic alloy.)

SECTION III

EXPERIMENTAL MATERIALS AND PROCEDURES

SECTION III

EXPERIMENTAL MATERIALS AND PROCEDURES

Candidate braze alloys were (TIG) arc melted in the form of 5.0 gram button ingots, using precision pre-weighed elemental charges (cold-crucible method; water-cooled copper crucible) (see Fig. 6). The weights of total charge and each alloying constituent were measured to the nearest milligram. Button ingots were also weighed after final melting to ensure retention and assimilation of all charge constituents. The melting chamber environment was static, titanium-gettered argon (one atmosphere). Each button ingot was turned over and remelted three times to promote chemical and structural homogeneity. Base elements and principal alloying agents were typically 99.9 (+) percent purity. (See Table 6 for characterization of elemental charge stocks.)

Manual ingot comminution (tool-steel mortar and 3.7 pound tool-steel pestle) was generally employed to obtain small chunks of braze suitable for specimen brazing tests. A good semi-quantitative estimate of relative braze toughness was derived from observations of apparent resistance to manual ingot crushing (e.g., "brittle, easy to crush manually", "tough, difficult to crush manually", or "very tough, requires hydraulic press to initiate ingot cracking"). (For Ingot Comminution Ratings (ICR), see data tables, Section IV.) Very tough ingots which could not be crushed manually or cracked on the press were drilled to obtain chips for braze screening tests. Inasmuch as the alloy design process was largely exploratory in nature, the application of the ingot comminution test (in conjunction with solidus-liquidus determination and general brazing characteristics; see below) were employed to cull out unpromising compositions as well as to identify promising directions for alloying experimentation.

The screening test configuration for solidus-liquidus temperature determinations and appraisal of general brazing characteristics was the foil T-joint illustrated in Figure 2. Inasmuch as neither program substrate alloy (Beta-C or Ti-6Al-4V) in either 0.050- or 0.062-inch thickness had been received at commencement of Phase I work, available 6-mil (0.006-inch) foil of Ti-6Al-4V alloy* was enlisted for all Phase I braze screening work. Particles or chips of braze alloy graded to -12/+20 mesh were positioned along and adjacent to the joint line on one side of the T-joint only. With this one-sided loading pattern and net fit-up of faying surfaces, uniform filletting

*Ti-6Al-4V (AMS-4911A); Rodney Metals, Inc., Heat No. D8941 (mill annealed).

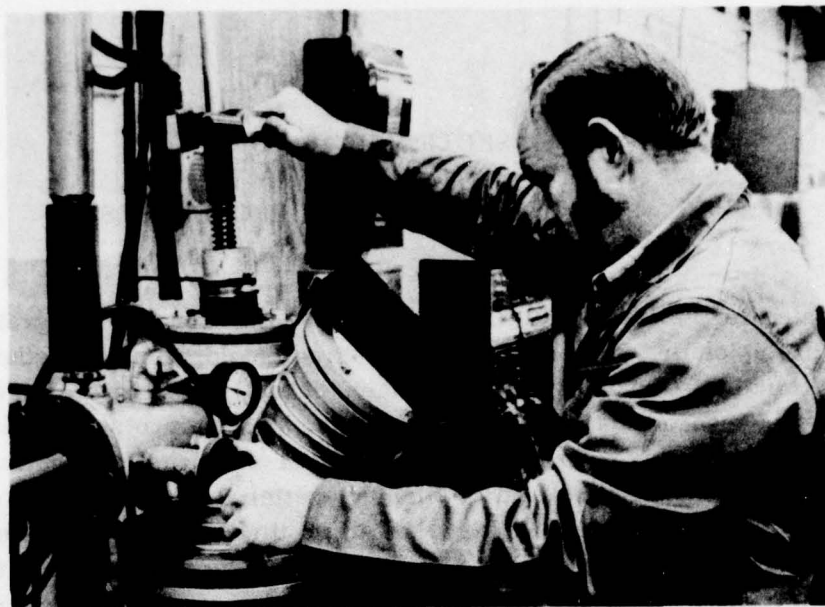


Figure 6. Controlled Atmosphere Arc Melter

and homogeneous microstructures (both sides) could be achieved only by total and near simultaneous braze melting and good-to-excellent braze flow. Most candidate braze alloys tested were culled out of contention by displaying poor brazing characteristics (see Appendix) and/or by not melting and flowing $\leq 1750^{\circ}\text{F}$. Each braze-loaded T-joint specimen was radiantly heated to the brazing temperature in high vacuum (1.0×10^{-5} Torr or better), inside of a transparent Vycor glass tube, so that the braze particles and the joint region could be viewed directly at all times (see Fig. 7). An inductively heated columbium or tantalum foil susceptor around the specimen served as the radiant heat source (Fig. 7). Normal heating rate was controlled at $\sim 100^{\circ}\text{F}/\text{min}$ above 1000°F . (This was to simulate a typical production braze heating rate.) Viewing with a Pyro Micro-Optical Pyrometer, Model No. 95, through a small hole in the susceptor (Fig. 7) permitted direct observation and measurement of initial braze melting (solidus temperature) and total braze melting (liquidus temperature) as well as flow and filleting behavior at the selected braze temperature. Brazing in the subject work (Phase I) was usually confined to the liquidus temperature plus $\sim 10\text{--}30^{\circ}\text{F}$, with brazing times at maximum temperature on the order of 15–30 seconds. Calibration of the pyrometer for the specific brazing environment described was carried out against the known melting temperatures for (particles of) pure copper (1981°F), pure silver (1761°F), and the minimum melting point alloy in the Cu-Mn system (viz., Cu-35Mn, 1600°F).

Table 6
HIGH-PURITY ELEMENTAL MELT STOCKS

Element	Source	Grade	Guaranteed Purity (% Wt)	Typical Interstitial Concentrations (ppm-Wt)
Titanium	Atomergic-Chemetals (New York, NY)	Crystal-Grade Granules	99.95 (+)	[O] ≤ 100 [N] ≈ 20 [C] ≤ 100
Zirconium	Wah-Chang (Albany, Ore.)	Iodide-Crystal Bar	99.9 (+)	[O] ≤ 150 [N] ≤ 40 [C] ≤ 100
Vanadium	Atomergic-Chemetals	Electrolytic Granules	99.9 (+)	
Nickel	Atomergic-Chemetals	Nickel Platelets (Electrolytic)	99.98	
Cobalt	Atomergic-Chemetals	High-Purity Melt-ing Grade	99.9 (+)	
Iron	Glidden Metals (Denver, Colorado)	Electrolytic Chips	99.95	
Chromium	Atomergic-Chemetals	Chromium Flake	99.95 (+)	
Columbium	Atomergic-Chemetals	Cb Nuclear-Grade Pellets	99.8 (+)	[O] ≤ 1000 [N] ≤ 200 [C] ≤ 300
Tantalum	Atomergic-Chemetals	Ta Capacitor-Grade Pellets	99.9 (+)	[O] ≤ 500 [N] ≤ 30 [C] ≤ 50
Copper	ASARCO (Denver, Colorado)	Special High-Purity Platelets (Spectro-graphically pure)	99.99 (+)	
Silicon	Research Organic/Inorganic Chemicals (Sun Valley, CA)	High-Purity Silicon Lump	99.7 (+)	
Manganese	Foots Mineral (Exton, PA)	Electrolytic Chip	99.99 (+)	

Table 6 (Contd)

Element	Source	Grade	Guaranteed Purity (% Wt)	Typical Interstitial Concentrations (ppm-Wt)
Beryllium	Kawecki-Beryco (Reading, PA)	Be Ingot-Sheet (Type IS)	99.8 (+)	[O] \leq 100 [C] \leq 400
Germanium	Atomergic-Chemetals	Semiconductor Grade (Ingot)	99.99 (+)	[O] \approx 100-500 [N] \approx 0-10
Gallium	Atomergic-Chemetals	Semiconductor Grade (Ingot)	99.99 (+)	
Palladium	Engelhard Industries (Newark, NJ)	High-Purity Wire (C. P. Grade)	99.98 (+)	
Tin	Atomergic-Chemetals	High-Purity Ingot	99.999	
Aluminum	ALCOA (Pittsburg, PA)	High-Purity Pig.	99.99	
Neodymium Cerium Gadolinium Lanthanum Yttrium	Lunex, Co. (Pleasant Valley, IA)	Nuclear Grade	99.9 (+)	
Scandium	Research Organic/ Inorganic Chemicals	Nuclear Grade	99.5 (+)	

Single-lap tensile shear specimens (Fig. 3) for Phase I and Phase II tests also were vacuum brazed by induction heating, inside a longer tantalum susceptor in the manner described above (Fig. 7). Shear specimens were positioned vertically (length axis) for brazing. Heating rate was similar to that for T-joints, and holding time at braze temperature was varied between 20 seconds and 5 minutes. For reasons of significantly greater economy of preparation, better adaptability to induction brazing and variable processing, and the need to rapidly screen and modify large numbers of braze alloy candidates within reasonable time schedules (Phases I and II), the standard shear specimen design (per AWS C3.2-63/60.105) was altered slightly to minimize machining, brazing and testing times. (See the dashed outline of the screening test specimen in Figure 3). The test section configuration and dimensions were maintained exactly the same as the standard specimen, but the grip ends were simplified to permit rapid positioning and tensile loading (wedge grips) by Hounsfield Tensometer. (In Phase III, Braze Alloy Characterization, the full size pin-loaded standard shear specimen was employed. See below for qualification.) The substrate sheet thickness is nominally 0.062-inch, per sponsor request, instead of the 0.125-inch thickness called out in the referenced AWS specification. For screening studies and all mechanical

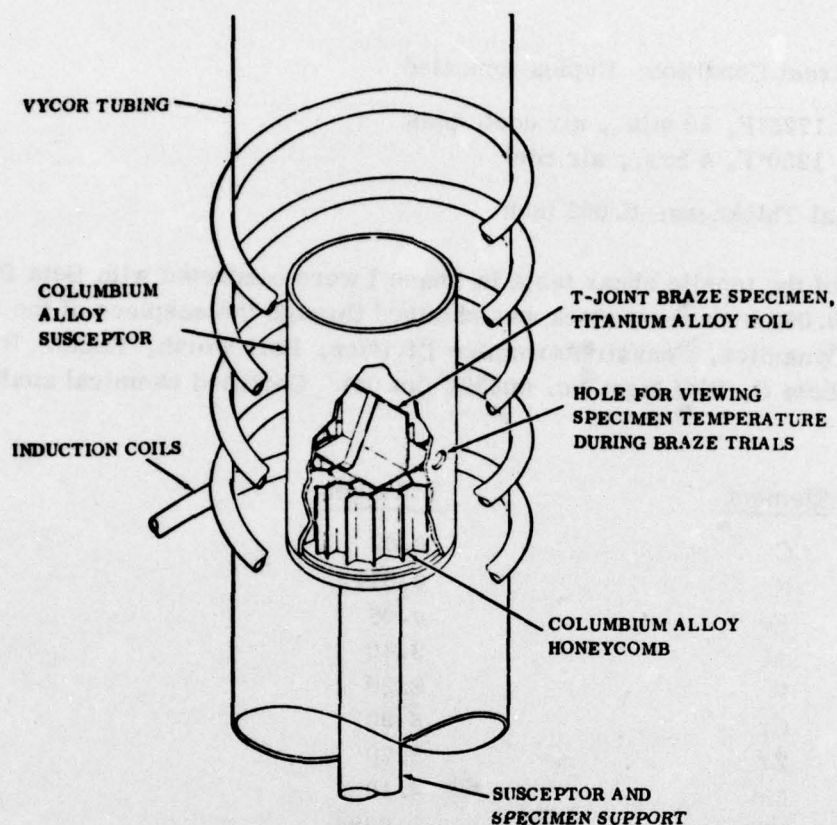


Figure 7. Schematic Diagram of the Laboratory Brazing Furnace

tests, joint overlap (A/t ; Fig. 3) was held constant at $2t$ (i.e., 0.125-inch) and faying surface clearance (gap) at 0.002-inch. Strain rate over the shear area was maintained at $\sim 1.0 \times 10^{-3}$ in./in./min in all-tensile shear testing.

The principal substrate sheet alloy used in Phase I and Phase II tensile and shear tests and all Phase III tests is Ti-6Al-4V, RMI Ingot No. 295406 (lot 13). It was obtained through the auspices of the sponsor. Certified chemical analysis is as follows:

<u>Element</u>	<u>% Weight</u>
C	0.02
N	0.013
Fe	0.17
Al	6.30
V	4.20
O	0.016
H	0.0040
Ti	Balance

Heat Treat Condition: Duplex Annealed

- (1) 1725°F, 10 min., air cool, plus
- (2) 1250°F, 4 hrs., air cool

Nominal Thickness: 0.062 inch

Some of the tensile shear tests in Phase I were conducted with Beta C alloy sheet. This 0.062 inch sheet stock was obtained through the auspices of the sponsor and General Dynamics, Convair Aerospace Division, Fort Worth, Texas. It was identified as Beta C, RMI Ingot No. 600393 (lot 04). Certified chemical analysis is as follows

<u>Element</u>	<u>% Weight</u>
C	0.02
N	0.014
Fe	0.06
Al	3.40
V	8.20
Cr	5.90
Zr	3.70
Mo	4.10
H	0.0084
O	0.104
Ti	Balance

Heat Treat Condition: H. R., STA and Cl (RMI designation)

Nominal Thickness 0.062 inch

Full size single-lap shear specimens for tensile-shear tests and stress-rupture tests (Fig. 3, Phase III) and double-lap-joint specimens for braze peel tests (Fig. 4, Phase III) were brazed by radiant heating in an NRC Model 3114 Vacuum Furnace, employing tantalum-strip resistance heating elements. Chamber vacuums of 1.0×10^{-5} Torr or better were maintained throughout the braze cycles. The NRC furnace is a small production-type brazing and heat treating furnace, which provided close simulation of the typical heating and cooling rates experienced in production vacuum brazing (viz. ~ 100 - $135^\circ\text{F}/\text{min.}$, heating from 1000°F to the actual braze temperature.) Holding time at the braze process temperature for specimen brazing was standardized at 15 minutes, to better simulate typical braze practice (cf. short-braze cycles for T-joints in prior Phase I and Phase II work). Except early in Phase I work where a light braze loading was evaluated (viz. 0.010-0.020 gm of braze alloy per shear specimen), heavy braze loading was made standard in all (other) Phase I, II, and III tensile-shear specimen preparation (viz. 0.120-0.140 gm of braze per

specimen). The heavier braze loads were selected to better simulate conventional braze processing. In all cases, candidate braze particles graded to -12/+20 mesh (-0.065 in./+0.033 in.) were used. No organic braze binders were employed in the subject program. All mill-finish faying surfaces were cleaned prior to brazing by:

- Acid etch; RT (61% distilled H_2O - 35% HNO_3 - 4% HF)
- Distilled water rinse
- Acetone rinse

In the course of work, it was determined that the sequence of machining and brazing of single-lap shear test specimens is very important. Shear test specimens in Phases I and II were machined to finish dimensions, assembled, and then brazed (all without problems). However, in Phase III work, finish specimens for tensile shear and stress rupture tests were machined from pre-brazed, nominally 1-1/8 in. wide x 9-7/8 in. long blanks (per AWS Spec. No. C3.2-63/60.105; see Figure 8). Attempts to gang-mill clamped stacks of specimens (each stack consisting of 5-8 brazed specimen blanks) to final gage dimensions resulted in significant damage to braze joints, of both candidate braze and baseline braze alloys. The tool-steel milling cutter used was contoured to provide final gage dimension and radii, as is common specimen-machining practice for superalloys and steels at Solar. Braze joint cracking was prevalent, whether milling cuts were made across the specimen length direction or along the length direction; true even at very low feeds. Consequently, it was decided to change to an electrochemical machining method (i.e., ECM), to avoid the tool-induced stresses associated with milling and other mechanical methods of machining. [This was a proper selection, inasmuch as it was learned subsequently that even finish hand filing or finish hand grinding can result in apparent braze damage and resultant premature test failures for ECM'd specimens (cf. Ref. 19). Therefore, all Phase III tensile-shear specimens and rupture specimens were tested with as-ECM'd finish surfaces.] The following ECM equipment and parameters were used for contour machining of gage dimensions:

- Basic ECM Facility: Cincinnati Milling Machine Co.; Model 2PS Elektrodyne Grinder
- Power Supply and Control: Anocut Engineering Co.; Model No. 600.
- Electrolyte: Cimlyte #7 (Cincinnati)
- Working Voltage: 16 volts
- Working Current: 300 amperes
- Maskant (applied to braze fillets) Organoceram Translucent Maskant #1-2021

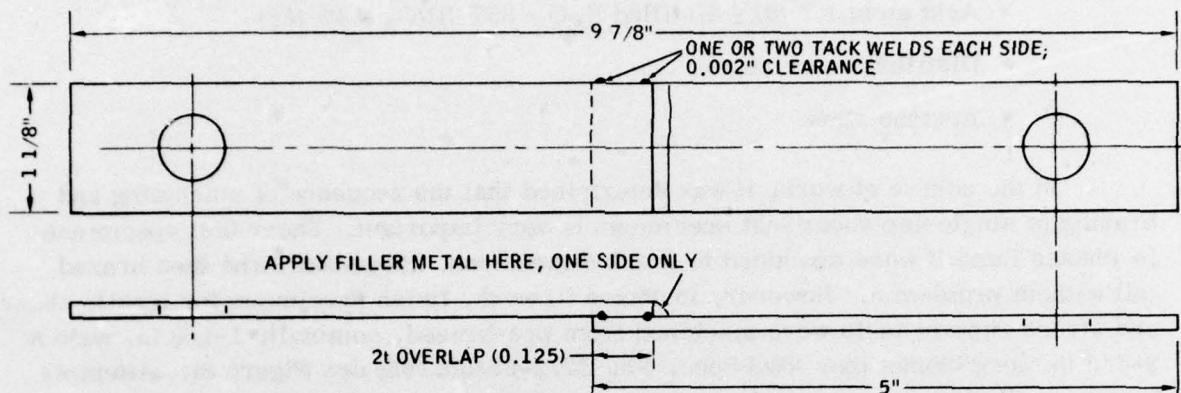


Figure 8. Pre-Brazed Shear Specimen Blanks

In the as-ECM'd condition, all brazements were found to be extremely brittle; apparently due to hydrogen generation and absorption during ECM (Ref. 20). This condition was corrected by vacuum dehydrating all specimens post-ECM in the NRC vacuum furnace (1 hour at 1025°F). In adopting ECM for Phase III specimen machining, two compromises were unfortunately found necessary in shear-specimen dimensions due to electrode and equipment limitations:

- Length of the gage section was reduced from 4 inches to 2 inches (cf. Fig. 3)
- Width of the gage section was maintained between 0.40 and 0.65 inch, rather than controlled at 0.50 inch (cf. Fig. 3)

However, by comparing tensile-shear data from Phases I, II, and III, it was concluded that the real effects of the above dimension changes upon shear properties were negligible.

Salt-spray conditioning of selected shear specimens prior to test was carried out in accordance with ASTM Specification Number B1117, using a 5 percent NaCl aqueous solution at a chamber temperature of 95-100°F. One-hundred hour exposures were made standard. Shear specimens were hung vertically in the salt-spray chamber with nylon cord.

Environmental conditioning to simulate the oxidation effects of service in 800°F air was carried out by suspending selected shear specimens in a Leeds and Northrup Homo circulating-air furnace, set at 800°F. Exposures for this 800°F air-oxidation (conditioning) were also standardized at 100 hours.

The environmental effects of hot-salt accretion in service were simulated by brush coating a slurry of 75 percent (vol.) NaCl-25 percent H₂O over all exposed joint regions of select shear specimens, then exposing the salt-coated specimens for 100 hours in 800°F air, as in the air-oxidation tests above. Salt coatings were oven-dried in air at 300°F, prior to 800°F exposures. Total NaCl applied per specimen was approximately 0.7 gm. This salt coating also covered all exposed substrate surfaces within ~1/4 inch of the braze fillets.

Isothermal aging treatments and cyclic annealing treatments of braze ingot were conducted in an NRC Model 3114 Vacuum Furnace, employing tantalum-strip resistance heating elements. Chamber vacuums of 1.0×10^{-5} torr or better were maintained throughout the heat treatment cycles.

All tensile shear tests at 800°F were conducted upon an Instron Universal Testing Machine, Model TT-D. Initial strain rate within the gage section was controlled at $\sim 1.0 \times 10^{-3}$ in./in./min. A SATEC Power Positioning Furnace (Model SF-15P) was employed.

All tensile shear tests and double-lap peel energy tests at room temperature (Phase III) were conducted upon a Tinus-Olsen Universal Testing Machine, Model 6000. Initial strain rate within the gage section (tensile shear) was controlled at $\sim 1.0 \times 10^{-3}$ in./in./min. Rate of crosshead motion in double-lap peel-energy testing was maintained at $\sim 5.0 \times 10^{-3}$ in./in./min. (Initial distance between crossheads; ~2.0 inches.)

Stress rupture tests of select single-lap shear specimens were conducted at 800°F in air, using Arcweld Creep-Rupture Testing Machines (Model JE). SATEC Power Positioning Furnaces (Model F6-1) were employed to maintain specimen temperature at 800°F \pm 15°F.

SECTION IV

EXPERIMENTAL RESULTS AND DISCUSSION

Section IV

EXPERIMENTAL RESULTS AND DISCUSSION

BRAZE ALLOY DESIGN AND SCREENING (PHASE I)

Salient experimental data derived from Phase I work (Braze Alloy Design and Screening) are given here. (Results of screening all of the 300(+) braze alloy designs are tabulated in the Appendix) Solidus, liquidus and flow temperatures, brazing and comminution characteristics, brazement microstructures as well as room temperature and 800°F shear strengths (as-brazed) are discussed for the most interesting candidate braze alloys, categorized into compositional systems. Over 300 alloy compositions were melted and screened in the quest for promising new braze systems applicable to 800°F service.

The main elements of the screening test regime for each braze candidate were as follows:

1. Determination: Solidus, liquidus, minimum flow temperatures
2. Determination: T-Joint brazing characteristics
 - Uniform flow and filleting
 - Absence of unmelted residues, shrinkage, surface roughness
3. Assessment: Relative resistance to RT comminution (cast button-ingot structures)
4. Single-lap tensile shear strengths
 - As-brazed condition (tests at RT and 800°F)
 - After 100 hours of 800°F air oxidation (RT tests)
 - After 100 hours of 100°F salt spray (RT tests)
5. Brazement microstructures.

Existing commercial braze alloys for titanium (i.e., the inherently corrosion-resistant varieties with Ti- or Zr-base and liquidus $\leq 1750^\circ\text{F}$) are all characterized by

high intermetallic contents, consequent high hardness relative to the substrate (Rc 45-58), and poor-to-marginal toughness and ductility levels. The new Ti-base, Ti-Zr base and Zr-Ti base braze alloy designs which were explored and evaluated in the subject work sought to achieve required melting-point depression combined with improved intrinsic "ductility-toughness" by eliminating (single-phase alloy approach) or minimizing (hypoeutectic alloy approach) the intermetallic compounds within the cast braze structures. This was the principal underlying theme in braze design.

There exist about seven (plausible) strong melting-point depressants capable of lowering liquidus temperatures of the above similar-metal (elemental) bases down fairly near to the desired 1650-1750°F range (see Table 4). In this context, "fairly near" means attainable liquidus temperatures of from 1720 to 2150°F. Beryllium was de-emphasized because of its toxicity; the precious metal palladium because of its high cost. Of the remaining five elements, most emphasis for study (especially in hypoeutectic-alloy design) was placed upon copper (Cu), nickel (Ni), and manganese (Mn); evaluated both for single-element alloying effects and in various combinations, searching for synergistic effects. The reasons for this selection are that these three melting point depressants display wide ranges of mutual miscibility in binary combinations, with little or no intermetallic-formation tendencies; and, in two cases, provide interesting low-melting combinations (troughs) of their own - viz., Cu-35Mn; minimum m. p., ~1600°F and Mn-39.5Ni, minimum m. p., ~1870°F.

Single-Phase Alloy Designs

Zr-V-Ti System. One of the most promising systems for use as a braze alloy base, from the combined viewpoints of (potential for) melting-point depression, beta-phase stabilization, corrosion resistance, and low hardness, high-toughness matrix, is Zr-V-Ti (see sections entitled "Melting-Point Depression", page 14 and "General Alloying Approach", page 17). In this system, 56 candidate base compositions were formulated and screened by hardness and visual solidus-liquidus temperature determinations (see Appendix). The screening objective was to define the most promising single-phase base compositions, i. e., those combining liquidus temperatures (on a Ti-6Al-4V substrate) below 2300°F, with hardness \leq Rc 30. Low-melting base compositions within this hardness limit (the maximum found in the single-phase Ti-Zr system) can reasonably be assumed single-phase metastable beta, with negligible intermetallic content (Ref. 14). (This assumption was later confirmed through metallography.) The candidate ternary base compositions are arrayed around the ternary eutectic point at Zr-28V-16Ti (2090°F) (Ref. 17 and 18). Figure 9 illustrates the individual hardness and liquidus temperature for each candidate base, as well as estimated isoliquidus lines (viz., 2200°F, 2300°F, 2400°F and 2500°F). Note the shaded area in Figure 9 which indicates the most promising base compositions as previously defined. (Incidentally, those bases with hardness \leq Rc 34 proved too tough to be crushed to produce small particles for brazing tests; instead, drilling chips had to be used.)

NOTE:
UPPER NUMBER ADJACENT TO
EACH DATA POINT INDICATES
THE APPARENT LIQUIDUS TEM-
PERATURE. LOWER NUMBER
IN PARENTHESES INDICATES
HARDNESS (ROCKWELL C SCALE).

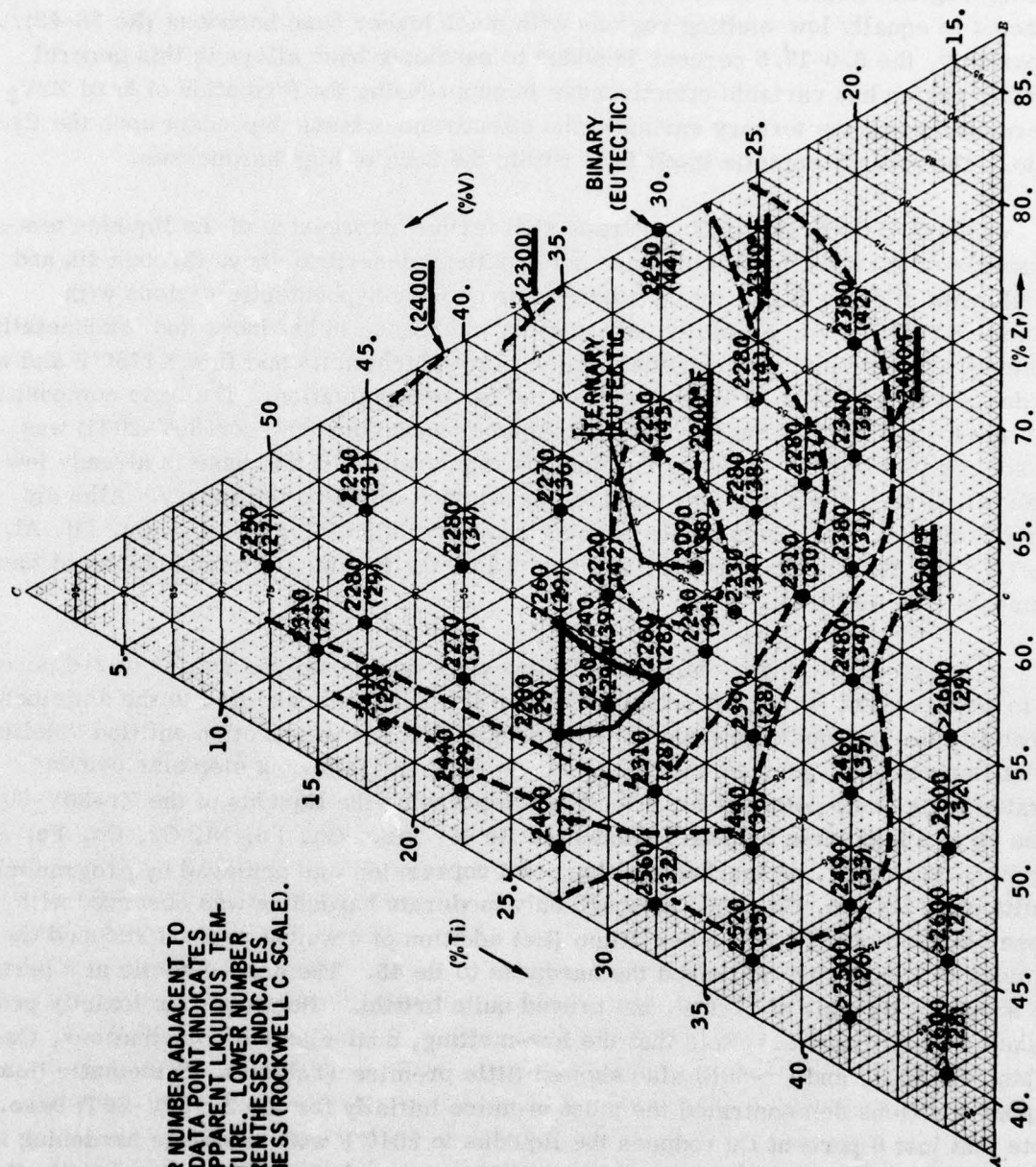


Figure 9. Portion of Ti-Zr-V Ternary Diagram

The most interesting compositional points, with no apparent high-hardness regions between them and the Ti-corner of the ternary, are Zr-30V-20Ti (2260°F liquidus, Rc 28) and Zr-32.5V-20Ti (2230°F liquidus, Rc 29). Note also that the subject low-melting regions (liquidus $\leq 2300^\circ\text{F}$) with low base hardness ($\leq \text{Rc } 30$) occur immediately adjacent to equally low-melting regions with much higher base hardness (Rc 36-43). Apparently, the 5.0-17.5 percent Ti added to candidate base alloys in this general eutectic region has variable effectiveness in suppressing the formation of hard ZrV_2 intermetallic (or the ternary variant), the effectiveness being dependent upon the Zr/V ratio. The ternary eutectic itself falls within the zone of high hardnesses.

Plans were drawn next to pursue still further depression of the liquidus temperatures of the most promising base compositions described above through 4th and 5th element alloying (i.e., into quaternary or quinary hypoeutectic regions with liquidus $\leq 1750^\circ\text{F}$, with hopefully only minimal increases in hardness and intermetallic content). Tentatively, any candidate braze alloy which melts and flow $\leq 1750^\circ\text{F}$ and with hardness ≤ 45 Rc would receive attention and further evaluation. The base composition with the lowest level of the intermetallic-former vanadium (viz. Zr-30V-20Ti) was chosen for this effort. Because the liquidus temperature of this base is already low (2260°F), it was hoped that only very minor alloying would be necessary. Alloying designs consisted of minor single element additions of Ni, Co, Fe, Cr, Cu, Pd, Al, Sn, Cb, Be, Si, Mn, Ga, and Ge, and select low-melting binary combinations of these elements (see Table 7).

Progressive single-element additions were made over the ranges of 2-6 percent up to 2-20 percent (wt.), the actual maximum limit in each case tied to the anticipated capability for liquidus depression of each single element (see section entitled "Melting-Point Depression", page 14 and Table 7). In fact, the following elements demonstrated little or no potential for effectively depressing the liquidus of the Zr-30V-20Ti base up to a maximum induced hardness of Rc 45: viz., Ga, Pd, Ni, Cr, Co, Fe, Al, and Mn. Similarly, no marked melting point depression was achieved by programmed additions of Cb, Sn, Ge or Si, although only moderate hardening was observed with these elements (Table 7). A beryllium (Be) addition of 4 weight percent reduced the liquidus to 1800°F and increased the hardness to Rc 45. The near-eutectic at 6 percent Be showed a liquidus of 1780°F, but proved quite brittle. (However, the toxicity problem makes Be unattractive.) Note that the low-melting, dual-element combinations, Cu-50Mn, Pd-50Ni, and Cr-50Ni also showed little promise (Table 7). Systematic (low) copper additions demonstrated the most promise initially for the Zr-30V-20Ti base. Note that just 6 percent Cu reduces the liquidus to 2040°F with moderate hardening to Rc 39. If this rate of liquidus depression held at somewhat higher copper levels, then 15-20 percent Cu should have been adequate to achieve brazing in the 1600-1750°F range. Unfortunately, progressive alloying additions in the range of 10.0-40.0 percent weight copper yielded no liquidus temperatures below 2000°F, and all alloys proved quite brittle in comminution studies (see Appendix).

Table 7

SUMMARY OF ALLOYING RESULTS WITH THE Zr-30V-20Ti BASE

Alloy Composition (Wt. %)		Melting Temperature (°F)		Hardness (Rc)	Ingot Comminution Rating ^(a)
Zr-30V-20Ti Base	Alloy Addition	Solidus	Liquidus		
Balance	2.0 - Ni	2090	>2200	38	3
Balance	4.0 - Ni	2090	>2200	40	3
Balance	6.0 - Ni	2070	2200	45	2
Balance	10.0 - Ni	2100	2190	48	1
Balance	15.0 - Ni	2050	2130	>48 (very brittle)	1
Balance	20.0 - Ni	2020	2090	>48 (very brittle)	1
Balance	2.0 - Co	2050	2170	40	3
Balance	4.0 - Co	2030	2100	41	3
Balance	6.0 - Co	2025	2090	47	2
Balance	2.0 - Fe	2100	2150	40	3
Balance	4.0 - Fe	2150	2200	48	2
Balance	6.0 - Fe	2190	2200	49	1(+)
Balance	2.0 - Be	1800	1975	39	3
Balance	4.0 - Be	1750	1800	45	2
Balance	6.0 - Be	1750	1780	47	2
Balance	2.0 - Cu	2170	>2300	31	3
Balance	4.0 - Cu	2050	2120	35	3
Balance	6.0 - Cu	2000	2040	39	3
Balance	10.0 - Cu	1860	>2110	44	2
Balance	15.0 - Cu	1780	>2150	45	2
Balance	20.0 - Cu	1910	>2000	43	2
Balance	30.0 - Cu	1860	2000	46 (very erosive)	1(+)
Balance	40.0 - Cu	1845	2020	49 (very erosive)	1(+)
Balance	2.0 - Mn	2150	2170	41	2
Balance	4.0 - Mn	2165	2180	45	2
Balance	6.0 - Mn	2120	2140	48	1(+)
Balance	2.0 - Sn	2230	2250	30	4
Balance	4.0 - Sn	2230	2270	31	4
Balance	6.0 - Sn	2230	2250	33	4
Balance	10.0 - Sn	2270	>2290	36	3(+)
Balance	15.0 - Sn	2250	>2280	37	3
Balance	20.0 - Sn	2225	>2300	39	3
Balance	2.0 - Al	2200	2220	42	3
Balance	4.0 - Al	2200	2250	49	2
Balance	6.0 - Al	>2300	--	51	1(+)
Balance	10.0 - Cb	>2300	--	32	4
Balance	15.0 - Cb	>2300	--	34	4
Balance	20.0 - Cb	>2300	--	36	4
Balance	10.0 - Pd	>2300	--	45	2
Balance	15.0 - Pd	2200	2225	47	1(+)
Balance	20.0 - Pd	2220	2280	48	1(+)

Table 7 (Contd)

Alloy Composition (Wt. %)		Melting Temperature (°F)		Hardness (Rc)	Ingot Comminution Rating ^(a)
Zr-30V-20Ti Base	Alloy Addition	Solidus	Liquidus		
Balance	2.0 - Ga	2160	2200	39	2
Balance	4.0 - Ga	2160	2175	44	2
Balance	6.0 - Ga	--	--	47	1(+)
Balance	2.0 - Si	>2300	--	38	3
Balance	4.0 - Si	2200	>2300	39	2
Balance	6.0 - Si	2200	>2300	41	2
Balance	2.0 - Ge	2150	2170	36	3(+)
Balance	4.0 - Ge	2150	2180	38	3
Balance	6.0 - Ge	2160	2190	38	3
Balance	5.0 - Cu 5.0 - Mn	2000	2090	46	2
Balance	10.0 - Cu 10.0 - Mn	2000	2025	47	1
Balance	15.0 - Cu 15.0 - Mn	1930	2020	>47 (very brittle)	1
Balance	5.0 - Pd 5.0 - Ni	2070	2080	46	2
Balance	10.0 - Pd 10.0 - Ni	2080	2170	47	1(+)
Balance	15.0 - Pd 15.0 - Ni	2080	2180	52	1
Balance	5.0 - Cr 5.0 - Ni	2000	2140	50	1
Balance	10.0 - Cr 10.0 - Ni	2000	2140	>52	1
Balance	15.0 - Cr 15.0 - Ni	2170	2240	>52 (very brittle)	1
Balance	2.0 - Cr	--	--	32	4
Balance	4.0 - Cr	>2020	--	39	3
Balance	6.0 - Cr	2145	2160	44	3
Balance	10.0 - Cr	2220	>2250	49	2
Balance	15.0 - Cr	--	--	50	1

^(a) Resistance to Crushing:
 (1) Brittle; easy to crush manually.
 (2) Marginally tough; moderately resistant to manual crushing.
 (3) Tough; strongly resistant to manual crushing.
 (4) Very tough; requires initial crushing on the hydraulic press.
 (5) Very tough and ductile; cannot be crushed. Requires drilling or rolling to obtain braze forms.

The disappointing results obtained with the Zr-30V-20Ti base were thought possibly related to this soft base's close proximity to the apparent boundary encompassing high-hardness, (probably) high-intermetallic-content compositions in the general area between the ternary and Zr-V binary eutectics (see Fig. 9). That is, the fourth and fifth element additions may have shifted the aforementioned boundary toward and beyond the subject (Zr-30V-20Ti) base, causing inordinate intermetallic compound formation and inducing brittle comminution behavior in the majority of cases (Table 7). With this in mind, two additional Zr-V-Ti base compositions were tested, both located in (other) single-phase, low-hardness areas (liquidus $\leq 2500^{\circ}\text{F}$, ≤ 35 Rc) appreciably farther distant from the boundary of the high-hardness compositions and the ternary

eutectic. One new base was Zr-25V-30Ti (2440°F liquidus, Rc 35), and the other was Zr-20V-35Ti (2490°F liquidus, Rc 33) (See Fig. 9). Near-maximal copper and nickel additions were made to these bases (viz. 25 and 30% Cu; 15 and 20% Ni) to determine whether intermetallic formation and embrittlement would be better suppressed than with the Zr-30V-20Ti base. (see Appendix; Alloy Series E9 and E27, respectively.) In fact, comminution resistances of the new alloys were generally improved over analogous alloys based on Zr-30V-20Ti (cf. Appendix and Table 7). Respectable degrees of melting-point depression also were obtained, but liquidus temperatures were all still $\geq 1900^\circ\text{F}$, and the solidus temperatures recorded did not indicate any eutectic troughs $\leq 1750^\circ\text{F}$ (i.e., of comminution-resistant nature; which might warrant further exploration). Consequently, design and screening work on the single-phase-alloy concept was suspended at this point in favor of studies of hypoeutectic alloys, which showed much better potential for attaining melt-and-flow temperature objectives (see below).

Hypoeutectic Alloy Designs

Ti-Zr-Cu System. Exploratory alloying was conducted in the ternary regions nearest to the Ti-Zr binary, searching for possible low-melting troughs between the first Ti-Cu and first Zr-Cu eutectics (refer to the AC1 Series of alloys in Appendix; and Table 4). Starting with the Ti-50Zr base (minimum m.p., 2950°F liquidus; Table 5), systematic copper additions over the range 10-50 percent Cu revealed a promising near-eutectic behavior at 30 percent copper (solidus 1635°F, liquidus 1660°F) (see Table 8). This can be compared favorably with the first eutectics formed by copper with the individual Ti and Zr bases (viz. Ti-36Cu, 1850°F and Zr-22Cu, 1820°F) (see Table 4). The hardnesses of the first (copper) intermetallics formed with pure Ti and pure Zr fortunately do not appear to be very hard, based upon eutectic and near-eutectic alloy hardness (Ti-30Cu, Rc 22; Zr-20Cu, Rc 33). (Analogous copper-alloying sequences with the pure Ti and pure Zr bases also show that good comminution resistance and lower hardness are associated more with the Ti base, Table 8.) The corresponding first (copper) intermetallic formed with the Ti-50Zr base, however, is ostensibly much harder [(Ti-50Zr) + 30 Cu, \geq Rc 47] and definitely induces some embrittlement, but melt temperatures potentially as low as 1630°F made further exploration worthwhile. The next alloying objective then was to find a suitable compromise among alloy hardness, comminution resistance, and low liquidus temperature, by systematically increasing the Ti/Zr ratio and/or altering (normally reducing) the copper level relative to the ternary eutectic toward more hypoeutectic structures, while retaining the liquidus temperature $\leq 1750^\circ\text{F}$. The most interesting hypoeutectic compositions found were those in the ternary corridor between copper levels of 29.0 percent and 31.5 percent and Ti/Zr ratios of 60/40 and 70/30 (See Fig. 10 and Table 9 for specific compositions). Braze flow and filleting characteristics were uniformly good brazing at or slightly above liquidus temperatures, in the range of 1690-1780°F. Solidus-liquidus spreads were reasonable. Microstructures in this

Table 8

SUMMARY OF ALLOYING RESULTS WITH Ti, Zr, Ti-V AND Ti-Zr BASES

Alloy Composition (Wt. %)		Melting Temperature (°F)		Hardness (Rc)	Ingot Comminution Rating ^(a)
Base	Alloy Addition	Solidus	Liquidus		
(1) <u>Pure Ti Base</u>					
90.0	10.0 - Cu	--	--	33	5
85.0	15.0 - Cu	--	--	31	5
80.0	20.0 - Cu	2050	2080	20	5
70.0	30.0 - Cu	1860	1880	22 (near-eutectic)	5
60.0	40.0 - Cu	1835	1885	8 (near-eutectic)	3
50.0	50.0 - Cu	1875	2000	17	2
80.0	10.0 - Cu 10.0 - Ni	1760	>>1900	30	4
70.0	15.0 - Cu 15.0 - Ni	1750	>>1900	38 (baseline) (TiCuNi)	3
(2) <u>Pure Zr Base</u>					
90.0	10.0 - Cu	--	--	14	5
85.0	15.0 - Cu	--	--	20	4(+)
80.0	20.0 - Cu	1880	1940	33 (near eutectic)	3
70.0	30.0 - Cu	1750	1860	29	3
60.0	40.0 - Cu	1675	1685	37 (very erosive)	3
50.0	50.0 - Cu	--	--	Very brittle	1
80.0	10.0 - Cu 10.0 - Ni	1700	1730	>46 (very brittle)	1
70.0	15.0 - Cu 15.0 - Ni	1650	1690	46 (erosive)	2
(3) <u>Ti-30V Base</u>					
90.0	10.0 - Cu	>2250	No Melt	31	4
85.0	15.0 - Cu	>2250	No Melt	37	4
80.0	20.0 - Cu	>2200	No Melt	37	4
70.0	30.0 - Cu	2020	>2200	37	3
60.0	40.0 - Cu	1830	~1975	39	3
50.0	50.0 - Cu	1850	~2075	31	2
70.0	15.0 - Cu 15.0 Ni	1950	>2070	42	3
(4) <u>Ti-50Zr Base</u>					
90.0	10.0 - Cu	1960	>2250	45	3
85.0	15.0 - Cu	1950	>2250	47	3
80.0	20.0 - Cu	1880	2020	47	3
70.0	30.0 - Cu	1635	1660	≥47	2
60.0	40.0 - Cu	1660	1680	Very brittle	1
50.0	50.0 - Cu	--	--	Very brittle	1
80.0	10.0 - Cu 10.0 - Ni	1725	>1880	43	2
70.0	15.0 - Cu 15.0 - Ni	1620	1675	38	2

^(a) Resistance to Crushing:

- (1) Brittle; easy to crush manually.
- (2) Marginally tough; moderately resistant to manual crushing.
- (3) Tough; strongly resistant to manual crushing.
- (4) Very tough; requires initial crushing on the hydraulic press.
- (5) Very tough and ductile; cannot be crushed. Requires drilling or rolling to obtain braze forms.

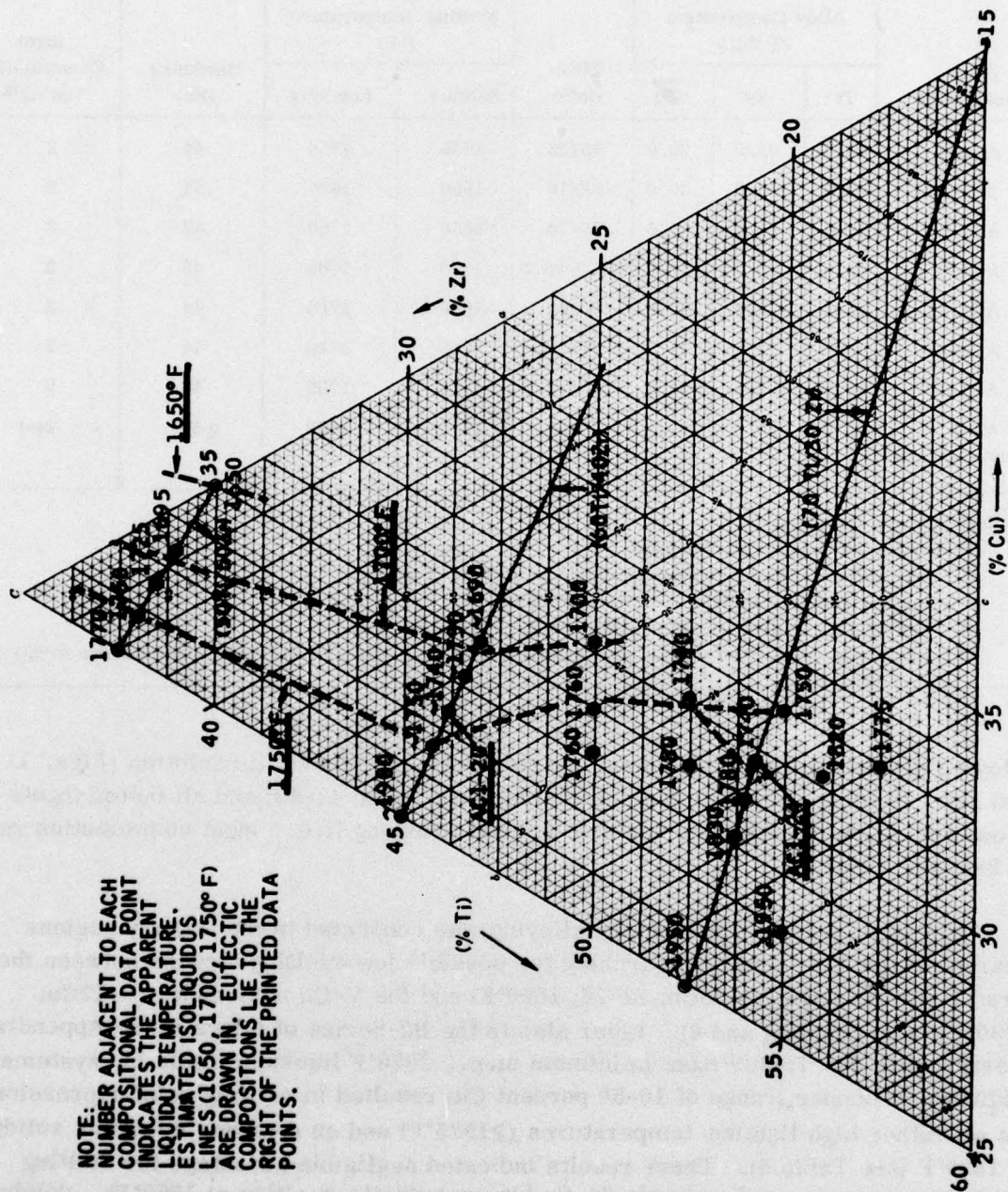


Figure 10. Portion of Ti-Zr-Cu Ternary Diagram

Table 9

PROMISING INITIAL BRAZE MATERIALS: Ti-Zr-Cu SYSTEM

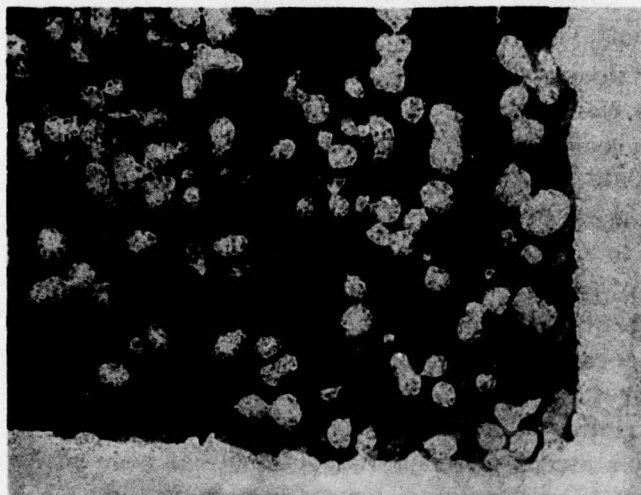
Alloy Designation	Alloy Composition (% Wt.)			Ti/Zr Ratio	Melting Temperature (°F)		Hardness (Rc)	Ingot Comminution Rating ^(a)
	Ti	Zr	Cu		Solidus	Liquidus		
AC1-8	46.0	25.0	29.0	65/35	1650	1760	44	2
AC1-1	42.0	28.0	30.0	60/40	1650	1690	44	2
AC1-2	49.0	21.0	30.0	70/30	1650	1760	42	3
AC1-9	45.0	25.0	30.0	64.5/35.5	1670	1760	45	2
AC1-11	47.5	22.5	30.0	68/32	1650	1780	44	2
AC1-12	46.0	22.5	31.5	67/33	1700	1740	44	2
AC1-10	43.5	25.0	31.5	63.5/36.5	1670	1700	43	2
A2-4 (near-eutectic)	35.0	35.0	30.0	50/50	1635	1660	≥ 47	2(-)

(a) Resistance to Crushing:

- (1) Brittle; easy to crush manually.
- (2) Marginally tough; moderately resistant to manual crushing.
- (3) Tough; strongly resistant to manual crushing.
- (4) Very tough; requires initial crushing on the hydraulic press.
- (5) Very tough and ductile; cannot be crushed. Requires drilling or rolling to obtain braze forms.

alloying series exhibit development of proeutectic terminal solid solution (Figs. 11 and 12). Hardnesses are in the acceptable range of Rc 42-45; and all button ingots showed fair to moderate resistance to manual crushing [i.e., ingot comminution ratings of 2-3 (see Table 8)].

Ti-V-Cu System. Exploratory alloying was conducted in the ternary regions nearest to the Ti-V binary, searching for possible low-melting troughs between the first Ti-Cu eutectic (Ti-36Cu; Rc 22; 1850°F) and the V-Cu monotectic (V-17Cu; 2790°F) (see Tables 4 and 8). Refer also to the B2-Series of alloys in the Appendix. Starting with the Ti-30V base (minimum m.p., 2950°F liquidus; Table 5), systematic additions of copper (range of 10-50 percent Cu) resulted in melting point depression, but all rather high liquidus temperatures (≥1975°F) and an apparent minimum solidus of 1830°F (see Table 8). These results indicated negligible advantage for melting point depression over the simple Ti-Cu binary eutectic (melting at 1850°F). Solidus-liquidus spreads in this region also were undesirably high. Although proving very tough in comminution studies, the Ti-V-Cu system alloys appeared too refractory to meet program melt-temperature objectives through further modification.



Moderately hypoeutectic braze structure, showing (light-etching) proeutectic "islands" (terminal Ti-Zr-Cu solid solution). No evidence of beta embrittlement, Ti-6Al-4V substrate.

Braze Tem: 1760°F
Magnification: 500X
Etchant: Kroll's

Figure 11. Microstructure of Ti-21.0Zr-30.0 Cu Brazement (AC1-2); T-Joint Intercept and Fillet Region



Strongly hypoeutectic braze structure, showing (dark etching) proeutectic dendrites (terminal Ti-Zr-Cu solid solution). Evidence of beta embrittlement, Ti-6Al-4V substrate.

Braze Temp: 2030°F
Magnification: 500X
Etchant: Kroll's

Figure 12. Microstructure of Ti-40.0Zr-20.0Cu Brazement (A2-3); T-Joint Intercept and Fillet Region

The Ti-Zr-Ni and Ti-Zr-Ni-Cu Systems. The first Ti-Ni eutectic (Ti-28.5Ni) is reported to melt $\sim 1750^{\circ}\text{F}$ (Ref. 14 and Table 4). Current experimentation has shown that this binary eutectic is brittle, and does not flow or form fillets well below $\sim 1900^{\circ}\text{F}$ (Alloy AC2-1/Appendix). Preliminary work with the Ti-50Zr base indicates a first eutectic point at approximately 20.0 percent Ni and $1700\text{--}1720^{\circ}\text{F}$ (Alloy AC2-3; Appendix). This eutectic is not very fluid between 1720°F to 1750°F , but the ingot structure is moderately resistant to manual crushing and therefore interesting. (Resistance to comminution was found to be a rare virtue in candidate braze alloys melting $\leq 1750^{\circ}\text{F}$). The circumstance of poor to marginal braze wetting and flow for both the binary (Ti-Ni) and ternary (Ti-Zr-Ni) eutectics, with both eutectic temperatures so close to the maximum process temperature limit, dictated a different alloying approach from that used with the Ti-Zr-Cu system. Consequently, work was undertaken to improve the brazing characteristics of this system by partial substitution of copper for nickel. (Copper is not only a strong m.p. depressant, but has been shown to confer excellent brazing characteristics, as in the Ti-Zr-Cu system.)

Experimental alloying with both nickel and copper additions to the Ti-50Zr base was carried out in the general compositional region between the [(Ti-50Zr) + 30Cu] near-eutectic (1635°F solidus/ 1660°F liquidus) and the [(Ti-50Zr) + 20Ni] near-eutectic (1700°F solidus/ 1720°F liquidus). Quaternary Ti-Zr-Ni-Cu compositions were designed and plotted on a pseudo-ternary diagram with termini of (Ti-50Zr), Ni, and Cu. [See Fig. 13 for a portion of this diagram, showing braze compositions of greatest interest.] A variety of Ni/Cu ratios were studied, inasmuch as there is no minimum m.p. in the Ni-Cu system. All quaternary alloy designs are given in the Appendix; Alloy Series A2 and AC5. Many of the quaternary alloys behaved very similarly to the Ti-Zr-Cu ternary eutectics, with regard to solidus and liquidus temperatures and short melt-down interval. Note the very flat liquidus surface (hovering about 1650°F) between alloy AC5-7 (12.5Ni, 12.5Cu), alloy AC5-2 (15.0Ni, 7.0Cu) and alloy AC5-3 (15.0Ni, 5.0Cu). Alloys in this compositional region possessed a very short interval between solidus and liquidus temperatures ($30\text{--}50^{\circ}\text{F}$), and exhibited excellent brazing characteristics, as hoped for with the Cu admixture. (See Table 10.) [With less than 5 percent Cu addition, brazing characteristics reverted to the sluggish flow and marginal filleting behavior of the Ti-Ni and Ti-Zr-Ni alloys mentioned above (see Fig. 13).] The major problem with the quaternary near-eutectic braze alloys described above (e.g., AC5-7) is marginal toughness, as measured by comminution resistance (see Table 10, where comminution ratings of 2 (-) were common). By intentionally altering the near-eutectic compositions to more strongly hypoeutectic designs (moving in the direction of the Ti-Zr terminus), notably tougher cast structures were developed without sacrificing any of the desirable brazing characteristics. [Typical alloys of this type are AC5-4, AC5-5, and AC5-21; with ingot comminution ratings (ICR) of 2; see Table 10 and Fig. 13.] Other promising candidate alloys of hypoeutectic design were obtained by systematically increasing the Ti/Zr ratio of the basic AC5-2 near-eutectic alloy, from the initial 50/50 (AC5-2; ICR = 2-) to 55/45 (AC5-14; ICR = 2), to 60/40 (AC5-15; ICR = 2+), then to 65/35

PORTION OF (50Ti/50Zr)-Ni-Cu QUATERNARY DIAGRAM (PSEUDO-TERNARY)

NOTE:
NUMBER ADJACENT TO EACH
COMPOSITIONAL DATA POINT
INDICATES THE APPARENT
LIQUIDUS TEMPERATURE.
ESTIMATED ISOLIQUIDUS
LINES (1650, 1700, 1750°F)
ARE DRAWN IN. ("B" INDICATES
A BRITTLE ALLOY.)
EUTECTIC COMPOSITIONS LIE
TO THE RIGHT OF THE 1650°F
ISOLIQUIDUS LINE (≥7% Cu)

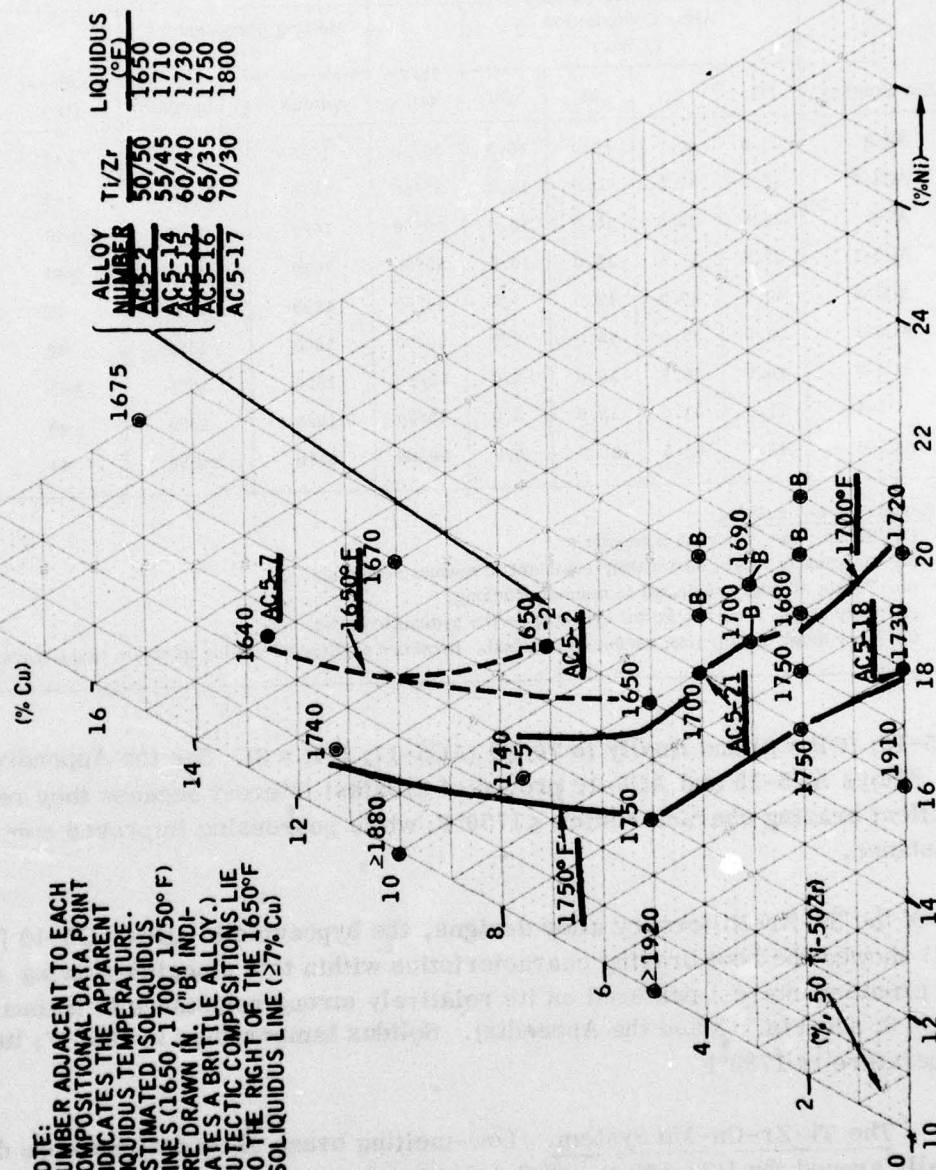


Figure 13. Portion of (50Ti/50Zr)-Ni-Cu Quaternary Diagram (Pseudo-Ternary)

Table 10
RESULTS OF PRELIMINARY SCREENING TESTS
THE Ti-Zr-Ni-Cu SYSTEM

Alloy Number	Alloy Composition (% Wt.)				Ti/Zr Ratio	Melting Temperature (°F)		Hardness (Rc)	Ingot Comminution Rating ^(a)
	Ti	Zr	Ni	Cu		Solidus	Liquidus		
A2-8	40.0	40.0	10.0	10.0	50/50	1725	1880	≥ 43	2(+)
AC5-7	37.5	37.5	12.5	12.5	50/50	1610	1640	≥ 44	2(-)
A2-5	35.0	35.0	15.0	15.0	50/50	1620	1675	≥ 45	2(-)
AC5-1	37.5	37.5	15.0	10.0	50/50	1625	1670	≥ 45	2(-)
AC5-5	40.0	40.0	12.5	7.5	50/50	1690	1740	47	2
AC5-2	39.0	39.0	15.0	7.0	50/50	1600	1650	42	2(-)
AC5-3	40.0	40.0	15.0	5.0	50/50	1600	1650	≥ 45	2(-)
AC5-4	41.0	41.0	13.0	5.0	50/50	1625	1750	≥ 46	2
AC5-6	42.5	42.5	10.0	5.0	50/50	1610	≥ 1920	44	2(+)

^(a) Resistance to Crushing:

- (1) Brittle; easy to crush manually.
- (2) Marginally tough; moderately resistant to manual crushing.
- (3) Tough; strongly resistant to manual crushing.
- (4) Very tough; requires initial crushing on the hydraulic press.
- (5) Very tough and ductile; cannot be crushed. Requires drilling or rolling to obtain braze forms.

(AC5-16; ICR = 3) and finally to 70/30 (AC5-17; ICR = 3). See the Appendix and Figure 13. Alloys AC5-15 and AC5-16 proved of greatest interest because they retained excellent brazing characteristics ≤ 1750°F; while possessing improved comminution resistance.

Of the Ti-Zr-Ni ternary alloy designs, the hypoeutectic alloy AC5-18 [(Ti-50Zr) + 18Ni] showed the best brazing characteristics within this sluggish-flowing system; with greatest interest centered on its relatively strong resistance to manual crushing (ICR = 3; see Fig. 13 and the Appendix). Solidus temperature is 1650°F; liquidus temperature is 1730°F.

The Ti-Zr-Cu-Mn System. Low-melting braze alloy designs were developed initially around the [(Ti-50Zr) + 30Cu] near-eutectic, with the objective of exploring for superior braze alloys (in terms of comminution resistance, lower braze temperatures and/or improved brazing characteristics) through partial substitution of manganese for copper, as melting-point depressant. (See the Ti-Zr-Cu Systems, above.) A variety of Cu/Mn ratios were evaluated around the (binary) minimum melting-point ratio of 65Cu/35Mn (~1600°F). In conjunction, Ti/Zr ratios were increased as high

as 80/20 in an attempt to obtain desired hypoeutectic behavior while maintaining liquidus temperatures $\leq 1750^{\circ}\text{F}$ (see the Appendix; Alloy Series AC6). Promising braze alloys in the quaternary Ti-Zr-Cu-Mn system were found in the region of 25-30 percent Cu, 8.3-10.0 percent Mn and Ti/Zr (base) ratios of 65/35 to 80/20 (Fig. 14 and see Alloy Series AC5; Appendix). Noticeable manganese volatilization was experienced in arc melting Cu-Mn master melts with Cu/Mn ratios $\leq 65/35$ (mixed with total charge). Best results were obtained with a high Cu/Mn ratio of 75/25 where there is definitely no problem of manganese volatilization, either in arc-melting or brazing. In fact, braze wetting, flow and filleting behaviors are among the very best noted for all braze candidates. Braze liquidus and minimum flow temperatures for the four superior hypoeutectic Ti-Zr-Cu-Mn alloys (selected for advanced screening tests) lie in the range, $1710\text{--}1750^{\circ}\text{F}$ (see Fig. 14 and the Appendix). The four Ti-Zr-Cu-Mn alloys are described in Table 11.

The major structural problem with the preferred Ti-Zr-Cu-Mn alloys is believed to be the extreme brittleness of their eutectic component and probably the intermetallic involved. This is reflected in the remarkably high alloy hardnesses (Table 11), and the notable brittleness of most alloys in and near the eutectic trough and in apparent hypereutectic regions (see Fig. 14). This, and possibly random ingot segregation, probably accounts for the marginal to sub-marginal comminution ratings obtained (Table 11).

The Ti-Cu-Ni System. Work on this system was restricted to two alloys because of the system's apparent refractoriness relative to the Ti-Zr-Cu, Ti-Zr-Ni-Cu, Ti-Zr-Ni, Ti-Zr-Cu-Mn and Zr-Ni-Cu systems previously described (see Tables 8 through 11). The two alloys investigated were Ti-10.0Cu-10.0Ni and Ti-15.0Cu-15.0Ni (the program baseline braze, "TICUNI"). (See Table 8 and alloys C2-8 and C2-5, respectively; Appendix.) The commercial brochure on foil TICUNI from WESGO (Ref. 5) indicates a liquidus or flow temperature of 1760°F ; however, the screening tests at Solar on alloy C2-5 indicate a liquidus temperature $>1950^{\circ}\text{F}$, and a minimum flow temperature of $1850\text{--}1890^{\circ}\text{F}$. At 1850°F the unmelted solid residue constitutes roughly 50 percent of total braze volume (see Fig. 15 which shows typical unmelted-braze residue on a lap-shear specimen brazement). This proved true for arc-melted button ingots of C2-5 crushed to $-12/+12$ mesh and -100 mesh powders, as well as for 2.0 mil thick TICUNI braze foil purchased from WESGO. The solidus temperature is $\sim 1750^{\circ}\text{F}$. TICUNI displays very good resistance to manual crushing ($\text{ICR} = 3$ to $3+$). This is undoubtedly due to the fact that it is a strongly hypoeutectic alloy, based upon the wide spread observed between solidus and liquidus temperatures (viz., 1750 to $>1950^{\circ}\text{F}$) and the typical strongly hypoeutectic microstructure (Figs. 16 and 17). When C2-5 is brazed at 1850°F , the Ti-6Al-4V substrate invariably shows beta-embrittlement structure overall (Fig. 16).

NOTE:
 NUMBERS ADJACENT TO EACH
 COMPOSITIONAL DATA POINT
 INDICATE APPARENT SOLIDUS/
 LIQUIDUS TEMPERATURES.
 ESTIMATED ISOLIQUIDUS
 TEMPERATURE LINES
 (1700, 1750° F) ARE DRAWN IN.
 EUTECTIC TROUGH IS IN THE
 GENERAL VICINITY OF THE
 1700° F ISOLIQUIDUS LINE.
 ("B" INDICATES A BRITTLE
 ALLOY.)

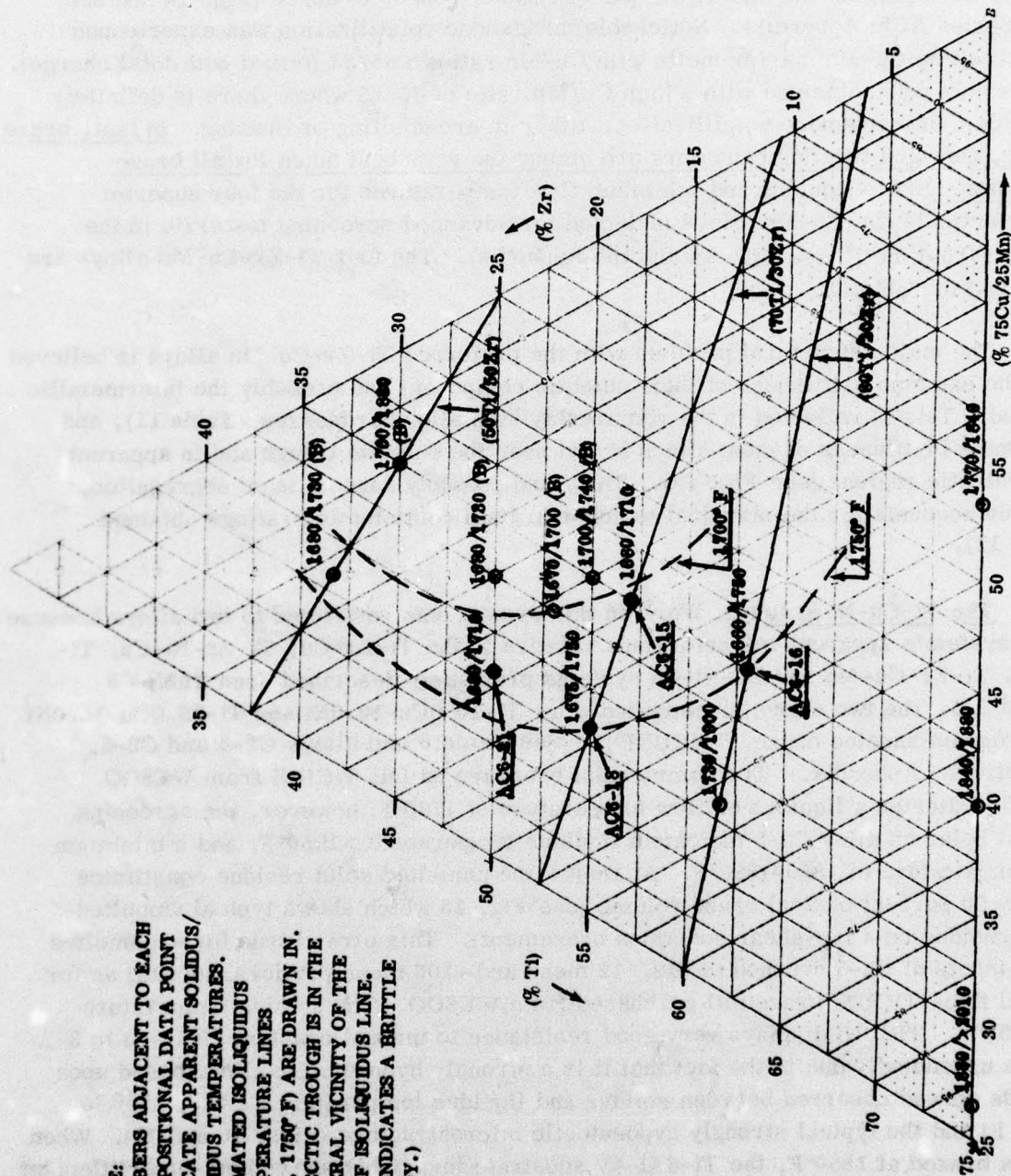


Figure 14. Portion of Ti-Zr-(75Cu/25Mn) Quaternary Diagram (Pseudo-Ternary)

Table 11

PROMISING INITIAL BRAZE ALLOYS: Ti-Zr-Cu-Mn SYSTEM

Alloy Designation	Alloy Composition (% Wt.)				Ti/Zr Ratio	Melting Temperature (°F)		Hardness (Rc)	Ingot Commination Rating ^(a)
	Ti	Zr	Cu	Mn		Solidus	Liquidus		
AC6-15	42.0	18.0	30.0	10.0	70/30	1680	1710	53	2 to 2(-)
AC6-16	48.0	12.0	30.0	10.0	80/20	1660	1750	53	2 to 2(-)
AC6-18	46.7	20.0	25.0	8.3	70/30	1675	1750	51	2 to 2(-)
AC6-21	41.7	25.0	25.0	8.3	65/35	1680	1710	49	2 to 2(-)

(a) **Resistance to Crushing:**

- (1) Brittle; easy to crush manually.
- (2) Marginally tough; moderately resistant to manual crushing.
- (3) Tough; strongly resistant to manual crushing.
- (4) Very tough; requires initial crushing on the hydraulic press.
- (5) Very tough and ductile; cannot be crushed. Requires drilling or rolling to obtain braze forms.

The Ti-Zr-Ni-Mn System. Low-melting braze alloy designs were sought within the Ti-Zr-Ni-Mn quaternary system in the vicinity of the sluggish [(Ti-50Zr) + 20 Ni] near-eutectic, with the objective of enhancing braze wetting, flow and filleting behavior; commination resistance and/or lowering melt and flow temperatures by partial substitution of manganese for nickel, as melting-point depressant. (See the Ti-Zr-Ni and Ti-Zr-Ni-Cu systems, above.) A variety of Ni/Mn ratios were evaluated around the (binary) minimum melting-point ratio of 39.5 Ni/60.5 Mn (~1870°F). (See the Alloy Series AC3; Appendix). It was learned that all quaternary alloys with ≥5% Mn were quite brittle, along a compositional tie-line connecting [(Ti-50Zr) + 18Ni] and [(Ti-50Zr) + 32.5Mn], on a pseudoternary diagram with termini of Ni, Mn, and (Ti-50Zr). Experimental alloys adjacent to the above tie-line on the side toward the Ti-Zr terminus, were all marginally tough or better (i.e., ICR ≥ 2); but all proved refractory, with liquidus temperatures apparently >>1850°F. The lowest solidus temperature recorded was 1780°F (AC3-8). Braze fluidity and filleting behaviors were uniformly poor, even for liquid fractions brazed >1800°F. Experimental alloys adjacent to the above tie-line, on the side toward the Mn and Ni termini, are all very brittle. Because of the general lack of promise exhibited by the Ti-Zr-Ni-Mn alloys, work on this quaternary system was suspended.

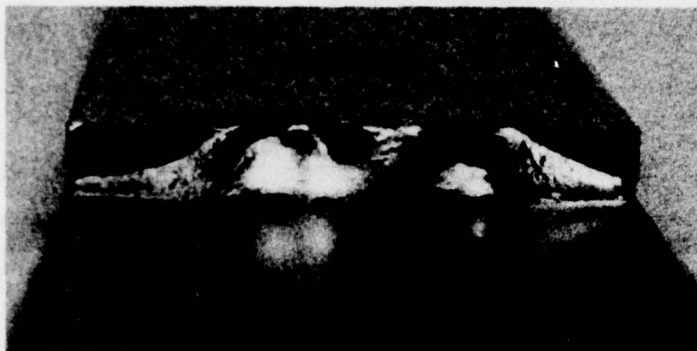
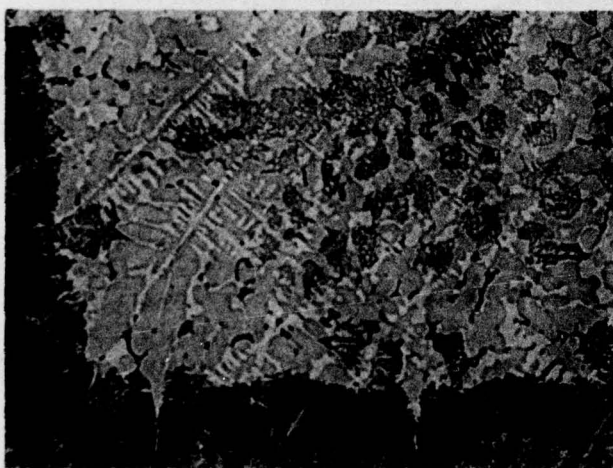


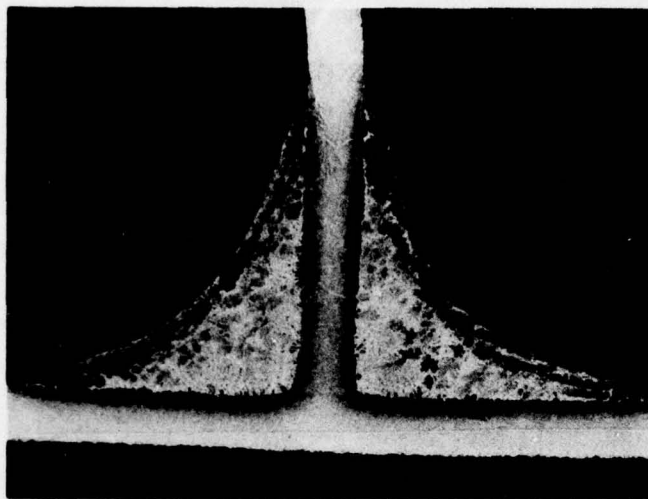
Figure 15. Lap-Shear Specimen Brazement, Made With Ti-15Cu-15Ni Alloy (Baseline)



Strongly hypoeutectic braze structure, showing (dark etching) proeutectic dendrites (terminal Ti-Cu-Ni solid solution). Note evidence of beta embrittlement structure, Ti-6Al-4V substrate.

Braze Temp: 1850°F
Magnification : 500X
Etchant: Kroll's

Figure 16. Microstructure of Ti-15.0Cu-15.0Ni Brazement: T-Joint Intercept and Fillet Region



Braze Temp: 1850°F
Magnification: 50 X
Etchant: Kroll's

Figure 17. Cross-Section of T-Joint Brazement Remote
From Unmelted Residue (Ti-15Cu-15Ni Braze Alloy)

Advanced Screening Tests

Work was directed at this point to more thorough screening and characterization of the most promising Ti- and Ti-Zr base braze-alloy designs identified thus far through preliminary screening, Phase I (Fig. 1). The screening test regime was expanded to include determination of single-lap tensile shear strengths (RT and 800°F), relative sensitivity to 800°F air-oxidation and 100°F salt-spray environments, brazing on Beta-C substrates, and metallographic analysis of braze structures. The number of candidate alloys was increased appreciably by this phase of work, through extensive exploratory alloying around those candidate hypoeutectic alloy compositions found most interesting during preliminary screening (See Section entitled "Hypoeutectic Alloy Designs", page 37 and Appendix). Concurrent screening by solidus-liquidus-flow temperature determinations and assessment of brazing characteristics and comminution resistance eventually reduced the total number of hypoeutectic braze candidates from ~200 (see Appendix) down to the 35 alloys with most promise and potential (See Table 12). These were the alloys subjected to advanced screening. The most critical appraisal was that concerning "braze characteristics", which constituted wetting, fluidity, fillet formation, and surface appearance. These performance characteristics and ratings naturally involve both objective and subjective considerations; the rankings becoming apparent after several braze runs. Representatives of each ternary and quaternary alloy system evaluated were included throughout this selection process, in order to permit continuing direct comparisons of the competing systems through the semi-final and final stages of alloy design. In this manner, the relative advantages and shortcomings of each alloy system were always in perspective. (Comparative baseline data are listed in Table 13.)

Table 12

**SUMMARY OF SCREENING TEST RESULTS (PHASE I) - SINGLE-LAP TENSILE
SHEAR TESTS (RT) - CANDIDATE BRAZE ALLOYS/AS-BRAZED CONDITION**

**Substrate Sheet Alloy: Ti-6Al-4V (0.062-Inch Thick) Duplex Annealed
Lap Joint: 2-t Overlap, 2-mil Faying Surface Clearance**

Brazing Alloy No.	Brazing Composition (Wt. %)	Ti/Zr Ratio	(ICR) Ingot Commutation Rating (a)	Characteristic Temperatures (°F) Solidus/Liquidus/Flow	Shear Stress and Fracture Location					
					Fracture (psi)			First Audible Crack (psi)		
					Process			Process		
					A	B	C	A	B	C
AC1-4 (Ti-Zr-Cu)	Ti-37.5Zr-25.0Cu	50/50	3	1640 1770 1800	28,600 ⁽¹⁾	29,500 ⁽¹⁾		14,400 ⁽¹⁾	16,000 ⁽¹⁾	
AC1-16 (Ti-Zr-Cu)	Ti-37.0Zr-26.0Cu	50/50	3	1680 1750 1780	27,900 ⁽¹⁾	28,000 ⁽¹⁾		15,800 ⁽¹⁾	19,800 ⁽¹⁾	
AC1-17 (Ti-Zr-Cu)	Ti-36.5Zr-27.0Cu Good flow and filletting	50/50	2	1640 1725 1760	29,800 ⁽¹⁾	29,100 ⁽¹⁾		11,800 ⁽¹⁾	21,100 ⁽¹⁾	
AC1-18 (Ti-Zr-Cu)	Ti-36.0Zr-28.0Cu Excellent flow and filletting	50/50	2	1620 1695 1710	30,600 ⁽¹⁾	30,000 ⁽¹⁾		13,200 ⁽¹⁾	19,900 ⁽¹⁾	
A2-4 (Ti-Zr-Cu)	Ti-35.0Zr-30.0Cu Excellent flow and filletting	50/50	2	1635 1650 1660	28,000 ⁽¹⁾	27,000 ⁽¹⁾		9,600 ⁽¹⁾	15,900 ⁽¹⁾	
AC1-20 (Ti-Zr-Cu)	Ti-28.8Zr-28.0Cu Excellent flow and filletting	60/40	3 (Rc 45)	1630 1740 1750	30,400 ⁽¹⁾ 32,400 ⁽¹⁾	27,400 ⁽¹⁾		16,000 ⁽¹⁾ 12,800 ⁽¹⁾	19,500 ⁽¹⁾	
AC1-21 (Ti-Zr-Cu)	Ti-28.4Zr-29.0Cu Excellent flow and filletting	60/40	3 (Rc 46)	1620 1730 1770	24,500 ⁽¹⁾	31,200 ⁽¹⁾		12,700 ⁽¹⁾	21,500 ⁽¹⁾	
AC1-1 (Ti-Zr-Cu)	Ti-28.0Zr-30.0Cu Excellent flow and filletting	60/40	2	1650 1690 1720	33,500 ⁽¹⁾	31,300 ⁽¹⁾		13,100 ⁽¹⁾	15,600 ⁽¹⁾	
AC1-8 (Ti-Zr-Cu)	Ti-25.0Zr-29.0Cu	65/35	2	1650 1760 1770	29,200 ⁽¹⁾	30,000 ⁽¹⁾		15,900 ⁽¹⁾	20,600 ⁽¹⁾	
AC1-9 (Ti-Zr-Cu)	Ti-25.0Zr-30.0Cu Excellent flow and filletting	64/36	2	1670 1760 1760	31,100 ⁽¹⁾	29,900 ⁽¹⁾		16,000 ⁽¹⁾	18,400 ⁽¹⁾	
AC1-10 (Ti-Zr-Cu)	Ti-25.0Zr-31.5Cu Excellent flow and filletting	63.5/ 36.5	2	1670 1700 1710	16,800 ⁽¹⁾	27,600 ⁽¹⁾		9,400 ⁽¹⁾	13,200 ⁽¹⁾	
AC1-11 (Ti-Zr-Cu)	Ti-22.5Zr-30.0Cu Excellent flow and filletting	68/32	2	1650 1780 1800	31,200 ⁽¹⁾	27,700 ⁽¹⁾		13,200 ⁽¹⁾	16,600 ⁽¹⁾	
(a) Resistance to Crushing:					Process A - Heavy braze load (0.120-0.140 gm); time at braze temperature, 20 seconds.					
1. Brittle; easy to crush manually.										
2. Marginally tough; moderately resistant to manual crushing.					Process B - Light braze load (0.010-0.020 gm); time at braze temperature, 20 seconds.					
3. Tough; strongly resistant to manual crushing.										
4. Very tough; requires initial crushing on the hydraulic press.					Process C - Light braze load (0.010-0.020 gm); time at braze temperature, 5 minutes.					
5. Very tough and ductile; cannot be crushed. Requires drilling or rolling to obtain braze forms.										
Fracture Location: (1) Braze fracture										
(2) Fracture through braze affected substrate										
(3) Base-metal fracture										

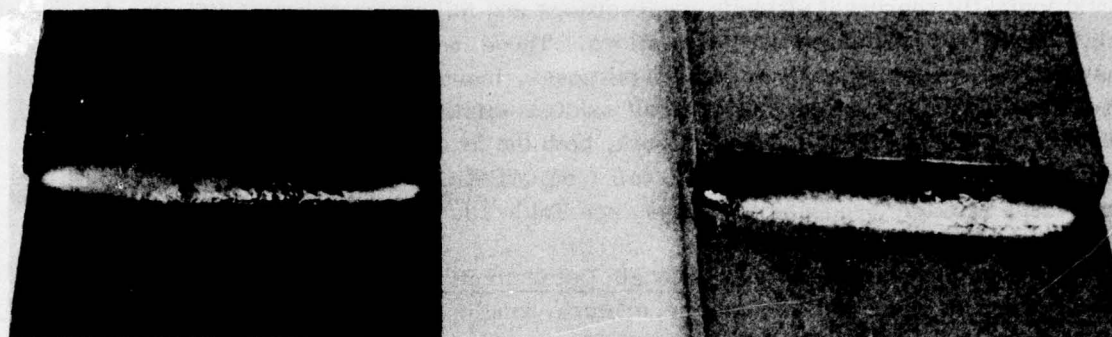
Table 12 (Contd)

Braze Alloy No.	Braze Composition (Wt. %)	Ti/Zr Ratio	(ICR) Ingot Commutation Rating (a)	Characteristic Temperatures (°F) Solidus/Liquidus/Flow	Shear Stress and Fracture Location					
					Fracture (psi)			First Audible Crack (psi)		
					Process			Process		
					A	B	C	A	B	C
AC1-12 (Ti-Zr-Cu)	Ti-22.5Zr-31.5Cu	67/33	2	1700 1740 1750	24,500 ⁽¹⁾	30,500 ⁽¹⁾		11,100 ⁽¹⁾	17,200 ⁽¹⁾	
AC1-2 (Ti-Zr-Cu)	Ti-21.0Zr-30.0Cu	70/30	3 (Rc 42)	1650 1760 1780	28,600 ⁽¹⁾ 25,600 ⁽¹⁾	28,600 ⁽¹⁾		17,300 ⁽¹⁾ 17,300 ⁽¹⁾	22,200 ⁽¹⁾	
AC1-24 (Ti-Zr-Cu)	Ti-20.7Zr-31.0Cu Excellent flow and filletting	70/30	3 (Rc 41)	1650 1740 1740-1760	29,500 ⁽¹⁾ 32,700 ⁽¹⁾	27,300 ⁽¹⁾ 27,700 ⁽¹⁾	26,200 ⁽¹⁾	19,000 ⁽¹⁾ 16,700 ⁽¹⁾	17,000 ⁽¹⁾ 19,700 ⁽¹⁾	24,100 ⁽¹⁾
AC1-13 (Ti-Zr-Cu)	Ti-20.0Zr-32.5Cu Excellent flow and filletting	70/30	2	1700 1750 1750	35,000 ⁽¹⁾	31,500 ⁽¹⁾ 30,000 ⁽¹⁾ 26,500 ⁽¹⁾	25,300 ⁽¹⁾	17,500 ⁽¹⁾	23,000 ⁽¹⁾ 13,900 ⁽¹⁾ 16,200 ⁽¹⁾	21,600 ⁽¹⁾
AC1-15 (Ti-Zr-Cu)	Ti-17.5Zr-32.5Cu Excellent flow and filletting	75/25	2	1740 1775 1775	30,500 ⁽¹⁾	30,500 ⁽¹⁾ 34,000 ⁽¹⁾	30,100 ⁽¹⁾	15,900 ⁽¹⁾	19,500 ⁽¹⁾ 19,100 ⁽¹⁾	18,100 ⁽¹⁾
A2-5 (Ti-Zr-Ni-Cu)	Ti-35.0Zr-15.0Ni-15.0Cu Good flow and filletting	50/50	2 to 2(-)	1620 1675 1690	30,100 ⁽¹⁾	30,200 ⁽¹⁾		16,000 ⁽¹⁾	23,400 ⁽¹⁾	
AC5-7 (Ti-Zr-Ni-Cu)	Ti-37.5Zr-12.5Ni-12.5Cu Excellent flow and filletting	50/50	2 to 2(-)	1610 1640 1650-1670	34,300 ⁽¹⁾ 36,200 ⁽¹⁾ --	30,800 ⁽¹⁾ 33,500 ⁽¹⁾		15,900 ⁽¹⁾ 13,600 ⁽¹⁾ 17,500 ⁽¹⁾	19,100 ⁽¹⁾ 15,100 ⁽¹⁾	
AC5-13 (Ti-Zr-Ni-Cu)	Ti-38.8Zr-11.2Ni-11.2Cu Fair to good flow and filletting	50/50	2	1650 1740 1790	25,300 ⁽¹⁾	36,800 ⁽¹⁾		17,900 ⁽¹⁾	18,100 ⁽¹⁾	
AC5-2 (Ti-Zr-Ni-Cu)	Ti-39.0Zr-15.0Ni-7.0Cu Excellent flow and filletting	50/50	2 to 2(-)	1600 1650 1650-1670	34,200 ⁽¹⁾ 34,800 ⁽¹⁾	33,700 ⁽¹⁾		14,000 ⁽¹⁾ 12,900 ⁽¹⁾	22,400 ⁽¹⁾	
AC5-3 (Ti-Zr-Ni-Cu)	Ti-40.0Zr-15.0Ni-5.0Cu Good flow and filletting	50/50	2 to 2(-)	1600 1650 1690	34,600 ⁽¹⁾	34,500 ⁽¹⁾		14,400 ⁽¹⁾	27,900 ⁽¹⁾	
AC5-15 (Ti-Zr-Ni-Cu)	Ti-31.3Zr-15.0Ni-7.0Cu Very good flow and filletting	60/40	2	1640 1730 1730-1765	35,500 ⁽¹⁾ 36,900 ⁽¹⁾	33,600 ⁽¹⁾		18,400 ⁽¹⁾ 14,400 ⁽¹⁾	19,800 ⁽¹⁾	
AC5-16 (Ti-Zr-Ni-Cu)	Ti-27.2Zr-15.0Ni-7.0Cu Excellent flow and filletting	65/35	3	1630 1750 1750-1780	34,800 ⁽¹⁾ 32,700 ⁽¹⁾	31,300 ⁽¹⁾	41,600 ⁽¹⁾	19,000 ⁽¹⁾ 16,000 ⁽¹⁾	20,300 ⁽¹⁾	24,300 ⁽¹⁾
AC5-19 (Ti-Zr-Ni-Cu)	Ti-40.0Zr-18.0Ni-2.0Cu	50/50	2	1640 1680 1740	35,300 ⁽¹⁾	33,300 ⁽¹⁾		18,400 ⁽¹⁾	15,600 ⁽¹⁾	
AC5-20 (Ti-Zr-Ni-Cu)	Ti-41.0Zr-16.0Ni-2.0Cu	50/50	2	1675 1750 1775	35,000 ⁽¹⁾	31,100 ⁽¹⁾		12,400 ⁽¹⁾	22,600 ⁽¹⁾	
AC5-21 (Ti-Zr-Ni-Cu)	Ti-40.0Zr-16.0Ni-4.0Cu Very good flow and filletting	50/50	2 to 2(+)	1640 1700 1700-1770	32,500 ⁽¹⁾ 31,500 ⁽¹⁾ --	30,600 ⁽¹⁾		20,000 ⁽¹⁾ 18,200 ⁽¹⁾ 20,500 ⁽¹⁾	19,800 ⁽¹⁾	

Table 12 (Contd)

Brazing Alloy No.	Brazing Composition (Wt. %)	Ti/Zr Ratio	(ICR) Ingot Commutation Rating ^(a)	Characteristic Temperatures (°F) Solidus/Liquidus/Flow	Shear Stress and Fracture Location					
					Fracture (psi)			First Audible Crack (psi)		
					Process			Process		
					A	B	C	A	B	C
AC5-22 (Ti-Zr-Ni-Cu)	Ti-40.5Zr-17.0Ni-2.0Cu Good flow and filletting	50/50	2	1640 1750 1775	34,800 ⁽¹⁾	31,000 ⁽¹⁾		16,900 ⁽¹⁾	16,200 ⁽¹⁾	
AC5-17 (Ti-Zr-Ni-Cu)	Ti-23.3Zr-15.0Ni-7.0Cu	70/30	3	1650 1775 1790	29,600 ⁽¹⁾	28,500 ⁽¹⁾		14,300 ⁽¹⁾	22,200 ⁽¹⁾	
AC2-3 (Ti-Zr-Ni)	Ti-40.0Zr-20.0Ni	50/50	3	1700 1720 1740	32,100 ⁽¹⁾	33,700 ⁽¹⁾		14,300 ⁽¹⁾	17,000 ⁽¹⁾	
AC5-18 (Ti-Zr-Ni)	Ti-41.0Zr-18.0Ni Good flow and filletting	50/50	3	1650 1730 1750	31,000 ⁽¹⁾ 32,400 ⁽¹⁾	29,000 ⁽¹⁾	34,700 ⁽¹⁾	15,800 ⁽¹⁾ 14,600 ⁽¹⁾	21,500 ⁽¹⁾	17,200 ⁽¹⁾
AC6-15 (Ti-Zr-Cu-Mn)	Ti-18Zr-30Cu-10Mn Excellent flow and filletting	70/30	2 to 2(-)	1680 1710 1710	34,700 ⁽¹⁾ 35,200 ⁽¹⁾			11,400 ⁽¹⁾ 11,800 ⁽¹⁾		
AC6-16 (Ti-Zr-Cu-Mn)	Ti-12Zr-30Cu-10Mn Excellent flow and filletting	80/20	2 to 2(-)	1660 1750 1750	32,500 ⁽¹⁾ 34,400 ⁽¹⁾			12,400 ⁽¹⁾ 12,800 ⁽¹⁾		
AC6-18 (Ti-Zr-Cu-Mn)	Ti-20Zr-25Cu-8.3Mn Excellent flow and filletting	70/30	2 to 2(-)	1675 1750 1750	34,900 ⁽¹⁾ 35,700 ⁽¹⁾			13,800 ⁽¹⁾ 13,700 ⁽¹⁾		
AC6-21 (Ti-Zr-Cu-Mn)	Ti-25Zr-25Cu-8.3Mn Excellent flow and filletting	63/37	2 to 2(-)	1680 1710 1710	30,800 ⁽¹⁾ 32,500 ⁽¹⁾			12,600 ⁽¹⁾ 13,500 ⁽¹⁾		

The following general comments can be made regarding the relative rankings of the 35 candidate alloys and 5 alloy systems listed in Table 12. Twelve alloying designs appeared superior in all or most respects. In the Ti-Zr-Cu system (Fig. 10), alloys AC1-20, AC1-21, AC1-2, and AC1-24 exhibited very good commutation resistances (ICR = 3), perhaps the best of all hypoeutectic alloys meeting the flow-temperature objective. High toughness levels and low hardnesses were later attributed to the lowest primary intermetallic contents of the subject brazing finalists (~23-29%, vol.; through metallography). Alloys AC1-20 and AC1-24 appeared to offer the best combination of desirable brazing characteristics, commutation resistance and high as-brazed shear strengths (Table 12). In the Ti-Zr-Ni-Cu system (Fig. 13), alloys AC5-7, AC5-2 and AC5-16 offer excellent brazing characteristics (well illustrated in Fig. 18), but superior commutation resistance only in the moderately hypoeutectic alloy AC5-16 (ICR = 3). Alloy AC5-16 displayed an outstanding combination of excellent brazing characteristics (perhaps the best of all in the advanced screening group), good commutation resistance and high shear strengths (Table 12). Fillets are extremely uniform and well-formed, and have a very smooth, mirror-like surface (Fig. 18), even after long-term environmental conditioning in 100°F salt spray or 800°F air. In spite of the marginal commutation resistances of the aforementioned near-eutectic alloys



After 100°F Salt Spray
(100 Hours)

After 800°F Air Oxidation
(100 Hours)

Alloy No. AC5-16
Ti-27.2Zr-15.0Ni-7.0Cu
Note Smooth Uniform Fillets

Figure 18. Typical Lap-Shear Specimen Brazements Made With No. AC5-16
Experimental Braze (1750°F)

(AC5-7 and AC5-2), they retained interest because of their very low melt and flow temperatures (1670°F) combined with high shear strength levels. Alloys AC5-15 and AC5-21 appeared to offer somewhat lower-melting (but similar-strength) alternatives to the promising AC5-16 alloy, which melts and flows in the high-limit range of 1750-1780°F. Both alloys AC5-15 and AC5-21 have very good brazing characteristics, and melt and flow in the ranges of 1730-1765°F and 1700-1770°F, respectively. Communion resistances of these two alloys were rated marginal (ICR = 2).

In the Ti-Zr-Ni system (Fig. 13), only alloy AC5-18 was rated as having adequately good brazing characteristics to warrant advanced screening. AC5-18 has good comminution resistance (ICR = 3) in spite of high intermetallic content (~45% vol.); and shear strengths comparable to the Ti-Zr-Cu and Ti-Zr-Ni-Cu alloys mentioned above (Table 12). AC5-18 is related generically to the better-flowing Ti-Zr-Ni-Cu alloys, and therefore of design interest. In the Ti-Zr-Cu-Mn system (Fig. 14), alloys AC6-15 and AC6-21 (1710°F) and alloys AC6-16 and AC6-18 (1750°F) revealed outstanding brazing characteristics, flowing and filleting superbly at their own liquidus temperatures. Brazing characteristics on all four are rated excellent and comparable to alloy AC5-16, the superior brazing alloy found in the Ti-Zr-Ni-Cu system (see Fig. 18). As-brazed shear strengths are uniformly high (Table 12). The common shortcoming of Ti-Zr-Cu-Mn alloys is marginal comminution resistance [ICR = 2 to 2(-)] (see Section entitled "Hypoeutectic Alloys Designs", page 37). Also included in the advanced screening group were several alloys with higher flow temperatures, in the range of 1850-1950°F, as comparison exemplars of more strongly hypoeutectic structures than those given in Table 12. The strongly hypoeutectic alloys

could logically represent ultimate compositions and microstructures of diffusion-brazed joints made with preferred candidate alloys. These inclusions also were felt to be justified for screening and comparison purposes, inasmuch as the strongly hypoeutectic Ti-15Cu-15Ni baseline braze alloy itself exhibits minimum flow temperatures of 1850-1890°F. In this advanced screening work, both the arc-melted baseline alloy (C2-5) in powder form and the 2-mil TICUNI foil from WESGO were evaluated. For results with these strongly hypoeutectic alloys, see Table 13.

Room Temperature Shear Strength Determinations (Correlations with Braze Ductility and Toughness). Room-temperature, single-lap shear strength tests were conducted to advance braze screening into the areas of relative mechanical strengths and ductilities (Tables 12 and 13). Single-lap tensile-shear specimens were fabricated with the principal process variables of braze loading and braze process time (Fig. 3 and Section III). Rather heavy conventional-placement braze loads were employed in the first test group (0.120-0.140 gms) resulting in fillet legs typically 0.040-0.050-inch long (Process A). Braze process time was intentionally kept short (~20 seconds) to minimize braze dilution and other possible braze/substrate interaction effects. The employment of heavy braze loads and short process times was designed to assess best the mechanical strengths and ductilities afforded by the essentially unreacted candidate braze structures. In the second and third test groups, the possibly beneficial aspects of braze dilution and braze/substrate interaction were emphasized by employing minimal (order-of-magnitude lower) braze loading, combined with short (20 seconds, Process B) or long (5 minutes, Process C) braze times. This was done to simulate diffusion-brazing processes. The minimal (conventional) braze loads of 0.010-0.020 gm are of the same order as braze loads used with the in-situ placement of WESGO "TICUNI" braze foil (Table 12). Fillet legs typically (only) 0.005-inch long were formed with these minimal braze loads.

Single-lap shear test specimens were fabricated and brazed with test section configuration per AWS Specification No. C3.2-63/60.105 (single exception - Ti-6Al-4V substrate alloy thickness was 0.062-inch rather than 0.125-inch, per sponsor's request). Overlap was controlled at 2-t (0.125-inch) and faying surface clearance at 0.002-inch. Strain rate over the shear area was maintained at 1.0×10^{-3} in./in./min. The single-lap tension test not only loads the braze joint progressively in shear, but exerts a significant bending or peel moment as well, which results in quite high peel stresses and surface strains (local; braze fillet region) as the joint rotates. Eccentric loading of the brazement derives from the fact that the tensile axis are not designed to be uniaxial (0.062-inch offset). (Joint rotation becomes increasingly apparent at nominal shear stresses $\geq 10,000$ psi. Permanent bend-deformation of the substrate sheet is obtained at nominal shear stresses ≥ 30 ksi.) This test then offers an assessment of relative braze ductility and strain accommodation (as well as braze strength) by measuring the nominal shear stress at which audible fillet cracking first occurs.

Table 13

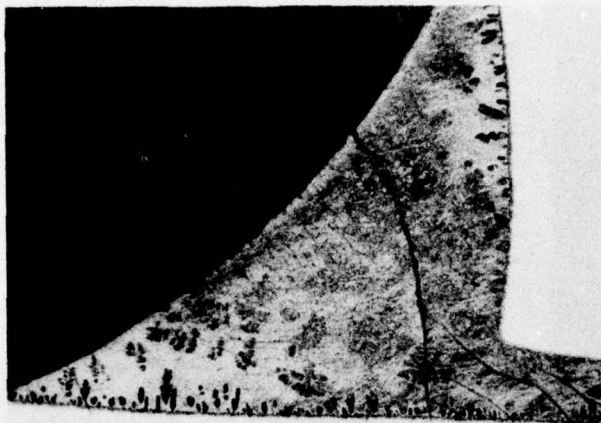
**SUMMARY OF SINGLE-LAP SHEAR TESTS (RT) - BASELINE AND STRONGLY
HYPOEUTECTIC BRAZE ALLOYS/AS-BRAZED CONDITION**

**Substrate Sheet Alloy: Ti-6Al-4V (0.062-Inch Thick) Duplex Annealed
Lap Joint: 2-t Overlap, 2-mil Faying Surface Clearance**

Braze Alloy No.	Braze Composition (Wt. %)	Ti/Zr Ratio	(ICR) Ingot 'Comminution' Rating ^(a)	Characteristic Temperatures (°F) Solidus/Liquidus/Flow	Shear Stress and Fracture Location					
					Fracture (psi)			First Audible Crack (psi)		
					Process			Process		
					A	B	C	A	B	C
C2-5 (Baseline) (Ti-Cu-Ni)	Ti-15.0Cu-15.0Ni	-	3 to 3(+)	1750 >1900 1850-1890	34,700 ⁽¹⁾ 36,700 ⁽¹⁾	35,400 ⁽¹⁾ 37,200 ⁽¹⁾		18,900 ⁽¹⁾ 13,100 ⁽¹⁾	28,100 ⁽¹⁾ 26,300 ⁽¹⁾	
WESGO TICUNI (Ti-Cu-Ni) Foil (2-mil) (Baseline)	Ti-15.0Cu-15.0Ni	-	-	1750 >1900 1850-1890	-	36,400 ⁽¹⁾ 37,600 ⁽¹⁾ (2)		-	36,000 ⁽¹⁾ 27,000 ⁽¹⁾	
C2-4 (Ti-Cu)	Ti-30.0Cu	-	5	1860 1880 1940	45,300 ⁽²⁾	40,800 ⁽¹⁾		34,800 ⁽¹⁾	36,500 ⁽¹⁾	
AC1-3 (Ti-Zr-Cu)	Ti-14.0Zr-30.0Cu	80/20	3	1650 1850 1870	38,200 ⁽¹⁾	34,600 ⁽¹⁾		19,700 ⁽¹⁾	24,000 ⁽¹⁾	
AC1-5 (Ti-Zr-Cu)	Ti-30.0Zr-25.0Cu	60/40	3 to 3(+)	1660 1880 1900	30,500 ⁽¹⁾	26,500 ⁽¹⁾		17,000 ⁽¹⁾	19,600 ⁽¹⁾	
C5-2 (Ti-Cu-Mn)	Ti-30.0Cu-10.0Mn	-	3 to 3(+)	1840 1880 1890	44,200 ⁽¹⁾	40,000 ⁽¹⁾		24,200 ⁽¹⁾	36,100 ⁽¹⁾	
AC2-2 (Ti-Zr-Ni)	Ti-42.0Zr-16.0Ni	50/50	3 to 3(+)	1750 1910 1950	35,200 ⁽¹⁾	30,500 ⁽¹⁾		24,500 ⁽¹⁾	22,000 ⁽¹⁾	
C6-2 (Ti-Cu-Si)	Ti-30.0Cu-3.0Si	-	4	1650 1900 1940	41,200 ⁽¹⁾	39,500 ⁽¹⁾		24,100 ⁽¹⁾	37,100 ⁽¹⁾	
(a) Resistance to Crushing: 1 Brittle; easy to crush manually. 2 Marginally tough; moderately resistant to manual crushing. 3 Tough; strongly resistant to manual crushing. 4 Very tough; requires initial crushing on the hydraulic press. 5 Very tough and ductile; cannot be crushed. Requires drilling or rolling to obtain braze forms.						Process A - Heavy braze load (0.120-0.140 gm); time at braze temperature, 20 seconds. Process B - Light braze load (0.010-0.020 gm); time at braze temperature, 20 seconds. Process C - Light braze load (0.010-0.020 gm); time at braze temperature, 5 minutes.				
Fracture Location: (1) Braze fracture (2) Fracture through braze-affected substrate (3) Base-metal fracture										

Additionally, relative resistance to catastrophic braze crack propagation at progressively higher stresses (above the stress for first cracking) becomes an indirect measure of braze toughness. For these reasons, braze fillet size was maintained uniform through equivalent braze loading; and the fillets were designed fairly large (~ 0.050 -inch leg) in the first test group, Process A, to preserve unreacted candidate braze structure in the fillet regions. As the unreacted braze fillet should possess the least hypoeutectic structure in the finished brazement, the lap-shear test (as described) becomes a stringent evaluation of the intrinsic ductility and strength of each candidate braze microstructure. Inasmuch as first fillet cracking was typically observed anywhere between about one-third to two-thirds the ultimate stress for brazement (i.e., braze joint) failure; and additional fillet cracking continued from this point on, the large fillets did not actually augment the effective joint area at the moment of failure over that obtained by the simple overlap consideration. This has been verified metallographically by examining fillet structures of shear specimens pulled only to the point of first audible cracking (Fig. 19 and 20). In spite of eccentric loading, there was not wide scatter noted in stress levels required to initiate cracking or to cause ultimate joint failure.

As a point of interest, the variable of braze loading was also found to influence the brazing characteristics of certain candidate braze alloys, some considerably more than others. With heavy braze loads, the ratio of braze-fillet volume to braze-joint volume (i.e., braze material located within the 2-mil gap zone) is $\sim 10/1$. With the light braze loads, which are probably somewhat more typical of actual braze practice, the same ratio is appreciably smaller, $\sim 10/25$. The strong capillary attraction afforded by the 2-mil gap tends to pull in liquid braze material, often as rapidly as it is formed, during braze heating above the solidus. Consequently, with light braze loads and moderate to strongly hypoeutectic braze alloys, significant liquid braze can be extracted (isolated) from the total braze load upon attainment of the solidus temperature, effectively disrupting the desired equilibrium between solid and liquid braze fractions in the fillet regions. The frequent end result is moderate to heavy residues of unmelted braze material at the normal liquidus temperature. Good examples are alloys with wide temperature interval between solidus and liquidus, such as AC1-4, AC1-8, AC1-2 and AC5-13. (With heavy braze loads, the influence of liquid-braze extraction upon solid-liquid equilibrium and effective liquidus temperature in the fillet region is logically not nearly so serious, because of the higher braze volume ratios mentioned.) Fortunately, it was found that certain hypoeutectic braze alloys (even with wide solidus/liquidus spreads) do braze consistently well, leaving no unmelted residues with light braze loading. The most reasonable explanation for this preferred behavior is that braze flow (into the joint capillary) is deferred until attainment of the liquidus temperature, possibly by the stronger capillary attraction of the braze alloy's own pro-eutectic solids. Good examples are AC1-20, AC1-11, AC1-24 and AC5-16 (Fig. 18). All of the 12 candidate braze alloys selected from the subject advanced screening studies for Phase II optimization work were shown to possess good to excellent brazing characteristics, even with light braze loads.



Magnification: 75X

Etchant: Kroll's



Magnification: 500X

Etchant: Kroll's

- Condition:**
- a) Loaded in shear to first audible crack (20,000 psi).
 - b) Loading increased to 26,000 psi (seven additional audible cracks); held 2 minutes under stress.
 - c) Unloaded; sectioned for metallography.

Note that (pre-failure) braze cracking is restricted to the fillet region and edge of faying surface joint.

Cracks are apparently arrested by the substrate BAZ, (Ti-6Al-4V) which shows no evidence of beta embrittlement.

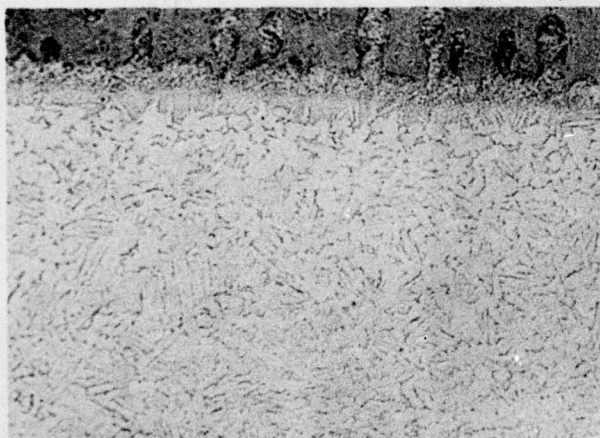
Figure 19. Microstructures of Braze Fillet Region; Single-Lap Shear Specimen Brazement, Braze Alloy AC5-21 (Ti-40Zr-16Ni-4Cu: 1770°F, 20 Seconds)



Magnification: 500X

Etchant: Kroll's

Braze



Note: Shear loaded to 25,500 psi without failure or cracking in faying-surface region. First audible cracking (fillet region) at 17,500 psi. Ti-6Al-4V substrate has retained the typical duplex annealed microstructure; no evidence of beta embrittlement. Braze eutectic structure is extremely fine.

Figure 20. Microstructures of Single-Lap Shear Specimen Brazement (Faying Surface Regions); Braze Alloy AC5-7 (Ti-37.5Zr-12.5Ni-12.5Cu; 1670°F, 20 Seconds)

To ascertain the probable maximum shear strengths obtainable from the candidate braze systems described, some very strongly hypoeutectic braze materials in these and related systems were also evaluated by lap-shear tensile testing (see Table 13). This group included the TICUNI baseline braze alloy. Their compositions and microstructures were chosen to simulate those developed in candidate alloy brazements due to substrate-braze interaction and dilution effects. Braze temperatures were in the range of 1850-1950°F.

Pertinent shear-strength data comparisons are as follows (Process A is discussed first; Tables 12 and 13). It is evident that taken together, the hypoeutectic braze candidates in the Ti-Zr-Cu system yield nominal shear strengths in the range of ~25,000-35,000 psi; those in the Ti-Zr-Cu-Mn, Ti-Zr-Ni and Ti-Zr-Ni-Cu systems, somewhat higher shear strengths more typically in the range of ~30,000-37,000 psi (Table 12). (Single exception; Alloy AC5-13 at 25,300 psi.) The maximum strength values are comparable (all systems; Processes A and B) to the strength ranges exhibited by the TICUNI baseline braze materials (Table 13). Shear strengths (Process A) of the 12 candidate braze alloys deemed most promising in the preceding commentary and repeated below* are all $\geq 30,000$ psi (range of ~30,000-37,000 psi), and were considered sufficiently close to the strength levels of the TICUNI baseline (~35,000-37,000 psi) and the other strongly hypoeutectic high-melting-point alloys studied (typically 35,000-45,000 psi, Table 13) to warrant continued development interest. The candidate braze alloys, additionally, braze some 100-200°F below the minimum braze temperature for TICUNI (1850°F), thus minimizing the likelihood of inducing beta embrittlement and grain coarsening in the Ti-6Al-4V substrate alloy.

Unfortunately, for the candidate alloys and baseline, there proved to be no sensitive, narrow-band, useful correlation between their nominal shear strengths (all were uniformly high) and comminution resistance as a measure of toughness (ICR's ranged from 2(-) to 3(+); or submarginal to very tough). This was true within each alloy system and overall (Table 14 and Fig. 21). Similarly, neither the average stress

*Tentative alloy selections for further screening work in Phase I and Phase II included the following twelve braze candidates: Alloy numbers AC1-20, AC1-24 (Ti-Zr-Cu); AC5-7, AC5-2, AC5-15, AC5-21 and AC5-16 (Ti-Zr-Ni-Cu); AC6-15, AC6-16, AC6-18 and AC6-21 (Ti-Zr-Cu-Mn); and AC5-18 (Ti-Zr-Ni) Table 12). These braze alloys were felt to offer the best combinations of good to excellent brazing characteristics (the first consideration), toughness as measured by crushing resistance, and potentials for mechanical strength and ductility. Strength and ductility potentials were believed especially good because these moderately hypoeutectic compositions possess the lowest levels of major melting-point depressants (Cu, Ni, Mn) and highest Ti/Zr ratios capable of providing acceptable braze characteristics (with light or heavy braze loads). These selections were approved by the sponsor at the completion of Phase I.

Table 14

COMPARISON OF NOMINAL RT SHEAR STRENGTH (a), STRESS FOR FIRST CRACKING (b), STRESS INTERVAL [(a) MINUS (b)], AND COMMINATION RESISTANCE FOR TWELVE PROMISING ALLOYS (PROCESS A)

Braze Alloy	(a) Nominal Shear Strength (Average) (psi)	(b) Stress for First Cracking (Average) (psi)	[(a) - (b)] Stress Interval Between First Crack and Fracture (psi)	Ingot Commination Resistance (ICR) (See Table XII)
C2-5 (baseline)	35,700	16,000	19,700	3 to 3 (+)
AC5-16	33,800	17,500	16,300	3
AC5-18	31,700	15,200	16,500	3
AC1-20	31,400	14,400	17,000	3
AC1-24	31,100	17,900	13,200	3
AC5-21	32,000	19,100	12,900	2 to 2 (+)
AC5-15	36,200	16,400	19,800	2
AC5-7	35,300	14,800	20,500	2 to 2 (-)
AC5-2	34,500	13,500	21,000	2 to 2 (-)
AC6-15	35,000	11,600	23,400	2 to 2 (-)
AC6-16	33,500	12,600	20,900	2 to 2 (-)
AC6-18	35,300	13,800	21,500	2 to 2 (-)
AC6-21	31,700	13,100	18,600	2 to 2 (-)

to induce first cracking nor the average stress interval between initial fillet cracking and ultimate joint failure, taken as a rough measure of the energy necessary to propagate the initial subcritical cracks to fracture, showed any logical or useful narrow-band correlation with commination resistance. (See Table 14 and Fig. 21.) The lack of correlation noted may be due to the obvious dissimilarity in strain rates between the two tests -- the shear strength tests conducted at a very slow strain rate of 1.0×10^{-3} in./in./min., requiring several minutes to induce cracking; contrasted with the shock loading of the ingot commination tests, resulting in cracking in less than a second. Consequently, testing for commination resistance (ICR) took on appreciably greater importance in subsequent Phase II work, as a more sensitive gage of cast-structure toughness, i.e., under the condition of high-rate, shock loading. Cast-structure toughness (ICR) appeared also to be the property most needy of improvement in most of the promising braze candidates (Tables 12 and 13) and this logically became the primary objective of Phase II, Optimization of Braze Structure (see section

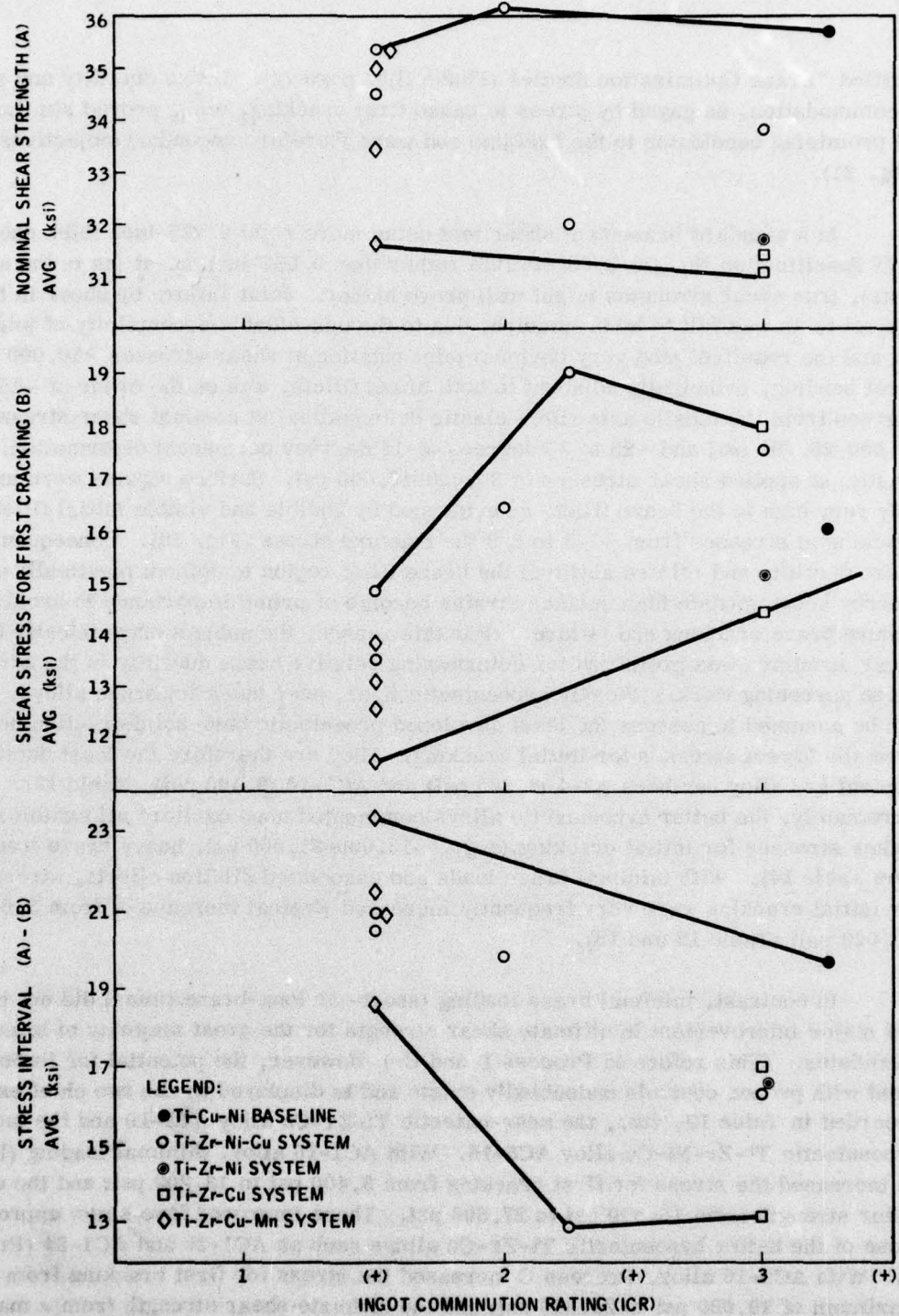


Figure 21. Variation in Shear Stress Parameters With Ingot Comminution Resistance (ICR)

entitled "Braze Optimization Studies (Phase II)", page 72). Braze ductility and strain accommodation, as gaged by stress to cause first cracking, etc., proved similar for all promising candidates to the baseline and were therefore secondary objectives (Fig. 21).

In a standard brazement shear test using more rigid 0.125-inch thick sheet (per AWS Specification No. C3.2-63/60.105) rather than 0.062-inch sheet (as in the subject tests), true shear strengths might well prove higher. Joint failure by shear in the subject tests was felt to be premature, due to the unavoidable eccentricity of joint loading and the resultant (and very obvious) joint rotation at shear stresses $\geq 10,000$ psi. Sheet bending, principally adjacent to both braze fillets, was on the order of ~ 15 to 20 degrees from the tensile axis (100% elastic deformation) at nominal shear stresses of 15,000-25,000 psi; and ~ 25 to 35 degrees (5-15 degrees permanent deformation, balance elastic) at applied shear stresses of 30,000-40,000 psi. Surface strains were undoubtedly very high in the braze fillet, as evidenced by audible and visible initial fillet cracking at stresses from $\sim 1/3$ to $2/3$ the fracture stress (Fig. 19). Consequently, braze ductility and related ability of the braze fillet region to deform plastically and thereby accommodate high surface strains become of prime importance to avoid premature braze cracking and failure. (For this reason, the subject eccentrically loaded shear specimen was preferred for determining relative braze ductility in the advanced braze screening work.) Weakly hypoeutectic (i.e., near eutectic) braze alloys, which can be assumed to possess the least developed proeutectic beta-solid-solution networks, show the lowest stresses for initial cracking. They are therefore the least ductile. Typical are alloy numbers A2-4 (9,600 psi) and AC1-10 (9,400 psi) (Table 12). Fortunately, the better hypoeutectic alloys commented upon earlier* all exhibit much higher stresses for initial cracking (e.g., $\sim 13,000$ - $21,000$ psi, heavy braze loading) (see Table 14). With minimal braze loads and associated dilution effects, stresses for initial cracking were very frequently increased (typical increase of from 3,000 to 10,000 psi) (Table 12 and 13).

In contrast, minimal braze loading (short- or long-braze times) did not induce any major improvement in ultimate shear strength for the great majority of braze candidates. (This refers to Process B and C.) However, the potential for improvement with proper controls undoubtedly exists and is displayed by the two chief exceptions, recorded in Table 12, viz., the near-eutectic Ti-Zr-Cu alloy AC1-10 and the moderately hypoeutectic Ti-Zr-Ni-Cu alloy AC5-16. With AC1-10 alloy, minimal loading (Process B) increased the stress for first cracking from 9,400 psi to 13,200 psi; and the ultimate shear strength from 16,800 psi to 27,600 psi. These improved levels now approach those of the better hypoeutectic Ti-Zr-Cu alloys such as AC1-20 and AC1-24 (Process A). With AC5-16 alloy, Process C increased the stress for first cracking from a maximum of 19,000 psi to 24,300 psi; and the ultimate shear strength from a maximum

*See footnote, page 59.

of 34,800 psi to 41,600 psi. These improved levels are now comparable to those of the best strongly hypoeutectic alloys (Process A; Table 13).

Environmental Conditioning and Elevated-Temperature Strength Tests. The twelve most promising braze alloy candidates discussed in the preceding section are characterized in Table 15, in terms of braze system; nominal compositions; solidus, liquidus and minimum flow temperatures; comminution resistance (ICR) and macro-hardness. These are the twelve braze alloys evaluated in the subject task for relative resistances to long-term 100°F salt-spray (ASTM Spec. B1117), long-term 800°F air oxidation, and determination of 800°F shear strengths. The actual effects of long-term environmental conditioning were assessed by visual examination and RT testing of single-lap tensile shear specimens. Tensile shear specimens for these evaluations were vacuum induction brazed for 20 seconds at minimum flow temperatures (Table 15), using heavy braze loading (equivalent and comparable to Process A of the preceding section). The substrate sheet alloy was Ti-6Al-4V.

Brazing characteristics of all 12 braze alloys in Table 15 have proven outstanding, with both rapid heating rates of 100-135°F/minute to the braze temperature (as in standard vacuum induction brazing tests and the subject specimen brazing runs) and in subsequent vacuum furnace brazing tests, at slower rates of 25-50°F/minute. Holding times up to 15 minutes at braze temperatures (1650-1750°F) have not resulted in any apparent grain growth or beta embrittlement in the Ti-6Al-4V substrate foils.

Table 16 lists the nominal RT shear strengths of the 12 candidate braze designs following 100 hours of 800°F air oxidation and 100 hours of 100°F salt spray, compared with corresponding strengths for the as-brazed condition (Process A, preceding section). The TICUNI baseline was evaluated in foil form, per sponsor request.

All braze alloys and lap shear specimen brazements have exhibited extraordinary resistances to 100°F salt-spray corrosion and 800°F air oxidation effects during programmed long-term environmental conditioning (Table 16). This was as anticipated. Retention of RT shear strengths, following both the referenced environmental conditioning regimes was excellent for all braze candidates (range of ~30 to 43 ksi), Table 16.

Candidate brazement shear strengths at RT (Ti-Zr-Cu, Ti-Zr-Ni, and Ti-Zr-Ni-Cu systems), following 100 hours air oxidation exposure at 800°F, typically increased ~5 to 15 percent over the as-brazed strength levels (Fig. 22). (The Ti-Zr-Cu-Mn alloys and the baseline alloy typically showed lesser changes. Average shear strengths were maintained ≥30 ksi and ≥35 ksi, respectively.) Curiously, 100 hours of 100°F salt spray exposure resulted in about the same range of minor increases in RT brazement strength for each affected alloy above, in the Ti-Zr-Ni, and Ti-Zr-Ni-Cu systems. (See Table 16.) Again, the Ti-Zr-Cu-Mn and baseline alloys were not

Table 15

CHARACTERIZATION OF RECOMMENDED BRAZE ALLOY DESIGNS (PHASE I)

Braze Alloy Designation	System	Nominal Composition (% Wt)	Characteristic Temperatures (°F)			(ICR) Ingot Communion Rating ^(a)	Ingot Hardness (Rc)	Ti/Zr Ratio (Base)
			Solidus	Liquidus	Minimum Flow (Brazing)			
AC6-15	Ti-Zr-Cu-Mn	Ti-18Zr-30Cu-10Mn	1680	1710	1710	2 to 2(-)	53	70/30
-16	Ti-Zr-Cu-Mn	Ti-12Zr-30Cu-10Mn	1660	1750	1750	2 to 2(-)	53	80/20
-18	Ti-Zr-Cu-Mn	Ti-20Zr-25Cu-8.3Mn	1675	1750	1750	2 to 2(-)	51	70/30
-21	Ti-Zr-Cu-Mn	Ti-25Zr-25Cu-8.3Mn	1680	1710	1710	2 to 2(-)	49	65/35
AC5-15	Ti-Zr-Ni-Cu	Ti-31.3Zr-15Ni-7Cu	1640	1730	1730-1765	2	47	60/40
-16	Ti-Zr-Ni-Cu	Ti-27.2Zr-15Ni-7Cu	1630	1750	1750-1780	3	46	65/35
-21	Ti-Zr-Ni-Cu	Ti-40Zr-16Ni-4Cu	1640	1700	1700-1770	2 to 2(+)	46	50/50
-7	Ti-Zr-Ni-Cu	Ti-37.5Zr-12.5Ni-12.5Cu	1610	1640	1650-1670	2 to 2(-)	44	50/50
-2	Ti-Zr-Ni-Cu	Ti-39Zr-15Ni-7Cu	1600	1650	1650-1670	2 to 2(-)	48	50/50
AC5-18	Ti-Zr-Ni	Ti-41Zr-18Ni	1650	1730	1750	3	46	50/50
AC1-20	Ti-Zr-Cu	Ti-28.8Zr-28Cu	1630	1740	1750	3	45	60/40
-24	Ti-Zr-Cu	Ti-20.7Zr-31Cu	1650	1740	1740-1760	3	41	70/30
C2-5 (Baseline)	Ti-Cu-Ni	Ti-15Cu-15Ni	1750	>1900	1850-1890 (Residue)	3 to 3(+)	38	--
WESGO "TICUNI" (2-mil foil) (Baseline)	Ti-Cu-Ni	Ti-15Cu-15Ni	1750	>1900 (In-Situ Brazing)	1850-1890	-	38	--

Notes: (a) Resistance to Crushing:

- (1) Brittle; easy to crush manually.
- (2) Marginally tough; moderately resistant to manual crushing.
- (3) Tough; strongly resistant to manual crushing.
- (4) Very tough; requires initial crushing on the hydraulic press.
- (5) Very tough and ductile; cannot be crushed. Requires drilling or rolling to obtain braze forms.

Table 16

COMPARATIVE LAP-SHEAR STRENGTH DATA
(As-Brazed Condition vs. Long-Term Environmental Exposures)
(Heavy Braze Loading) 2t Overlap, RT Tests

Braze Alloy	System	Composition (wt %)	Nominal Shear Strengths (ksi) [Duplicate Tests]		
			As-Brazed	After 100 hrs 100°F Salt Spray (5% NaCl)	After 100 hrs 800°F Air Oxidation
AC6-15	Ti-Zr-Cu-Mn (1710°F)	Ti-18Zr-30Cu-10Mn	34.7-35.2	32.7-32.8	31.9-32.6
AC6-16	Ti-Zr-Cu-Mn (1750°F)	Ti-12Zr-30Cu-10Mn	32.5-34.4	29.5-31.4	32.3-34.8
AC6-18	Ti-Zr-Cu-Mn (1750°F)	Ti-20Zr-25Cu-8.3Mn	34.9-35.7	30.4-31.4	34.4-35.5
AC6-21	Ti-Zr-Cu-Mn (1710°F)	Ti-25Zr-25Cu-8.3Mn	30.8-32.5	29.8-30.5	31.0-32.8
AC5-15	Ti-Zr-Ni-Cu (1730-1765°F)	Ti-31.3Zr-15Ni-7Cu	35.5-36.9	42.0-43.0	40.0-41.4
AC5-16	Ti-Zr-Ni-Cu (1750-1780°F)	Ti-27.2Zr-15Ni-7Cu	32.7-34.8	35.5-36.3	34.5-35.5
AC5-21	Ti-Zr-Ni-Cu (1700-1770°F)	Ti-40Zr-16Ni-4Cu	31.5-32.5	32.8-33.6	35.1-36.5
AC5-7	Ti-Zr-Ni-Cu (1650-1670°F)	Ti-37.5Zr-12.5Ni-12.5Cu	34.3-36.2	38.1-39.0	39.3-40.1
AC5-2	Ti-Zr-Ni-Cu (1650-1670°F)	Ti-39.0Zr-15Ni-7Cu	34.2-34.8	37.0-38.7	37.1-38.2
AC5-18	Ti-Zr-Ni (1750°F)	Ti-41Zr-18Ni	31.0-32.4	33.6-33.6	34.2-35.5
AC1-20	Ti-Zr-Cu (1750°F)	Ti-28.8Zr-28.0Cu	30.4-32.4	30.9-32.0	33.1-34.9
AC1-24	Ti-Zr-Cu (1740-1760°F)	Ti-20.7Zr-31Cu	29.5-32.7	34.3-34.5	35.5-36.4
TiCuNi foil baseline	Ti-Cu-Ni (1850°F)	Ti-15Cu-15Ni	36.4-37.6	35.6-36.7	36.1-36.1
Substrate Alloy: Ti-6Al-4V (0.062-inch thick) Braze Loading: 0.120 to 0.140 gm Common Brazing Procedure: Process A (All Braze Fractures)					

significantly affected (Fig. 22). Largest strength increases and highest RT strengths (both long-term exposures) were observed for the Ti-Zr-Ni-Cu alloys, especially AC5-15, (40.0 to 43.0 ksi), AC5-7 (38.1 to 40.1 ksi) and AC5-2 (37.0 to 38.7 ksi). (See Table 16 and Fig. 22.) [The TICUNI-foil baseline brazements, after both 800°F oxidation and 100°F salt-spray exposures, maintained essentially equivalent strength levels with the as-brazed condition (viz., ~36 to 37 ksi).] The underlying cause of the observed minor strength increases may be beta-matrix transformation effects, which were studied later (though indirectly) through post-braze thermal treatments in Phase II. In any event, brazement shear strengths were not adversely affected by long-term salt spray or 800°F air oxidation.

Of equal importance, none of the candidate or baseline braze alloys tested have shown any visible sign of structural deterioration due either to salt-spray exposure or 800°F oxidation exposure. Surface oxides developed on the braze fillet surfaces (800°F) are very light, uniform, continuous, coherent, and tenaciously adherent (see Fig. 18). (In all cases, oxidation of braze surfaces was less than substrate alloy oxidation; i.e., Ti-6Al-4V.) Braze fracture surfaces (after test) revealed no visible sign of internal oxidation. Braze surfaces after 100°F salt-spray exposure (and test) showed no evidence of general corrosion* or crevice corrosion, all surfaces retaining the bright metallic lustre of the as-brazed condition (see Fig. 18). Three other favorable aspects support the conclusion of general insensitivity of these similar-metal braze alloy designs to long-term environmental exposure (viz., 100°F salt spray and 800°F oxidation):

- No change in the apparent mode or locus of failure (invariably braze-line fracture)
- Little or no change in first-fillet-cracking behavior
- No reduction in RT joint strength due to exposure.

Elevated temperature brazement strengths were surveyed next. The shear strength data listed in Table 17 shows the variation in strength between RT and 800°F test temperatures for the 12 most promising braze alloy candidates. (Typical strength comparisons are illustrated in Figure 22.) All RT shear strengths (as-brazed condition) lie in the range of ~30 to 37 ksi, including the TICUNI foil baseline. Best strength retention, with the test temperature increased to 800°F, is exhibited by the TICUNI baseline and the two Ti-Zr-Cu system alloys, AC1-20 and AC1-24. (Strengths

*Exceptions: Light superficial staining on the fillet areas and environs of brazements made with the Ti-Zr-Cu alloys, AC1-20 and AC1-24.

Table 17
COMPARATIVE LAP-SHEAR STRENGTH DATA
(RT and 800°F)
(Heavy Braze Loading) 2t Overlap

Braze Alloy	System	Composition (wt %)	Nominal Shear Strengths (Duplicate Tests)	
			RT (ksi)	800°F (ksi)
AC6-15	Ti-Zr-Cu-Mn (1710°F)	Ti-18Zr-30Cu-10Mn	34.7-35.2	27.4-28.0
AC6-16	Ti-Zr-Cu-Mn (1750°F)	Ti-12Zr-30Cu-10Mn	32.5-34.4	28.7-29.3
AC6-18	Ti-Zr-Cu-Mn (1750°F)	Ti-20Zr-25Cu-8.3Mn	34.9-35.7	24.9-25.7
AC6-21	Ti-Zr-Cu-Mn (1710°F)	Ti-25Zr-25Cu-8.3Mn	30.8-32.5	25.6-28.7
AC5-15	Ti-Zr-Ni-Cu (1730-1765°F)	Ti-31.3Zr-15Ni-7Cu	35.5-36.9	24.2-25.0
AC5-16	Ti-Zr-Ni-Cu (1750-1780°F)	Ti-27.2Zr-15Ni-7Cu	32.7-34.8	24.4-25.3
AC5-21	Ti-Zr-Ni-Cu (1700-1770°F)	Ti-40Zr-16Ni-4Cu	31.5-32.5	22.8-24.4
AC5-7	Ti-Zr-Ni-Cu (1650-1670°F)	Ti-37.5Zr-12.5Ni-12.5Cu	34.3-36.2	22.6-22.8
AC5-2	Ti-Zr-Ni-Cu (1650-1670°F)	Ti-39.0Zr-15Ni-7Cu	34.2-34.8	22.5-24.4
AC5-18	Ti-Zr-Ni (1750°F)	Ti-41Zr-18Ni	31.0-32.4	23.4-24.1
AC1-20	Ti-Zr-Cu (1750°F)	Ti-28.8Zr-28.0Cu	30.4-32.4	30.5-30.7
AC1-24	Ti-Zr-Cu (1740-1760°F)	Ti-20.7Zr-31Cu	29.5-32.7	33.6-33.9
TiCuNi foil baseline	Ti-Cu-Ni (1850°F)	Ti-15Cu-15Ni	36.4-37.6	32.7-35.1
Notes: Common Conditions: As-brazed (Process A) Substrate Alloy: Ti-6Al-4V (0.062-inch thick) Braze Loading: 0.120 to 0.140 gm (All Braze Fractures)				

are retained ≥ 30 ksi.) With the Ti-Zr-Ni-Cu, Ti-Zr-Ni, and Ti-Zr-Cu-Mn braze alloys, 800°F shear strengths show moderate reductions to the ~ 22.6 to 29.3 ksi range.

A typical example of 800°F data is provided by the promising Ti-Zr-Ni-Cu alloy, AC5-16, which experienced a drop in average shear strength (as-brazed condition) from 33.8 ksi (RT) to 24.9 ksi (800°F). (see Fig. 22). However, in subsequent work (see section entitled "Phase III, Braze Characterization", page 112) it was learned that 800°F shear strengths for alloy AC5-16 could be maintained ≥ 30 ksi (range of 30-37 ksi), even after long-term salt-spray and 800°F air-oxidation exposures, merely by imposing a post-braze thermal treatment of 1.0 hour at 1025°F (high vacuum). [This vacuum thermal treatment was not originally imposed for the express purpose of improving 800°F strength, but only as a means of de-hydriding specimens after ECM machining.] Therefore, the potential does exist for restoration of 800°F brazement strengths through post-braze thermal treatment, and the examples of strength reduction noted above for the as-brazed condition should not be considered irreversible on the basis of this screening data. The strong indication that braze strength can be altered by short-term thermal treatment suggested also that beta-matrix instability might be a major determinant of braze toughness and ductility, as well as shear strength. This possibility was investigated systematically in Phase II, Braze Optimization (page 71). Oxidation effects were not particularly suspect for the subject strength reductions at 800°F, because:

- Long-term 800°F air oxidation had no significant effect on braze shear strength or ductility properties in prior tests at RT, where the embrittling effects of interstitial-solute contaminants (if present) should have been most pronounced (Table 16).
- Oxidation effects would be expected to affect adversely all of the compositionally-similar candidate braze alloys; instead, some were affected, and some not.

It should be remembered that the referenced single-lap shear tests (employed for screening) do not provide design data for pure shear; in fact, considerable joint rotation and progressive fillet cracking occur prior to joint failure in all cases, due to eccentric loading and high localized surface strains. (For example, at a nominal shear stress of ~ 30 ksi, plastic bend-deformation of the substrate sheet first becomes evident at and near the base of the lap-fillet, implying local substrate and braze fiber stress ≥ 120 ksi (Ref. 20). For screening purposes, these pre-failure phenomena are useful in monitoring and comparing individual braze capabilities for strain accommodation and resistance to peel cracking. However, joint failures invariably occur by a combination of peel and shear modes through the braze metal. Therefore, true "shear strengths" determined under uniaxial loading conditions might be expected to be ranged

somewhat higher than the 30-37 ksi (RT) and 23-34 ksi (800°F) recorded above. Reasonable expectations for limiting maximum shear strengths were derived from the aforementioned work of A. Freedman who conducted uniaxial shear tests on diffusion brazed Ti-6Al-4V specimens (viz., ~72 ksi at RT; ~56 ksi at 800°F). [True diffusion brazing studies and shear-strength determination under uniaxial loading conditions were not carried out in the subject work, as this was beyond the scope of our screening studies.]

Screening Tests With Beta-C Alloy Substrate. A final braze screening test was the trial application of the 12 candidate braze alloys to make single-lap shear specimens of 0.062 inch Beta-C alloy sheet. Brazing characteristics were uniformly excellent for all 12 braze candidates on Beta-C, with flow temperatures and behavior essentially identical to those observed with the Ti-6Al-4V alloy substrate. Comparative lap-shear strength tests (RT) were conducted using Beta-C sheet specimens, in both the as-brazed condition and after 100 hours exposure to salt-spray environment. Shear strengths for the as-brazed condition were in the typical range of 22-29 ksi, somewhat lower on average than those recorded for corresponding Ti-6Al-4V shear specimens (cf. Tables 16 and 18 and Fig. 22). The TICUNI foil baseline also developed lower shear strength with Beta-C (viz., 28 ksi versus 37 ksi). The anomalous strength increases associated sporadically with long-term salt-spray conditioning (see preceding section) improved the strengths of certain Ti-Zr-Ni-Cu, Ti-Zr-Cu and Ti-Zr-Cu-Mn alloys -- especially AC5-2 and AC1-24 -- but the overall range of strengths (21 to 30 ksi) remained about the same as before salt-spray conditioning. However, there was one notable high-strength exception, braze number AC5-16 (35.3 ksi, as-brazed; 43.8 ksi, after 100 hours salt spray, 100°F). Thus AC5-16 alloy proved superior all-around for both Beta-C and Ti-6Al-4V substrates. Also, braze alloys AC6-18, AC5-15, AC5-21, AC1-20 and the TICUNI foil baseline braze yielded RT shear strengths ≥ 27 ksi for both test conditions; i.e., as-brazed and after 100 hours of 100°F salt spray. These higher-strength braze alloys show most consistent promise for Beta-C joining.

Metallography failed to reveal any significant structural differences between the Beta-C brazements and the Ti-6Al-4V brazements tested previously. However, inasmuch as specimen braze failures for both substrate alloys invariably occurred through the braze-metal regions (all candidates), subtle differences in the degree of braze dilution, due to braze/substrate interaction, can logically be considered responsible for the noted shear strength differences.

Salt-spray conditioning of the Beta-C lap-shear specimens resulted in no discernible evidence of general corrosion or crevice corrosion on any candidate brazement. This was true even for the Ti-Zr-Cu alloys, AC1-20 and AC1-24, which had shown very light, superficial staining on Ti-6Al-4V substrates. First-cracking behaviors (Beta-C specimens) were essentially the same as for corresponding Ti-6Al-4V specimens.

Table 18

**COMPARATIVE LAP-SHEAR STRENGTH DATA (BETA-C SUBSTRATE ALLOY)
As-Brazed Condition vs. Long-Term Salt-Spray Exposure
(Heavy Loading; 2t Overlap; RT Test Temperature)**

Braze Alloy	System and Braze Temperature (°F)	Nominal Shear Strengths (ksi) (Single Test per Condition)	
		As-Brazed Condition	After 100 hrs, 100°F Salt Spray
AC6-15	Ti-Zr-Cu-Mn (1710)	24.5	24.7
AC6-16	Ti-Zr-Cu-Mn (1750)	25.2	28.1
AC6-18	Ti-Zr-Cu-Mn (1750)	27.2	29.2
AC6-21	Ti-Zr-Cu-Mn (1710)	23.2	21.4
AC5-15	Ti-Zr-Ni-Cu (1730-1765)	27.5	27.9
AC5-16	Ti-Zr-Ni-Cu (1750-1780)	35.3	43.8
AC5-21	Ti-Zr-Ni-Cu (1700-1770)	29.4	29.4
AC5-7	Ti-Zr-Ni-Cu (1650-1670)	25.3	28.1
AC5-2	Ti-Zr-Ni-Cu (1650-1670)	22.6	30.2
AC5-18	Ti-Zr-Ni (1750)	27.5	23.4
AC1-20	Ti-Zr-Cu (1750)	27.7	27.0
AC1-24	Ti-Zr-Cu (1740-1760)	21.6	26.2
TiCuNi foil baseline	Ti-Cu-Ni (1850°F)	28.2	30.8
Substrate Alloy: Beta-C (0.062-inch thick) Braze Loading: 0.120-0.140 gm (Process A) (All Braze Fractures)			

Metallography and Microhardness Surveys. Microstructural analyses were conducted principally during Phase II, Braze Optimization Studies and are therefore discussed under that heading below.

General Comments, End of Phase I

Exploratory alloying studies and selective screening tests had narrowed 300(+) candidate braze compositions down to the 12 semi-finalist braze designs listed in Table 15. These 12 hypoeutectic alloys consistently demonstrated superior conventional brazing characteristics with Ti-6Al-4V and Beta-C substrates (a primary criterion), combined with good RT strain accommodation and ductility (measured by nominal shear stress for first fillet cracking in single-lap tensile shear tests) and marginal-to-good levels of RT toughness (measured by relative resistance to ingot comminution). (In this context, "good" signifies levels comparable to the TICUNI baseline alloy.) All candidate alloys are of similar-metal design, and all displayed extraordinary resistances to structural deterioration and shear-strength impairment related to long-term exposures in 100°F salt-spray or 800°F air oxidation. Shear strength levels of all semi-finalist candidates at 800°F also were fair-to-good, relative to RT strength levels (and baseline levels). The common characteristic most in need of improvement or optimization (Phase II) was RT toughness, as gaged by resistance to (high-strain-rate) ingot comminution. From an overall viewpoint (at this stage), the two braze alloys with most outstanding promise were AC5-16 (Ti-Zr-Ni-Cu system) and AC1-20 (Ti-Zr-Cu system).

BRAZE OPTIMIZATION STUDIES (PHASE II)

At the commencement of Phase II work, the twelve semi-final braze alloy designs (Fig. 1 and Table 15) had passed advanced screening tests, but were not regarded as finished or optimized braze materials, either as to composition or processing. The purpose of Phase II was to attempt correction of structural shortcomings made evident in Phase I work, through minor alloying variation, alteration in braze processing, and/or post-braze thermal treatment. Particular emphasis was placed upon improving cast-structure toughness, as gaged by relative resistance to (high-strain-rate) ingot comminution, i. e., "ICR", see Section 3. As discussed in the section entitled "Braze Alloy Design and Screening (Phase I)", page 31, ingot comminution resistance (RT) was the common candidate property most in need of enhancement, relative to the TICUNI baseline alloy; and was also, in fact, a more sensitive gage of cast-structure toughness than the various shear-strength parameters evaluated in Phase I. Figure 23 illustrates the principal tools involved in manually determining ingot comminution resistance of 5 gram arc-melted button ingots.



Note relative size of 5-gm button ingot.

Figure 23. Steel Mortar and Pestle Used to Determine ICR

Braze Design Problems and Possible Solutions

In the semi-final alloy designs, principal melting point depression is provided by the beta-eutectoid-type alloying agents, copper (Cu), nickel (Ni), and manganese (Mn), used singly or in combination (see basic problem discussion, page 14). In simple binary combinations with the titanium base, all characteristically exhibit both eutectic and eutectoid formation, with appreciable associated generation of hard intermetallic compounds (the first structural problem). Primary intermetallics constitute from 23 to 49 percent by volume of the subject braze structures (see section entitled "Post-Braze Thermal Treatments", page 76).

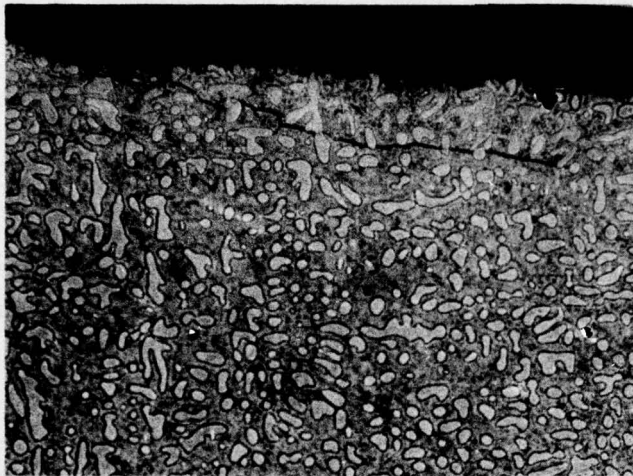
Only minor melting point depression is provided by the beta-isomorphous agent, zirconium, but this minor contribution appears essential to obtain the total depression required (i.e., for brazing $\leq 1750^{\circ}\text{F}$). However, all of the alloying agents used in this study (Zr, Cu, Mn, Ni) are strong beta-phase stabilizers; with the total beta stabilization in each of the 12 subject braze alloys undoubtedly much stronger than in any commercial beta-stabilized alloy. It might be ideal from a braze ductility-and-toughness viewpoint if the beta-phase could be retained untransformed; but this is not very plausible when considering adaptability to long-term 800°F service. However, it does force consideration of the (optimum) beta-transformation process, which constitutes the second structural problem. Although the beta-transformation characteristics of the subject alloys are not known, possible products (of an adverse nature) could include transition or meta-stable structures such as omega phase or autoaged martensite (α''), and/or

near-equilibrium structures such as fine precipitates of alpha and intermetallic compound(s) in partially transformed beta. (A plausible third structural problem related to partial beta transformation might be partitioning and concentration of interstitial-element contaminants into relatively small volumes of alpha-phase product.) To circumvent and/or alleviate these hard, potentially embrittling structures then was the main underlying theme of Phase II (Braze Structure Optimization).

Because of two key observations made early in the microstructural examination of crushed braze ingot (Phase II), and another earlier macrostructural observation from Phase I, work was concentrated first upon isothermal aging studies over a range of temperatures (viz. 800 to 1400°F) in the proximate vicinity of estimated beta-eutectoid temperatures of the candidate alloys (see Table 19). The purpose was to determine post-braze thermal treatments which best promote (for each alloy) equilibrium transformation of matrix beta culminating in the softest (and toughest) possible transformation structure. The apparently dominant role of matrix beta in controlling brazement ductility and "toughness" was inferred from the following three observations. First, in prior tensile-shear tests of lap-joint brazements (Phase I; RT and 800°F), initiation and primary propagation of shear cracking invariably occurred within the microcast (i.e., as-brazed) braze structures (Fig. 19). Secondary (tributary) cracks were observed to be arrested by the braze-affected-zone structures (BAZ) for both program substrate alloys; Ti-6Al-4V and Beta-C (Fig. 19 and section entitled "Braze Alloy Design and Screening (Phase I), page 31). Therefore, it was apparent that the as-cast braze structures inherently possess the least useful ductilities and strain-accommodation capabilities of the three principal structures in each brazement; viz. the annealed substrate alloy, the BAZ, and the cast braze structure. A second important general observation was made early in Phase II during thorough metallographic examination of crushed braze ingot (simulating massive as-brazed structures). It was that propagation of primary and secondary comminution cracks occurs preponderantly through the (proeutectic) beta-matrix phases, and not through or along the intermetallic networks or their boundaries. In fact, comminution cracks often appeared to be arrested upon encountering massive intermetallics (see Figs. 24, 25, 25). All of this suggested that the weakest, most vulnerable structural link (common) in shear fracture and in comminution cracking is the quasi-continuous beta-matrix phase; and optimization studies should logically start with attempts to ductilize this structural component. A third general observation made early in Phase II was that most as-cast braze structures are typically quite hard (e.g., Knoop 475-510) and normally prove significantly harder than most equilibrium-aged braze structures studied (of the same alloy chemistry). (Braze alloy hardness also varied markedly with different isothermal aging temperatures.) (Table 19). Indirectly, this suggested that the terminal solid-solution matrix phases have the potential to undergo undesirable modes of beta transformation on solidification and rapid cooling from the brazing (or casting) temperatures to RT. The capacity for appreciable transformation hardening on holding below estimated

DATA FROM POST-BRAZE ISOTHERMAL AGING STUDY (PHASE II)

- 3) Kneads 500 gms (K50N)
- 4) 100% Crumb
- 5) 1. Brittle; easy to crush manually.
- 6) 2. Marginally tough; moderately resistant to manual crushing.
- 7) 3. Tough; strongly resistant to manual crushing.
- 8) 4. Very tough; requires initial crushing on the hydraulic press.
- 9) 5. Very tough but ductile; cannot be crushed. Requires friction or rolling to obtain briare forms.
- 10) 6. Common Aging Cycle: (Frocam)
1600° F., 1/2 hour, F. C. to 1400° F. (in preheaters); 24 hours, F. C. to R. T.
Based upon aged oilfines (microprecipitate striations with active temperatures)



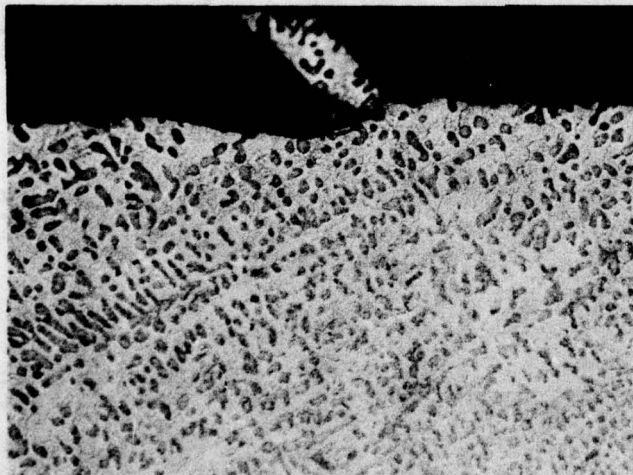
Alloy AC1-20 (Ti-Zr-Cu)
Matrix phase etches light,
primary intermetallic dark

Etchant: Kroll's (+)H₂O₂

Magnification: 500X

(See Note Below)

Figure 24. Primary Comminution Crack Surfaces (Edge Mounts) in As-Cast Braze Alloys



Alloy AC5-16 (Ti-Zr-Ni-Cu)
Matrix phase etches dark,
primary intermetallic light

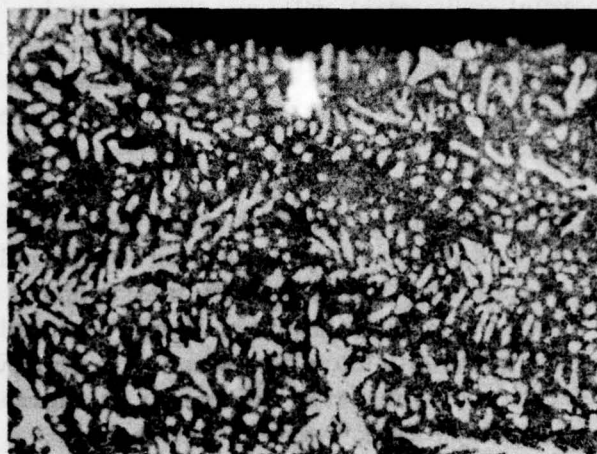
Etchant: Kroll's (+)H₂O₂

Magnification: 500X

(See Note Below)

Figure 25. Primary Comminution Crack Surfaces (Edge Mounts) in As-Cast Braze Alloys

NOTE: Note that the primary crack surfaces (edges) occur predominately along the matrix phases (primary intermetallics remain uncracked). The secondary comminution crack in Alloy AC5-16 also initiated and propagated within the matrix phase. The crack skirted nodular intermetallic particles in its path, and was apparently terminated by one.



Alloy AC6-16 (Ti-Zr-Cu-Mn)
Matrix phase etches dark,
primary intermetallic light

Etchant: Kroll's (+)H₂O₂

Magnification: 500X

(See Note, Page 75)

Figure 26. Primary Comminution Crack Surfaces (Edge Mounts)
in As-Cast Braze Alloys

beta eutectoid temperatures was also strongly indicated, for certain aging temperature ranges (Table 19). These corroborative observations all tended to support the general advisability of controlling beta decomposition processes post brazing and prior to service.

Post-Braze Thermal Treatments

This work addressed the first and second structural problems described in the section entitled "Braze Design Problems and Possible Solutions", page 72. The critical problem of determining optimum beta-matrix transformations was studied first. Three different approaches to design of post-braze heat treatment were considered in Phase II. First, intermediate- to long-term holding at sub-eutectoid temperatures (directly after brazing and cooling to RT) might be applied to attempt general coarsening, softening and overaging of autoaged α' , omega or other hypothetical transition structure, assuming undesirable transition products to be the primary problem. Matrix transition structures in commercial titanium alloys are often quite persistent and fine, however, so that even when softening by thermal treatment is obtained, improvement in ductility frequently is not a co-result (Ref. 22). A second approach would attempt to circumvent undesirable transition structures by initially heating to a beta-solution temperature above the eutectoid, post-brazing, followed by furnace cooling to and long-term isothermal holding at a select sub-eutectoid temperature to obtain soft, coarse-structured equilibrium beta-decomposition products. A further benefit anticipated from beta-solutioning (e.g., at 1400°F) as in the subject work) is the chemical homogenization and stress-relief of the cast beta matrix, to promote a more uniform beta-transformation structure on isothermal aging. This

second approach appeared to have advantages, and was the one evaluated in initial studies (see Isothermal Aging Studies, this section). It was recognized that any untransformed beta retained after isothermal aging might still have the potential to transform to undesirable transition structures on subsequent cooling to RT, or later during periods of elevated temperature service and/or stress. Therefore, the optimum post-braze thermal treatment might consist of a combination of the second approach with the first approach.

Precipitation of intermetallic compound(s) can be expected within the matrix phase during the eutectoid decomposition of beta (as for example, during isothermal aging below the eutectoid temperature). If dislocation mobility in the matrix phase is hampered by a fine, intense dispersion of intermetallic precipitate, it was reasoned that a corrective third heat-treatment approach might also prove effective in improving matrix ductility. To this end, post-braze cyclic annealing treatments at alternate temperatures just above and just below each alloy's eutectoid temperature were programmed to coalesce and spheroidize intermetallic particles, hopefully, to the degree required to confer improved ductility. Cyclic annealing here would be somewhat analogous to certain spheroidization treatments used commercially to coalesce carbides in steels (pearlite eutectoid) or the spheroidization of lamellar cast beryllide structures in Ti-Zr-Be and Ti-Zr-Ni-Be braze alloys (Refs. 23 and 24). This third heat-treatment approach addressed both the first and second structural problems defined in the section entitled "Braze Design Problems and Possible Solutions", page 72.

Of actual pertinence to program objectives, the resistances to comminution of four of the Ti-Zr-Ni-Cu system braze alloys were significantly increased above the as-cast ratings by isothermal aging in the vicinity of the beta-eutectoid temperatures; viz. AC5-18 (1050°F), AC5-16 (1025 and 1050°F), AC5-15 (1025°F) and AC5-21 (1025 and 1050°F). (Details are given under Isothermal Aging Studies, this section.) All four alloys were rated "tough; strongly resistant to manual crushing" after isothermal aging under the above conditions (see Table 19). (Alloys AC5-16 and AC5-18 were given ICR ratings of 3(+), post-aging; high levels of toughness equivalent to the C2-5 baseline alloy.) The best previous ratings for AC5-21 and AC5-15 were "marginally tough; moderately resistant to manual crushing". Although these comminution ratings are based upon semi-quantitative measures of energy input to initiate ingot cracking, they have proved to be very reproducible and reliable gages of cast alloy toughness in the subject screening studies.

Isothermal Aging Studies. The following is a discussion of results obtained using post-braze isothermal aging treatments (second approach, described in the preamble of the section entitled "Post-Braze Thermal Treatments", page 76) to alter cast microstructure in the direction of improved braze ductility and toughness. Arc-melted 5 gm button ingots of each candidate braze alloy were used to simulate (and isolate) as-brazed braze structures, and to facilitate both heat-treatment and comminution studies and

subsequent metallographic examination of braze structures, unaffected by braze/substrate interaction. Crushed ingot chunks were examined metallographically after comminution testing (both as-cast and after thermal treatment) in an attempt to correlate microstructural features with both primary (new surface) and secondary (internal) comminution cracks. Post-braze thermal treatments showing the most promise, in terms of reduced braze hardness and/or improved resistance to comminution were identified. Lap-shear tests of brazements (RT) were also conducted to determine the possible beneficial influence of post-braze thermal treatment upon braze strain-accommodation and strength properties.

Vacuum heat treatment of braze ingot started with common beta-solutioning at 1400°F, 1/2 hr., followed by furnace hold or cool to a select isothermal aging temperature in the range, 800 to 1400°F, and then isothermal holding for 24 hours. Beta decomposition to equilibrium products on isothermal holding below the eutectoid temperature probably proceeds very sluggishly, and may reasonably require from 2-5 hours for initiation and 10-20 hours for appreciable partial transformation, even at the equilibrium transformation "nose" temperature(s) (Ref. 10). Because neither the true eutectoid temperatures (estimated range, 910 to 1290°F; Table 19) nor the TTT transformation "nose" temperatures are known, 25-100°F temperature intervals were used within the 800-1400°F range in the aging study. It was reasoned that the chances for omega formation would be minimized by aging at or above 800°F, as would the chances for martensite formation in the subject, highly-beta-stabilized matrices (Refs. 10 and 25 and Section 2).

Isothermal aging data are listed in Table 19 and plotted in Figures 27 through 32. Anticipated patterns of microhardness versus aging temperature were obtained for the Ti-Zr-Cu-Mn series alloys (AC6-15, -16, -18, -21; Figs. 27 and 28). Hardness minimums (range of 434-451 Knoop; significantly below as-cast hardness levels) were obtained by aging at 1025°F, just below estimated beta eutectoid temperatures. Metallography did not reveal any specific structural basis for the noted softening, but it is assumed due to extensive equilibrium transformation of beta matrix, under conditions which induce thermal overaging and avoid hard, undesirable transition products. Hardnesses typically rise steeply on either side of the hardness minimum for each alloy, presumably due to more intense and stable aging effects (lower aging temperatures) and reformation of hard transition products on cooling (higher aging temperatures, above the eutectoid). Generally, the higher the aging temperature in this latter region, the lower the hardness on cooling, possibly due to increased matrix enrichment and stabilization of (homogeneous) beta with temperature. (Because of the rather high alloying levels of Mn, Ni and Cu, all braze alloys are believed to be hyper-eutectoid.) Variation in ingot comminution rating with aging temperature shows roughly an inverse pattern to that previously described for hardness versus temperature, particularly in the vicinity of each hardness minimum. That is, the lower the hardness, the better the resistance to comminution, as a general rule. However, there are some obvious exceptions, and there is obviously only a very broad-band

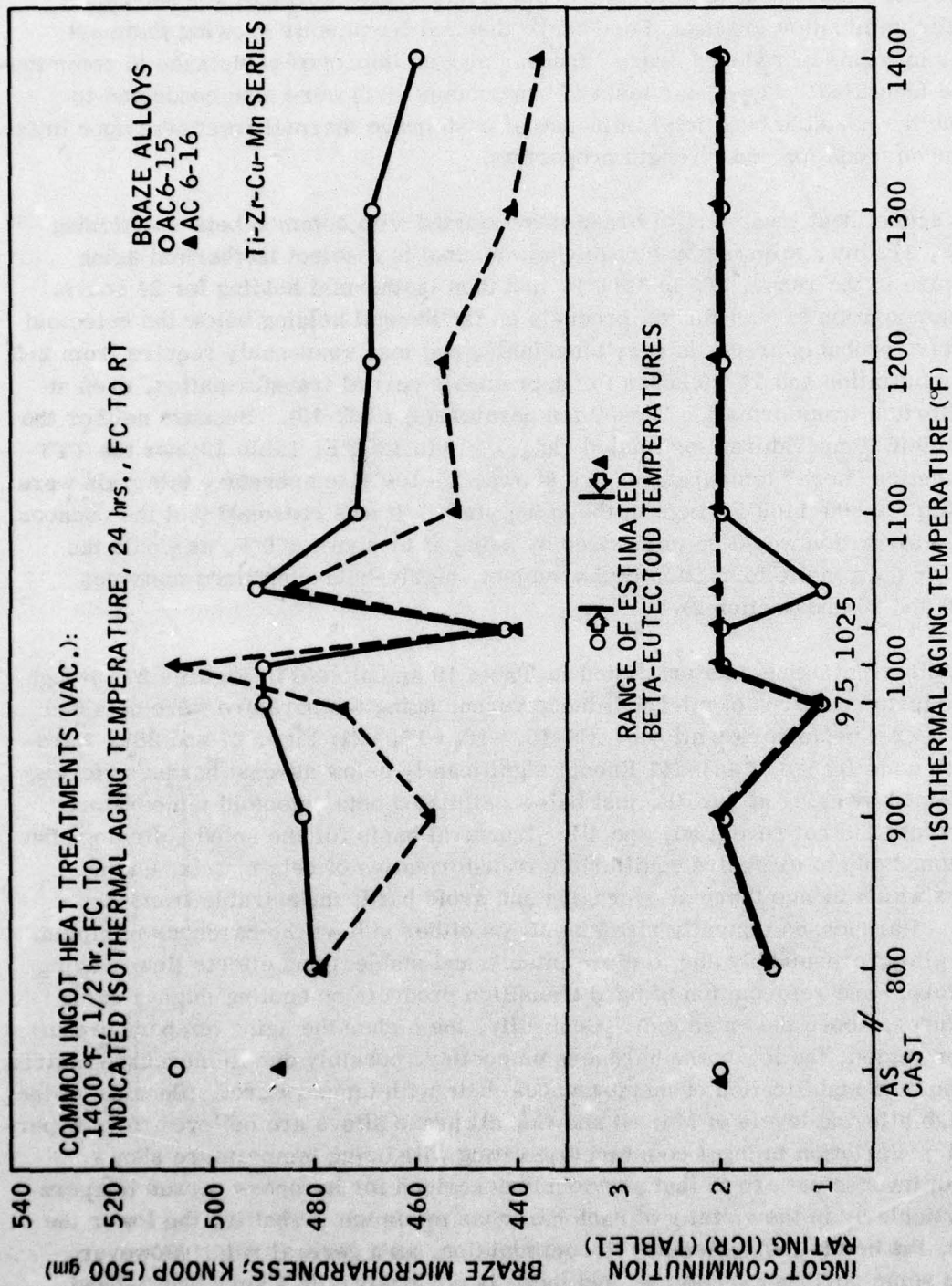


Figure 27. Braze Microhardness and Ingot Comminution Rating (ICR) Plotted Versus Isothermal Aging Temperature (Alloys AC6-15 and AC6-16)

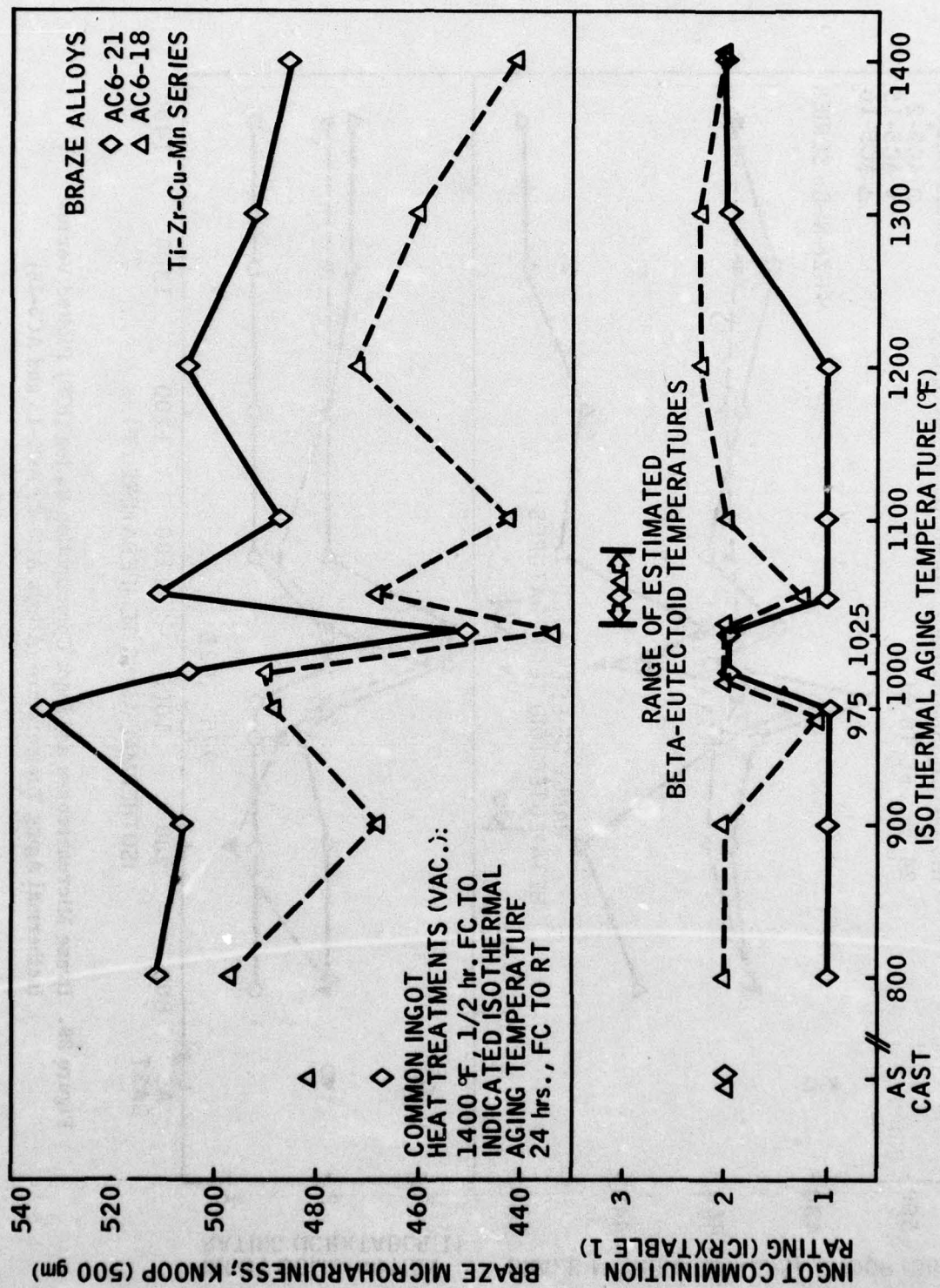


Figure 28. Braze Microhardness and Ingot Commutation Rating (ICR) Plotted Versus Isothermal Aging Temperature (Alloys AC6-18 and AC6-21)

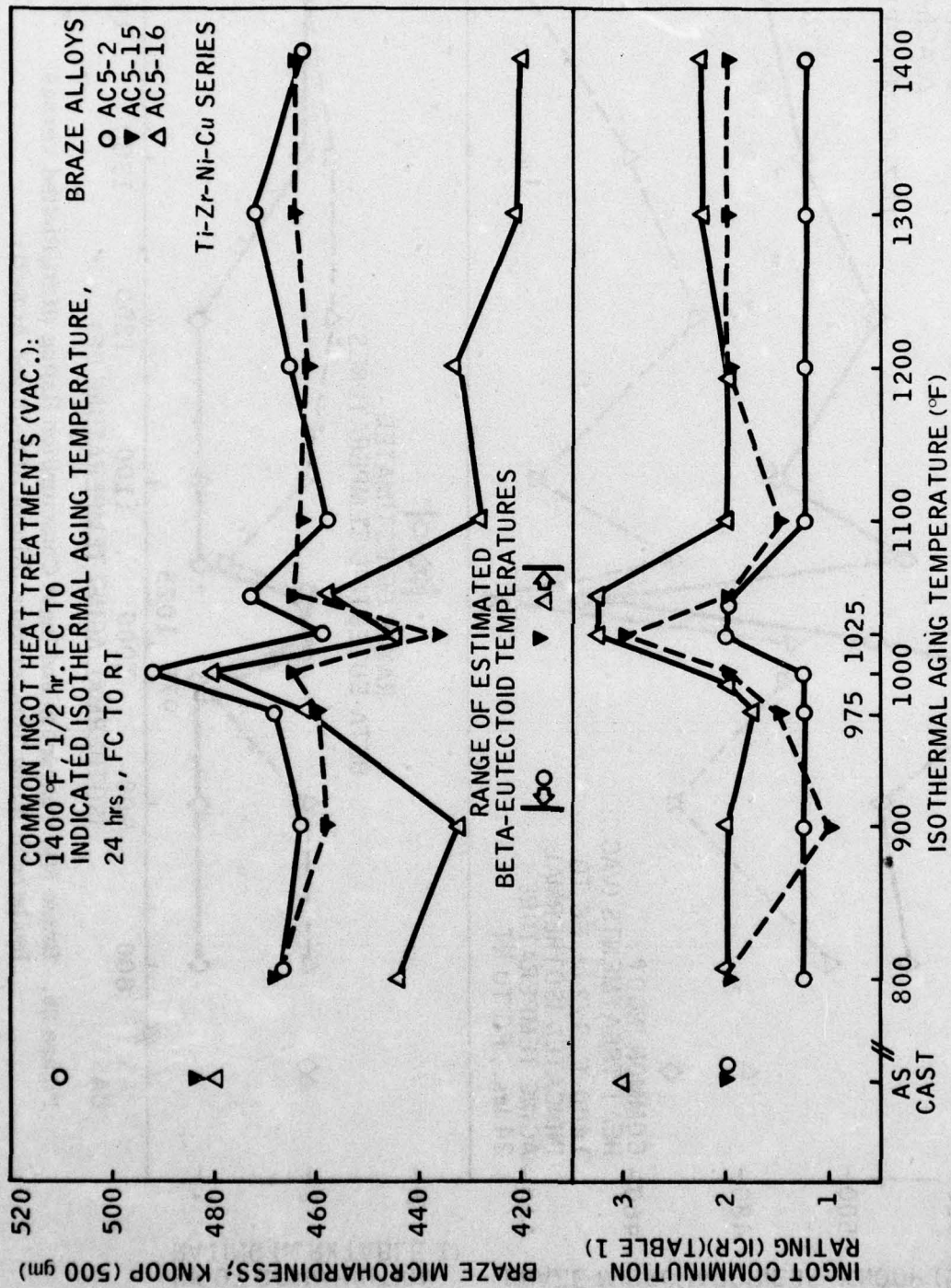


Figure 29. Braze Microhardness and Ingot Comminution Rating (ICR) Plotted Versus Isothermal Aging Temperature (Alloys AC5-2, AC5-15 and AC5-16)

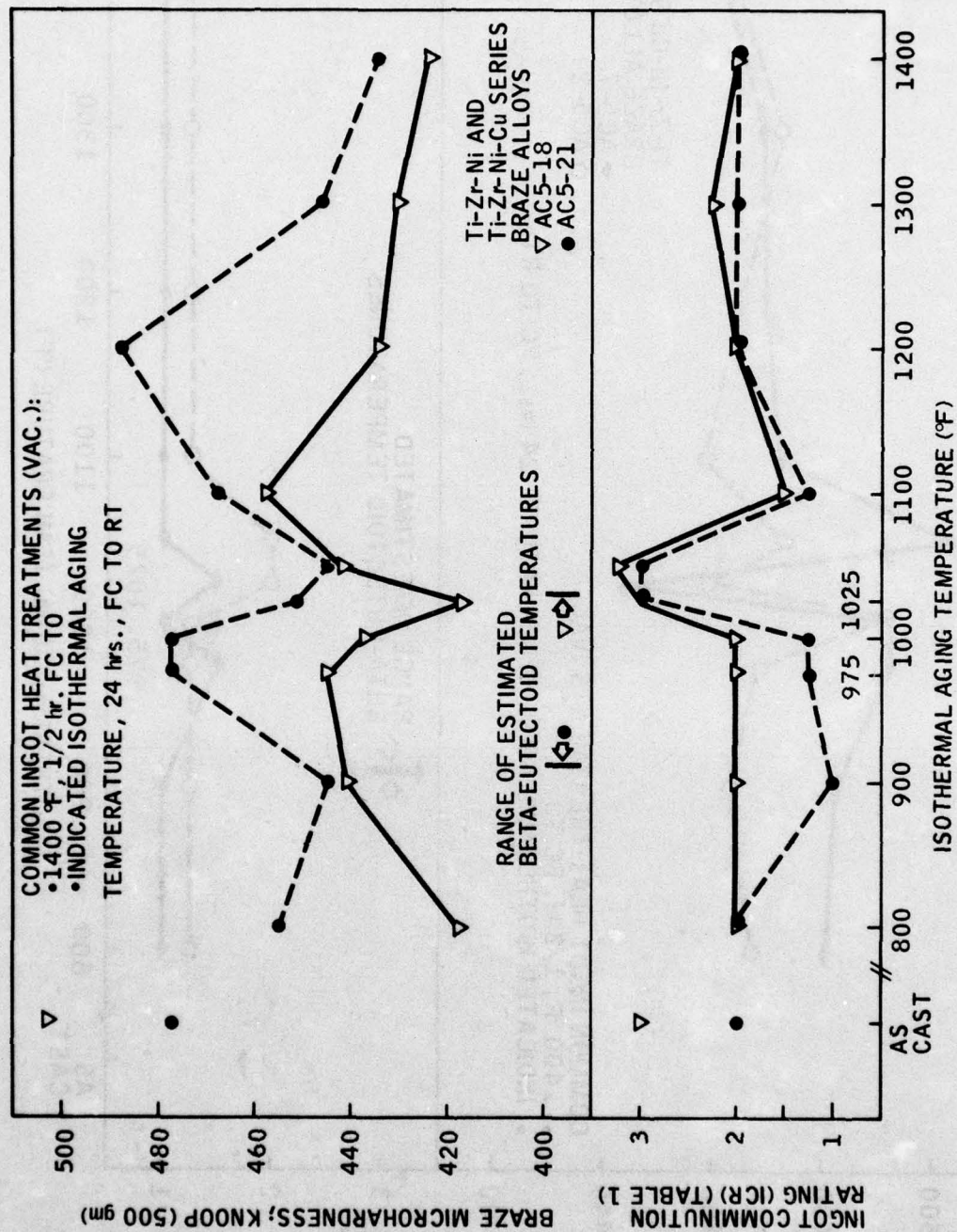


Figure 30. Braze Microhardness and Ingot Communitation Rating (ICR) Plotted Versus Isothermal Aging Temperature (Alloys AC5-18 and AC5-21)

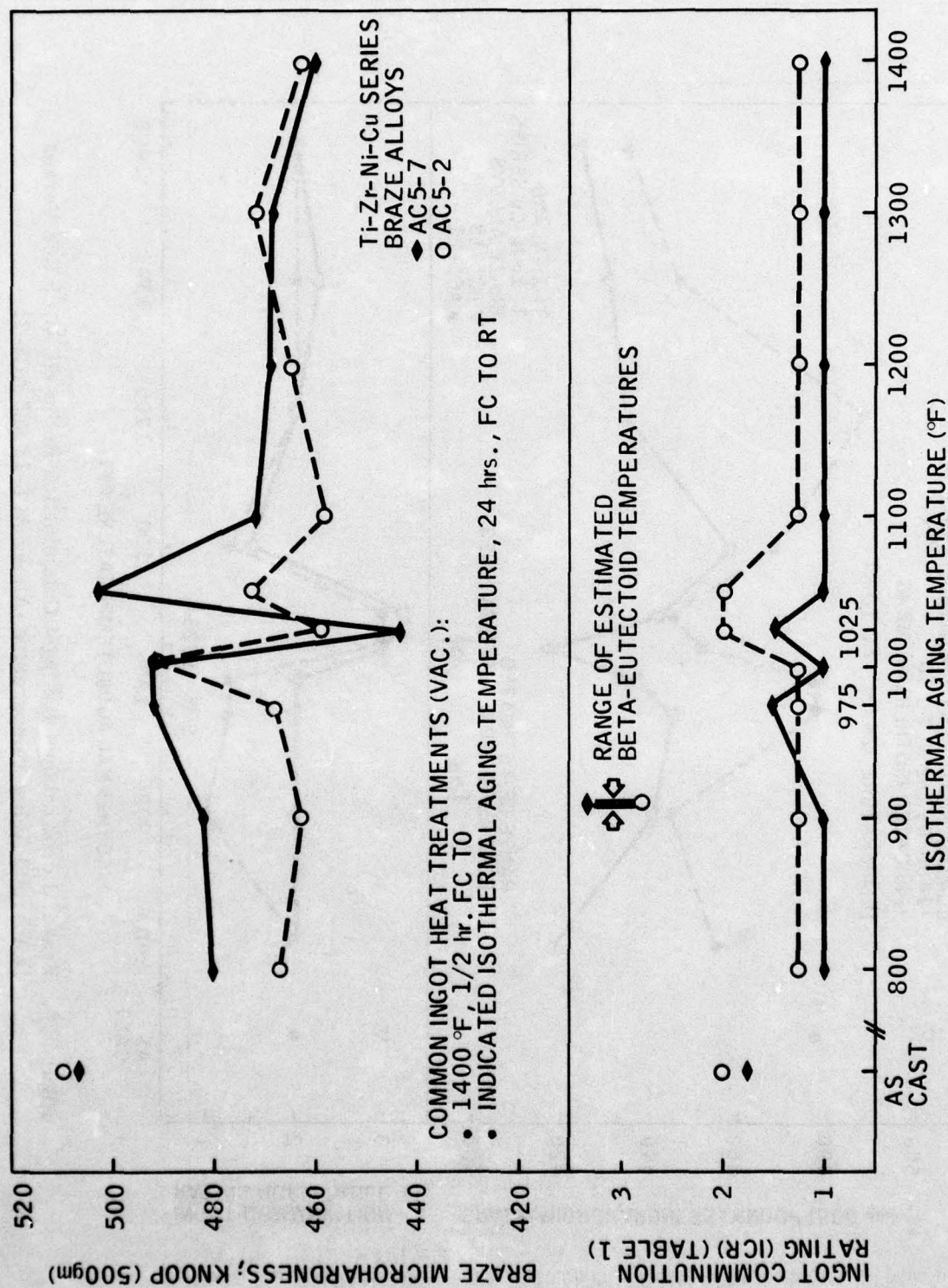


Figure 31. Braze Microhardness and Ingot Communion Rating (ICR) Plotted Versus Isothermal Aging Temperature (Alloys AC5-2 and AC5-7)

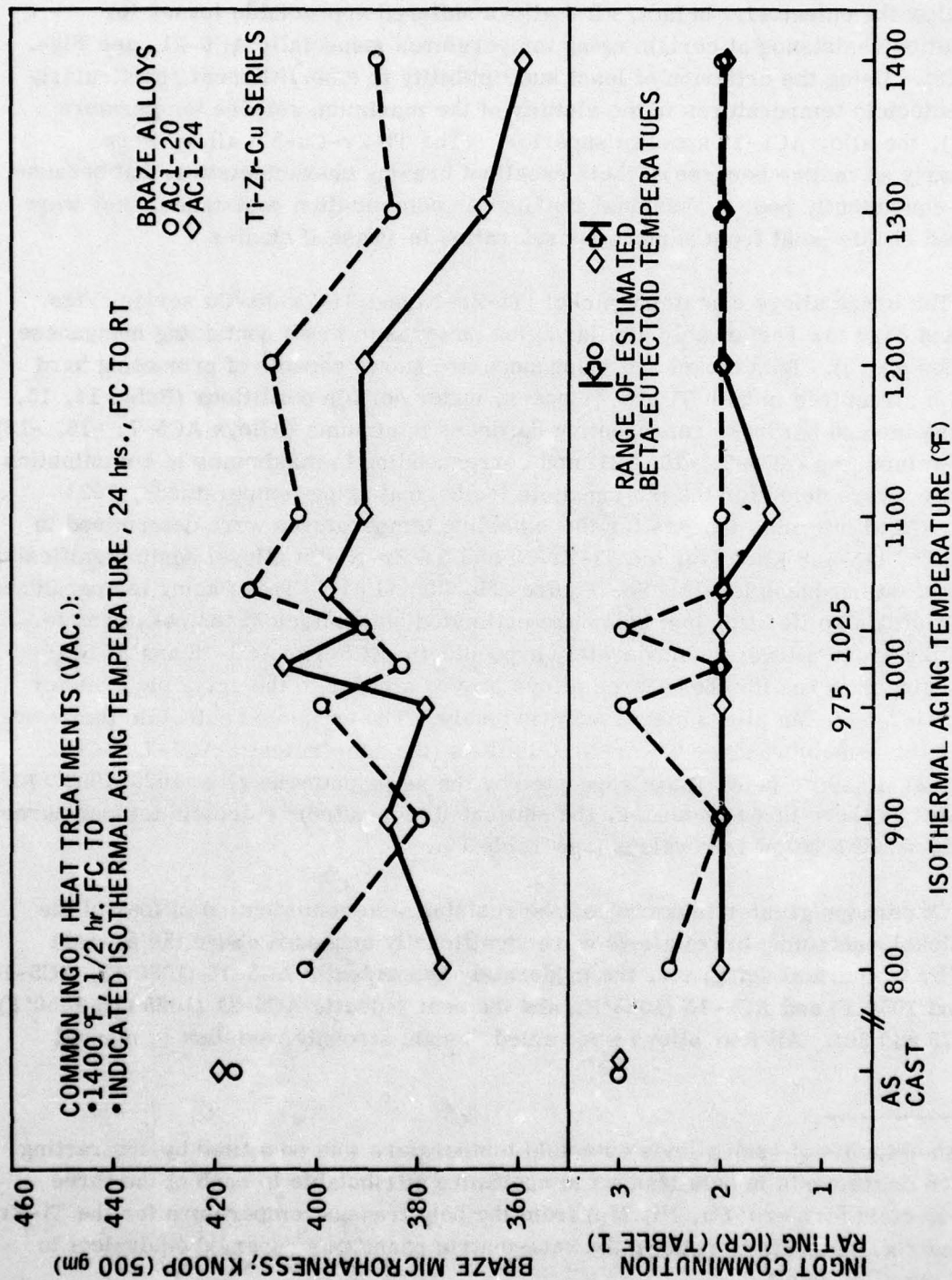


Figure 32. Braze Microhardness and Ingot Communion Rating (ICR) Plotted Versus Isothermal Aging Temperature (Alloys AC1-20 and AC1-24)

AD-A036 575

SOLAR SAN DIEGO CALIF

F/G 11/6

TITANIUM BRAZE SYSTEM FOR HIGH TEMPERATURE APPLICATIONS.(U)

AUG 76 C E SMELTZER, A N HAMMER

F33615-74-C-5118

UNCLASSIFIED

RDR-1786-6

AFML-TR-76-145

NL

2 OF 2

AD
A036575



relationship between microhardness and comminution rating, probably because all hardnesses still range quite high. For the Ti-Zr-Cu-Mn series alloys, resistance to comminution was not notably improved (over the as-cast ranking) through isothermal aging below the eutectoid. In fact, all 4 alloys suffered appreciable losses in comminution resistance at certain aging temperatures (especially AC6-21, see Figs. 27 and 28). Using the criterion of least susceptibility to embrittlement, particularly at sub-eutectoid temperatures in the vicinity of the maximum service temperature ($\leq 900^\circ\text{F}$), the alloy AC6-18 appears superior. (The Ti-Zr-Cu-Mn alloys were particularly attractive because of their excellent brazing characteristics, but because of their consistently poor to marginal rankings in comminution resistance, they were dismissed at this point from serious consideration in Phase II studies.

The braze alloys containing nickel (Ti-Zr-Ni and Ti-Zr-Ni-Cu series; Figs. 29, 30 and 31) show remarkably similar aging patterns to those containing manganese (described above). Both nickel and manganese are known capable of promoting hard transition structures in both Ti and Zr bases, under certain conditions (Refs. 14, 15, 16). Dips in aged hardness representing hardness minimums (Alloys AC5-7, -15, -18) or near-minimums (AC5-2, -15, -21) and corresponding to maximums in comminution resistance, were noted for the intermediate isothermal aging temperatures, 1025-1050°F. (Aged microhardnesses for these holding temperatures were determined in the range of 415-459 Knoop for the Ti-Zr-Ni and Ti-Zr-Ni-Cu alloys; again significantly below as-cast hardness levels. See Figures 29, 30 and 31.) These aging temperatures (1025-1050°F) also lie at or just below the estimated beta eutectoid temperatures for three of the braze alloys; the moderately hypoeutectic AC5-18, AC5-15 and AC5-16; and the aging patterns for these three alloys proved similar to the aging patterns for the four Ti-Zr-Cu-Mn alloys discussed previously. The estimated eutectoid temperatures for the remaining three Ti-Zr-Ni-Cu alloys (the near-eutectic AC5-7, AC5-2 and AC5-21 lie 100°F below those suggested by the aging patterns (viz. 1025-1050°F). Therefore, in these three instances, the estimated (computed)* eutectoid temperatures are likely $\sim 100^\circ\text{F}$ below true values (see Table 19).

Of perhaps greater importance, the resistance to comminution of four of the above nickel-containing braze alloys were significantly enhanced above the as-cast ratings by isothermal aging; viz. the moderately hypoeutectic AC5-18 (1050°F), AC5-16 (1025 and 1050°F) and AC5-15 (1025°F); and the near eutectic AC5-21 (1025 and 1050°F) (Figs. 29 and 30). All four alloys were rated "tough; strongly resistant to manual

*A rough estimate of each alloy's eutectoid temperature was computed by subtracting weighted decrements in beta transus temperature attributable to each of the three beta-eutectoid formers (Cu, Ni, Mn) from the beta transus temperature for the Ti-Zr base matrix. The Ti/Zr ratio in the beta-matrix phase was assumed equivalent to that of the alloy itself.

crushing" after isothermal aging under the above conditions (see Table 19). Alloys AC5-16 and AC5-18 were given ICR rankings of 3(+), post-aging; superior levels of toughness equivalent to the C2-5 baseline alloy (cf Tables 15 and 19). The best previous ICR ratings for AC5-21 and AC5-15 were "marginally tough; moderately resistant to manual crushing". Although these comminution ratings are based upon semi-quantitative measures of energy input to initiate ingot cracking, they have proved to be very reproducible and reliable gages of cast alloy toughness in screening studies (see Section III). A negative aspect which must be considered is the appreciable reduction in comminution resistance noted for certain aging temperatures, (for some alloys) both above and below estimated beta eutectoid temperatures. Particularly vulnerable are the weakly hypoeutectic, near-eutectic alloys, AC5-7 and AC5-2; rated "brittle" over a wide range of post-braze aging temperatures (Fig. 31). In contrast, the moderately hypoeutectic alloys, AC5-18 and AC5-16, showed very little susceptibility toward embrittlement due to aging (especially $\leq 900^\circ\text{F}$); and, in view of their noted ability to be "toughened" by aging treatment, were considered prime candidates for further structural optimization studies (Phase II). In a somewhat similar (favored) category are the structurally intermediate alloys, AC5-15 and AC5-21 (Fig. 31), although these alloys do experience embrittlement at certain elevated aging temperatures [(900, 975, 1100°F) and (900, 975, 1000, and 1100°F) resp.]. Again, the Ti-Zr-Ni-Cu alloy, AC5-16, appeared most promising overall; with the Ti-Zr-Ni alloy, AC5-18, a close second.

The two braze alloys containing only copper (beta-eutectoid former; Ti-Zr-Cu system) exhibited appreciably lower microhardnesses than those recorded for the previously discussed alloys (both as-cast and isothermal-aged conditions) (see Fig. 32). Minimum aged hardnesses (subeutectoid aging) also proved significantly lower than as-cast hardnesses for both the subject alloys, AC1-20 and AC1-24 [viz. minimums of 379 Knoop (900°F) and 375 Knoop (800°F), resp.]. Aged hardnesses obtained for the (subeutectoid) aging temperature range, 800-1100°F, all lie within the relatively low and narrow range of 375-413 Knoop. (The absence of hardness peaks and valleys in the vicinity of the eutectoid temperatures differentiate the subject copper-only alloys from the preceding ones containing admixtures of nickel or manganese or nickel-only.) However, there were not corresponding improvements in comminution resistance recorded at the noted low hardness levels post-aging (Fig. 32). In fact, only alloy AC1-20 preserved the "tough; strongly resistant to manual crushing" rating after aging at 975°F and 1025°F, dropping to a "marginally tough" rating for all other aging temperatures. Alloy AC1-24 dropped to a similar marginal rating for all aging temperatures. (Fortunately, like AC5-16 and AC5-18 discussed previously, neither AC1-20 nor AC1-24 showed any notable tendency toward serious embrittlement due to aging.) This overall behavior was surprising in light of the aforementioned low hardness levels and associated relatively low volume percentages of primary intermetallics (viz. 23-29%, see Table 19). Curiously, the highest comminution rating for the Ti-Zr-Cu alloys coincided with rather high levels of hardness.

There appear to be, in the overall scheme, expected general relationships between microhardness and comminution resistance as well as between intermetallic content and comminution resistance (i.e., toughness) (Table 19 and Figs. 27-32). These relationships, however, are obviously quite broad-band and of limited usefulness. This broad-band correlation, typical of the data presented, may be due to the fact that alloy hardnesses, even after preferred aging, are still rather high for engineering metals, per se. Examination of comminution crack paths in aged ("softened") ingot structures show essentially no change in propagation mode; the cracking still occurring predominantly through the metallic terminal-solution matrix phases, as in the as-cast condition.

At this stage of Phase II, a series of single-lap shear test specimens (Ti-6Al-4V; Fig. 3) were vacuum brazed and isothermally aged post-braze for comparison tensile-shear tests versus the as-brazed condition (cf. Table 20 and Tables 12 and 13; screening test data, Phase I). Test brazements made with the more promising alloys AC5-15, AC5-16, AC5-21, AC5-18 and AC1-20 were aged and tested. Alloy AC6-16 was included to represent the Ti-Zr-Cu-Mn system. The 1025°F aging treatment was evaluated, inasmuch as it had been associated most commonly with increased or stabilized comminution resistance and/or minimum braze hardness. Nominal shear stresses at fracture and at the point of first audible braze cracking were compared with corresponding stress levels for the as-brazed condition (Table 20). In overview, the Ti-Zr-Ni and Ti-Zr-Ni-Cu alloys experienced roughly a 5-10 ksi drop in fracture stress and a 1-4 ksi drop in minimum stress for first cracking, attributable to 1025°F aging (AC5-15, -16, -18, -21). Although these were rather minor (and largely insignificant) changes, they are not in the direction hoped for. The Ti-Zr-Cu and Ti-Zr-Cu-Mn alloys tested (AC1-20 and AC6-16) did not experience any significant changes in shear properties due to 1025°F aging. All joint fractures occurred through braze metal, as in previous testing. As discussed first in the section entitled "Braze Alloy Design and Screening (Phase I)", page 31, shear-strength parameters still were not showing any improvement of sensitivity relative to high-rate comminution properties.

At this juncture in Phase II work, it was not clear what specific directions might be most promising, in the areas of post-braze thermal treatment and/or minor alloying, to develop optimum braze structures. The work to date had shown the feasibility of obtaining significantly reduced hardnesses and, in some cases, increased resistances to comminution through selective heat treatments of as-cast ingot structures. Undesirable forms of beta-matrix transformation were suspect for the rather prevalent marginal toughness and strain accommodation ratings, but the exact nature(s) of these transformations are undoubtedly subtle, and not apparent from metallographic examination. (Suspect transformation products include hard transition structures; fine, homogeneous precipitation of intermetallics within the matrix; possible strong partitioning of interstitial contaminants, etc.) In this regard, phase analysis of transformation structures would have been useful in helping select and

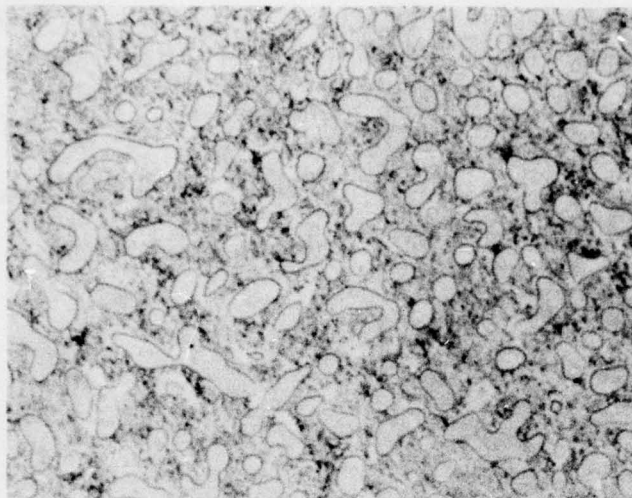
Table 20
COMPARATIVE RT LAP-SHEAR STRENGTH DATA⁽¹⁾
(As-Brazed Condition vs. Post-Braze 1025°F Aging)

Braze Alloy	System and Braze Temperature (°F)	Nominal Shear Strengths (ksi)			
		As-Brazed Condition		Isothermally Aged, Post-Brazing ⁽²⁾	
		At Fracture ⁽³⁾	At First Audible Crack	At Fracture ⁽³⁾	At First Audible Crack
AC6-15	Ti-Zr-Cu-Mn (1710°F)	34.7 35.2	11.4 11.8		
AC6-16	Ti-Zr-Cu-Mn (1750°F)	32.5 34.4	12.4 12.8	34.8 36.0	13.7 13.6
AC6-18	Ti-Zr-Cu-Mn (1750°F)	34.9 35.7	13.8 13.7		
AC6-21	Ti-Zr-Cu-Mn (1710°F)	30.8 32.5	12.6 13.5		
AC5-15	Ti-Zr-Ni-Cu (1730-1765°F)	35.5 36.9	18.4 14.4	25.3 26.4	12.3 12.4
AC5-16	Ti-Zr-Ni-Cu (1750-1780°F)	32.7 34.8	16.0 19.0	28.4 29.3	12.4 13.9
AC5-21	Ti-Zr-Ni-Cu (1700-1770°F)	31.5 32.5	18.2 20.0	25.8 26.1	12.9 12.8
AC5-7	Ti-Zr-Ni-Cu (1650-1670°F)	34.3 36.2	15.9 13.6		
AC5-2	Ti-Zr-Ni-Cu (1650-1670°F)	34.2 34.8	14.0 12.9		
AC5-18	Ti-Zr-Ni (1750°F)	31.0 32.4	15.8 14.6	23.9 24.2	13.3 14.0
AC1-20	Ti-Zr-Cu (1750°F)	30.4 32.4	16.0 12.8	29.3 31.0	13.4 13.6
AC1-24	Ti-Zr-Cu (1740-1760°F)	29.5 32.7	19.0 16.7		
C2-5 (Baseline)	Ti-Cu-Ni (1850°F)	34.7 36.7	18.9 13.1		
TiCuNi foil baseline	Ti-Cu-Ni (1850°F)	36.4 37.6	36.0 27.0		
⁽¹⁾ Heavy Braze Loading (0.12 to 0.14 gms); 2t overlap (0.125 in.); Substrate Alloy: Ti-6Al-4V (0.062 in. tk.). (Process A) ⁽²⁾ 1400°F, 1/2 hr; FC to 1025°F, 24 hrs; FC to RT (1.0 x 10 ⁻⁴ torr, vacuum). ⁽³⁾ All Braze Fractures					

tailor most beneficial post-braze thermal treatments and minor alloying changes. However, rigorous phase analysis was beyond the scope of the subject exploratory alloying program; and, therefore, optimization studies continued on an iterative basis in Phase II.

Metallographic examination did reveal the following pertinent structural information on the more promising braze alloys.

- The moderately hypoeutectic Ti-Zr-Ni-Cu alloys, AC5-15 and AC5-16, are characterized by moderate levels of (ostensibly) a single primary intermetallic (33% and 31% vol., respectively), which exhibits typically nodular, round-edged particle shapes (Fig. 33). The as-cast and etched matrix phases contain fine precipitates; which, on subsequent aging (softening) at 1025°F, tend to coalesce into more visible, spheroidal shapes (Fig. 34). These "globules" etch similarly to the primary intermetallic.
- The moderately hypoeutectic Ti-Zr-Ni and Ti-Zr-Ni-Cu alloys, AC5-18 and AC5-21, with higher Ni and lower Cu contents than the above, have considerably higher levels of primary intermetallics (45% and 37%, vol., respectively), but these intermetallics also exhibit rather rounded, nodular shapes. In the as-cast condition, two different-etching intermetallics are evident (dark and light) (Fig. 35 and 36). On subsequent aging at 1025°F, matrix softening is accompanied by coalescence and spheroidization of matrix precipitates, apparently identical to the light-etching primary intermetallic (as described above) (Fig. 37 and 38). The proportion of dark-etching primary intermetallic also decreases noticeably during 1025°F aging. On isothermal aging at 1200°F, above the eutectoid temperatures, the trend toward edge-rounding coalescence, and nodularization of all intermetallics becomes very discernible (Fig. 39).
- The weakly hypoeutectic (near-eutectic) Ti-Zr-Ni-Cu alloys (viz., AC5-2 and AC5-7) are also characterized by high levels of primary intermetallics (42% and 38% vol., respectively) but of a much finer texture and morphology than AC5-18 and AC5-21. (See the fine, lamellar, as-cast structure of AC5-7; Fig. 40.) On subsequent aging at 1025°F, braze softening is again accompanied by visible trends toward coalescence and spheroidization of formerly lamellar intermetallics (Fig. 41). These two alloys have low brazing temperatures, but are not promising from the standpoint of toughness (Fig. 31).

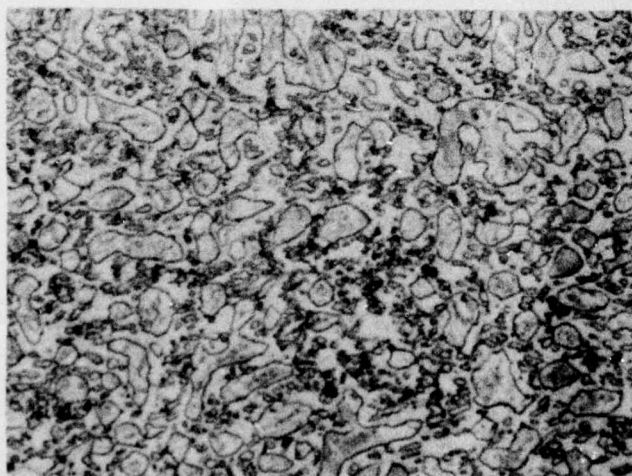


As-Cast

Etchant: Kroll's (+)H₂O₂

Magnification: 1200X

**Figure 33. Microstructure of Alloy AC5-16 (Ti-Zr-Ni-Cu)
(As Cast Condition)**

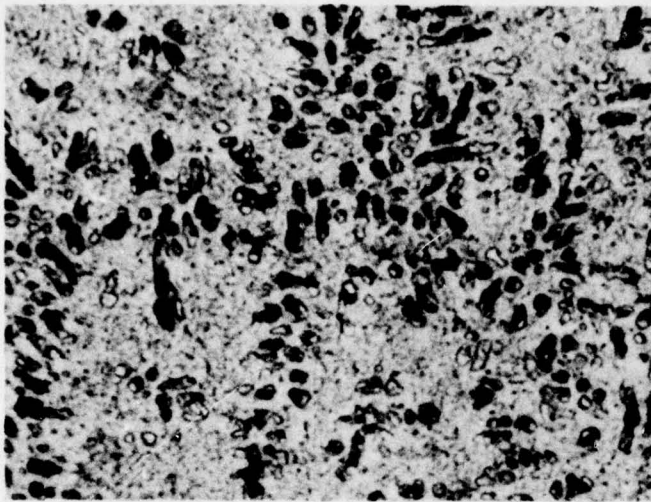


Aged 24 Hrs. at 1025°F

Etchant: Kroll's (+)H₂O₂

Magnification: 1200X

**Figure 34. Microstructure of Alloy AC5-16 (Ti-Zr-Ni-Cu)
(Isothermally Aged at 1025°F)**

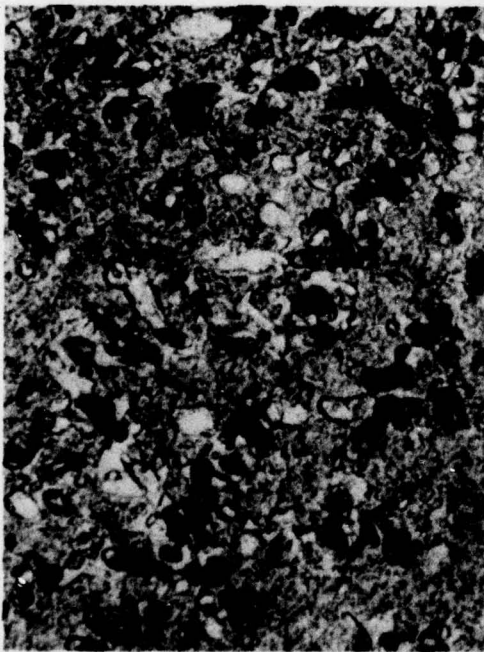


As-Cast

Etchant: Kroll's (+)H₂O₂

Magnification: 1200X

Figure 35. Microstructures of Alloy AC5-21 (Ti-Zr-Ni-Cu)
(As-Cast vs. 1025°F and 1200°F Aging)



As-Cast

Etchant: Kroll's (+)H₂O₂

Magnification: 1200X

Figure 36. Microstructures of Alloy AC5-18 (Ti-Zr-Ni)
(As-Cast vs. 1025°F Aging)



Aged 24 Hrs. at 1025°F

Etchant: Kroll's (+)H₂O₂

Magnification: 1200X

Figure 37. Microstructures of Alloy AC5-21 (Ti-Zr-Ni-Cu)
(As-Cast vs. 1025°F and 1200°F Aging)

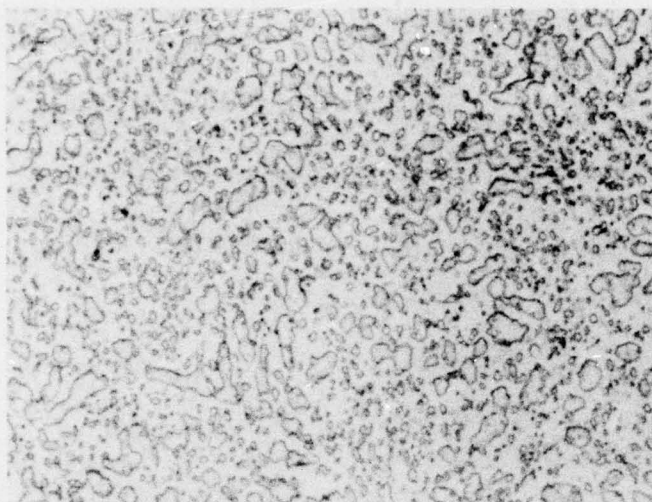


Aged 24 Hrs. at 1025°F

Etchant: Kroll's (+)H₂O₂

Magnification: 1200X

Figure 38. Microstructures of Alloy AC5-18 (Ti-Zr-Ni)
(As-Cast vs. 1025°F Aging)

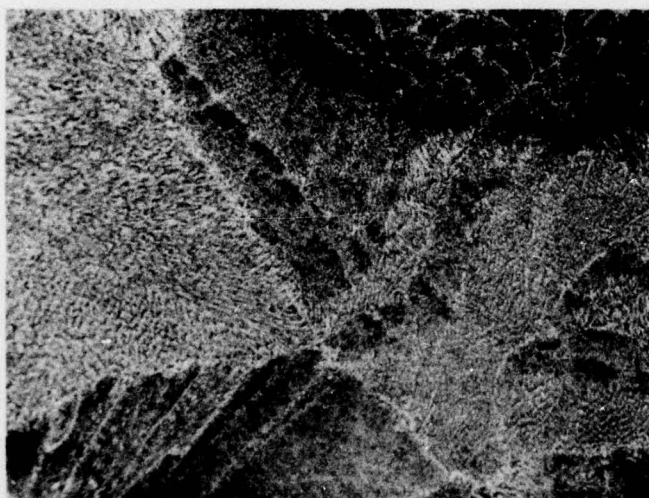


Aged 24 Hrs. at 1200°F

Etchant: Kroll's (+)H₂O₂

Magnification: 1200X

**Figure 39. Microstructure of Alloy AC5-21 (Ti-Zr-Ni-Cu)
(As-Cast vs. 1025°F and 1200°F Aging)**

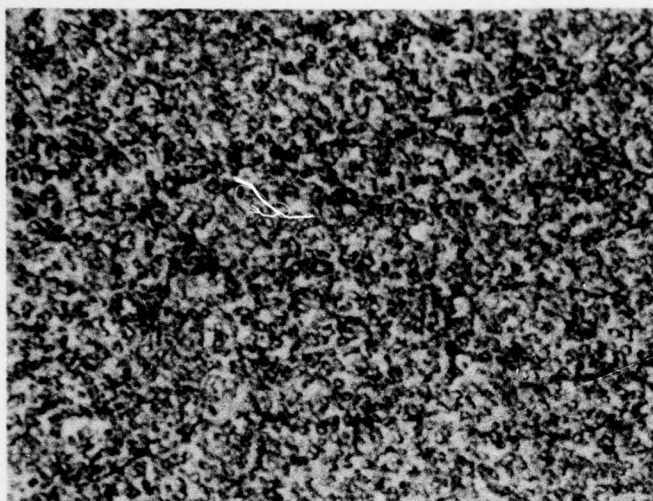


As-Cast

Etchant: Kroll's (+)H₂O₂

Magnification: 1200X

**Figure 40. Microstructures of Alloy AC5-7 (Ti-Zr-Ni-Cu)
(As-Cast vs. 1025°F Aging)**



Aged 24 Hrs. at 1025°F

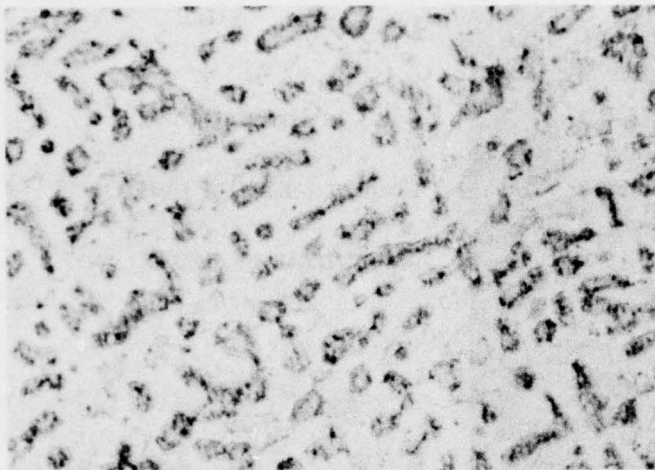
Etchant: Kroll's (+)H₂O₂

Magnification: 1200X

Figure 41. Microstructures of Alloy AC5-7 (Ti-Zr-Ni-Cu)
(As-Cast vs. 1025°F Aging)

- The moderately hypoeutectic Ti-Zr-Cu alloys, AC1-20 and AC1-24, have somewhat similar cast structures to AC5-15 and AC5-16, except that there appear to be two primary intermetallics (light and dark etching), and there is no discernible precipitation in the as-cast (or aged) matrix phases. Primary intermetallic levels are 29% and 23% vol., respectively; the lowest of all 12 braze candidates (Fig. 42). There appears to be little tendency toward change of primary intermetallic particle shape, etching characteristic, or dendritic pattern associated with isothermal aging (cf. Figs. 42, 43 and 44).

Cyclic Annealing Studies. The following is a discussion of results obtained using post-braze cyclic annealing treatments (third approach, described above in the preamble of the section entitled "Post-Braze Thermal Treatments", page 76) to alter cast microstructure in the direction of improved braze ductility and toughness. Arc-melted 5 gm button ingots of each candidate braze alloy were used to simulate (and isolate) as-brazed braze structures, and to facilitate both heat-treatment and comminution studies and subsequent metallographic examination of braze structures, unaffected by braze/substrate interaction. Crushed ingot chunks after comminution testing were examined metallographically (both as-cast and after thermal treatment) in an attempt to correlate microstructural features with both primary (new surface) and secondary (internal) comminution cracks. In order to keep the number of program tests manageable for the various optimization procedures, work was concentrated on those candidate braze alloys in each alloy system which appeared to possess best inherent potential for high toughness and strain-accommodation, and/or which have responded most favorably

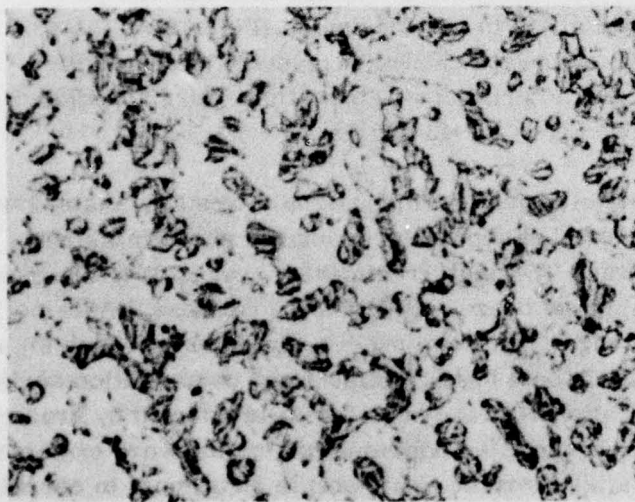


As-Cast

Etchant: Kroll's (+)H₂O₂

Magnification: 1200X

Figure 42. Microstructures of Alloy AC1-20 (Ti-Zr-Cu)
(As-Cast vs. 1025°F and 1200°F Aging)

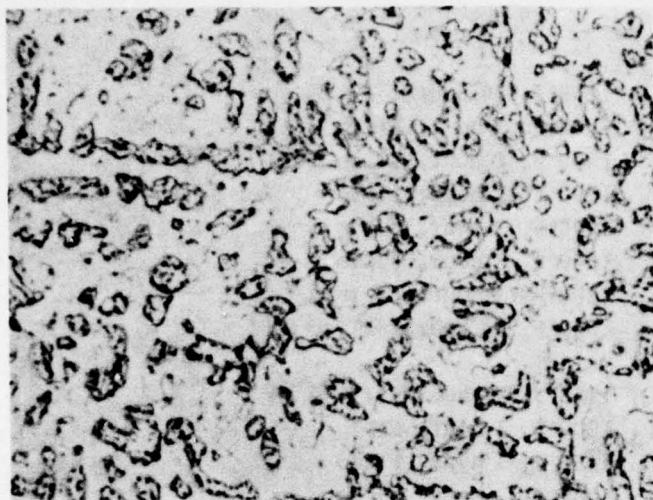


Aged 24 Hrs. at 1025°F

Etchant: Kroll's (+)H₂O₂

Magnification: 1200X

Figure 43. Microstructures of Alloy AC1-20 (Ti-Zr-Cu)
(As-Cast vs. 1025°F and 1200°F Aging)



Aged 24 Hrs. at 1200°F

Etchant: Kroll's (+)H₂O₂

Magnification: 1200X

Figure 44. Microstructures of Alloy AC1-20 (Ti-Zr-Cu)
(As-Cast vs. 1025°F and 1200°F Aging)

to post-braze thermal treatment in prior study (i.e., isothermal aging). The candidate braze alloys examined were the four which showed most promise for improved toughness in isothermal aging studies [viz. AC5-15, AC5-16 and AC5-21 (Ti-Zr-Ni-Cu system) and AC5-18 (Ti-Zr-Ni system)], the best of the lower-melting-temperature braze alloys [viz. the near-eutectic AC5-2 (Ti-Zr-Ni-Cu system)], and the most consistent high-toughness alloy in the low-hardness Ti-Zr-Cu system (viz. AC1-20). Estimated beta eutectoid temperatures are AC5-15 (1025°F); AC5-16 (1070°F); AC5-21 (~1050°F revised); AC5-18 (1030°F); AC5-2 (~1025°F revised); and AC1-20 (1185°F) (Table 19). Consequently, experimental cyclic annealing studies were conducted between the temperature limits of 1000°F (common minimum temperature) and 1100-1200°F (maximum temperature range). (See treatment schedule below). Vacuum heat treatment of braze ingot started with common beta-solutioning at 1400°F, 1/2 hour, followed by furnace cooling to one of the three different cyclic annealing schedules tabulated below:

- Schedule "A"
(1100°F \rightleftharpoons 1000°F)

1100°F, 16 hours, FC to
1000°F, 1 hour, FH to
1100°F, 1 hour, FC to
1000°F, 1 hour, FH to
1100°F, 1 hour, FC to
1000°F, 1 hour, FH to
1100°F, 1 hour, FC to
1000°F, 16 hours, FC to RT

- Schedule "B" (1200°F \rightleftharpoons 1000°F)
 - 1200°F, 16 hours, FC to
 - 1000°F, 1 hour, FH to
 - 1200°F, 1 hour, FC to
 - 1000°F, 1 hour, FH to
 - 1200°F, 1 hour, FC to
 - 1000°F, 1 hour, FH to
 - 1200°F, 1 hour, FC to
 - 1000°F, 16 hours, FC to RT

- Schedule "C" (1150°F \rightleftharpoons 1000°F)
 - 1150°F, 16 hours, FC to
 - 1000°F, 1 hour, FH to
 - 1150°F, 1 hour, FC to
 - 1000°F, 1 hour, FH to
 - 1150°F, 1 hour, FC to
 - 1000°F, 1 hour, FH to
 - 1150°F, 1 hour, FC to
 - 1000°F, 16 hours, FC to RT

Schedule "D" indicates beta-solutioning treatment only (i.e., 1400°F, 1/2 hour, FC to RT). The objectives of cyclic annealing were to promote and accelerate the coalescence and spheroidization of intermetallic precipitates through repeated employment of the energy of eutectoid reaction (Refs. 23 and 24). Although coalescence and spheroidization of intermetallic precipitates was observed to occur (especially with Schedule "C", 1150°F-1000°F), none of the cyclic annealed ingots showed improvement in resistance to comminution over the respective as-cast ingot structures. In fact, in all instances but three, the cyclic annealed ingots suffered decreased resistance to comminution (see Table 21). The generally superior alloy, AC5-16, and the low-hardness alloy, AC1-20, suffered the least serious impairment to comminution resistance, and maintained ICR rankings of 2 or better throughout this cyclic-annealing work.

Metallographic examination of cyclic-annealed and crushed AC5-16 ingot chunks have revealed the following relationships among microstructure, microhardness and comminution resistance. (AC5-16 is felt to be the most promising candidate braze overall, based upon prior work.) The microstructures of Schedule B (1200°F \rightleftharpoons 1000°F; Fig. 45), Schedule D (1400°F; Fig. 46) and the as-cast condition (Fig. 33) all show a fairly uniform dispersion of the fine intermetallic precipitate within the matrix phase; typical of homogeneous nucleation of precipitate following beta-solutioning at a temperature well above the estimated eutectoid temperature (1070°F). The as-cast structure of AC5-16 possesses the highest rating for comminution resistance among these three conditions (viz., 3 rating versus 2), in spite of somewhat greater hardness (481 Knoop versus 430/422 Knoop; Table 21). As expected, the lower beta-solutioning temperatures employed in the cyclic annealing study promoted discernible coalescence (growth and spheroidization) of structurally stable intermetallic precipitates. A rough estimate of stable intermetallic-particle growth can be given in terms of the change in size range

Table 21

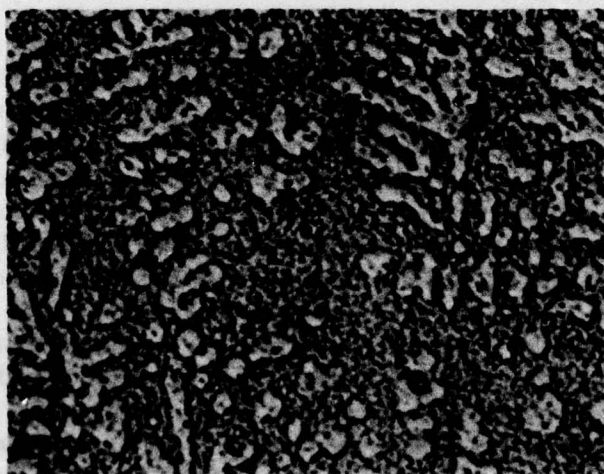
**INGOT COMMINATION RATINGS FOR CYCLIC ANNEALED
VERSUS AS-CAST STRUCTURES**

Braze Alloy	Ingot Comminution Rating ^(a)				
	As-Cast	Schedule A	Schedule B	Schedule C	Schedule D
AC5-15	2	1(+)	2 ^(b)	2 ^(b)	2(-)
AC5-16	3 (481) ^(c)	2 (430) ^(c)	2 (442) ^(c)	2(+) (453) ^(c)	2 (430) ^(c)
AC5-21	2 to 2(+)	1	2 ^(b)	1(+)	1
AC5-18	3	2	1	1	1
AC5-2	2 to 2(-)	1	1	1	1
AC1-20	3	2	2	2	2

^(a) Resistance to Crushing
 (1) Brittle; easy to crush manually.
 (2) Marginally tough; moderately resistant to manual crushing.
 (3) Tough; strongly resistant to manual crushing.
 (4) Very tough; requires initial crushing on the hydraulic press.
 (5) Very tough and ductile; cannot be crushed. Requires drilling or rolling to obtain braze forms.

^(b) No change in comminution rating over as-cast condition.

^(c) Knoop microhardness number (500 gm).



Schedule B

Etchant: Kroll's (+) H₂O₂

Magnification: 1200X

**Figure 45. Microstructure of Alloy AC5-16 (Ti-Zr-Ni-Cu) Cyclic
Annealed Between 1200°F and 1000°F (Schedule B)**



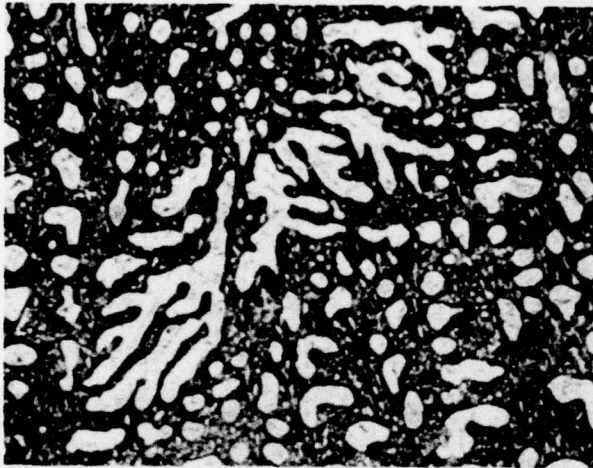
Schedule D

Etchant: Kroll's (+) H_2O_2

Magnification: 1200X

Figure 46. Microstructure of Alloy AC5-16 (Ti-Zr-Ni-Cu) Beta-Solutioned At 1400°F, 1/2 Hour, FC to RT (Schedule D)

of discernible particles; for the as-cast condition ($\sim 0.08-0.2\mu$) and following Schedule "C" ($\sim 0.2-1.1\mu$). This effect was most pronounced with Schedule "C" ($1150 \pm 1000^\circ F$; Fig. 47 and 48); and to a slightly lesser extent, Schedule "A" ($1100^\circ F \pm 1000^\circ F$; Fig. 49). The degree of precipitate coalescence and spheroidization (or nodularization) noted here is similar to that obtained in prior work involving isothermal aging of AC5-16 at $1025^\circ F$ (see Fig. 34). [This is an important comparison because the $1025^\circ F$ isothermal age has developed the highest comminution resistance noted for AC5-16; viz. 3+.] The microhardness levels of these three spheroidized structures are also fairly similar (viz., 453 Knoop for Schedule "C"; 430 Knoop for Schedule "A"; and 444 Knoop for $1025^\circ F$ isothermal aging). However, in spite of these proximate similarities in hardness and apparent structure, comminution ratings (ICR) are markedly different (viz. 3+ rating for $1025^\circ F$ isothermal aging versus only 2+ for Schedule "C" and only 2 for Schedule "A") (see Tables 19 and 21). Very probably, then, the spheroidized intermetallics in the $1025^\circ F$ aged structure are only coincidental, and are not primarily responsible for its superior comminution rating. Comminution cracks for all cyclic annealed conditions invariably propagate through the matrix (terminal-solid-solution) phase and intermetallic particulates are almost never cracked, as were the cases noted previously for the as-cast condition and isothermally aged conditions in earlier work. [See Figs. 25, 48, 50 and 51 which illustrate typical crack-propagation paths.] Consequently, it is felt that the above observations constitute further supportive evidence indicting the structure and heat-treat condition of the beta-matrix phase as the principal determinants of comminution resistance (i.e., of braze toughness, per se). Phase analysis of beta transformation structures is again indicated as the most logical prerequisite for efficiently selecting and tailoring post-braze thermal treatments

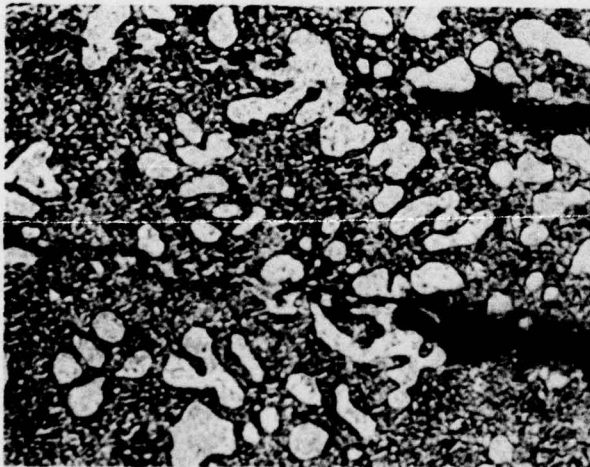


Schedule C

Etchant: Kroll's (+) H_2O_2

Magnification: 1200X

Figure 47. Microstructure of Alloy AC5-16 (Ti-Zr-Ni-Cu) Cyclic Annealed Between 1150°F and 1000°F (Schedule C)



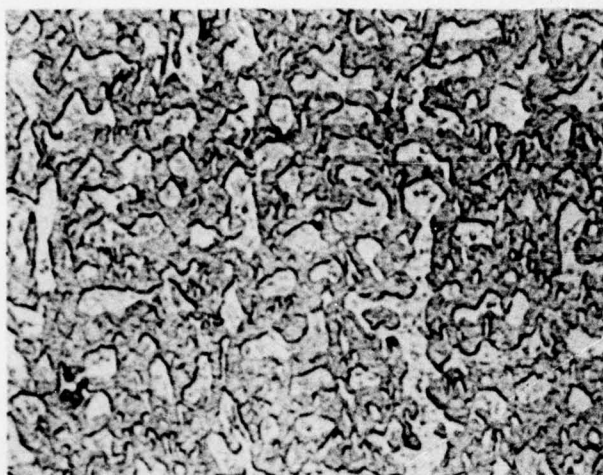
Schedule C

Etchant: Kroll's (+) H_2O_2

Magnification: 1200X

[Note that cracks propagate largely through the matrix phase, skirting around the light-etching, primary intermetallics.]

Figure 48. Microstructure of Alloy AC5-16 (Ti-Zr-Ni-Cu) Showing Secondary Comminution Cracks; Cyclic Annealed Between 1150°F and 1000°F (Schedule C)

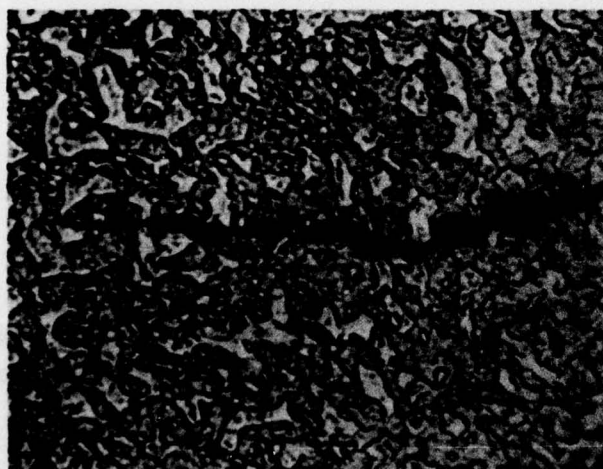


Schedule A

Etchant: Kroll's (+) H_2O_2

Magnification: 1200X

Figure 49. Microstructure of Alloy AC5-16 (Ti-Zr-Ni-Cu) Cyclic Annealed Between 1100°F and 1000°F (Schedule A)



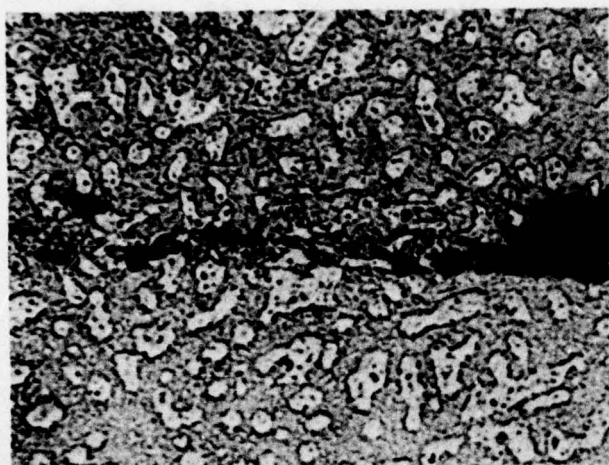
Schedule A

Etchant: Kroll's (+) H_2O_2

Magnification: 1200X

[Note that the crack propagates largely through the matrix phase, skirting around the lighter-etching, primary intermetallic.]

Figure 50. Microstructure of Alloy AC5-16 (Ti-Zr-Ni-Cu) Showing Secondary Comminution Crack; Cyclic Annealed Between 1100°F and 1000°F (Schedule A)



Schedule B

Etchant: Kroll's (+) H_2O_2

Magnification: 1200X

[Note the crack front advancing from the right side, with void formation in the matrix phase ahead of the crack tip. The crack propagates largely through the matrix phase, skirting around the lighter-etching primary intermetallics.]

Figure 51. Microstructure of Alloy AC5-16 (Ti-Zr-Ni-Cu) Showing Secondary Comminution Crack; Cyclic Annealed Between 1200°F and 1000°F (Schedule B)

most beneficial to braze toughness. However, in-depth phase analysis is beyond the scope of the subject exploratory alloying program (Section I).

Coalescence and spheroidization of the intermetallic precipitates has been demonstrated feasible through cyclic annealing. However, inasmuch as these structural changes have not been associated with any corresponding improvement in ingot comminution resistance, no further study of intermetallic coalescence and spheroidization was conducted in Phase II.

Rare-Earth-Metal Scavenging

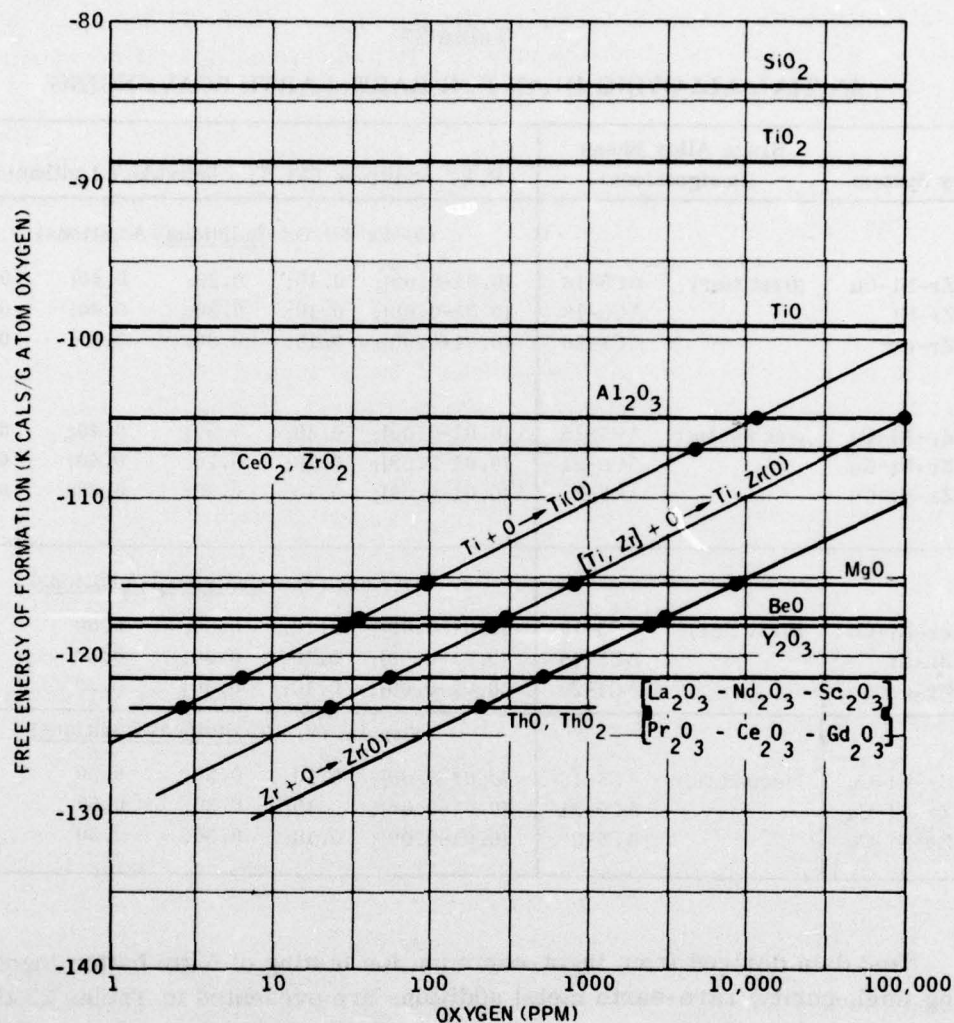
Final studies in Phase II (Braze Optimization) were concentrated on minor rare-earth (RE) metal additions made to melt charges of select candidate alloys, in an effort to scavenge possibly excessive interstitial element solutes (O, N, C) down to very low levels. (This approach was chosen to address the third and last structural problem cited in the section entitled "Braze Design Problems and Possible Solutions", page 72.) The rare-earth (and rare-earth-like) metals adopted for this study include representatives of both the yttrium subgroup (viz. yttrium and gadolinium), the cerium subgroup (viz. cerium, lanthanum and neodymium) as well as scandium (Ref. 26). The above rare earth metals are attractive as scavenging agents due to the very high free energies of formation of their extraordinarily stable oxides, nitrides and carbides; and they are frequently employed in the melting practices of specialty

steels and superalloys and (occasionally) titanium alloys (Ref. 27 and 28). In fact, rare-earth metals are just about the only reactive agents capable of scavenging interstitial contaminants from Ti and Zr alloys (see below).

The best rationale for RE scavenging can be made for oxygen removal. Figure 52 is a plot of the free-energies of formation of various oxygen solutions in liquid Ti, Ti-50Zr, and Zr metals (1600°F), relative to the free energies of formation of different rare-earth oxides (competitors for oxygen with the liquid-metal solutions). Assuming that R_2O_3 -type oxides are the stable forms and that the Ti-50Zr base solutions fairly represent the subject braze alloys, one might expect effective oxygen scavenging with adequate yttrium (Y) additions down to about 200-250 ppm (O), solute limit at equilibrium, and with adequate cerium (Ce), lanthanum (La), neodymium (Nd), scandium (Sc), or gadolinium (Gd) additions, down to 50-70 ppm (O), solute limit (Fig. 52). Driving the interstitial solutes down to such low maximum levels, (actually levels well below those normally found in commercial titanium alloys) should serve to neutralize the problem of excessive interstitials, if this is indeed a pertinent problem.

The key word here is "adequate" rare-earth addition -- too little addition, and not all the available oxygen in solution can be reacted to form RE oxides for slagging away; too much addition, and the solid-solubility limits for residual rare-earths in the braze matrix may be exceeded, resulting in internal (RE/Ti, Zr) intermetallic formation and possible further loss of ductility (Ref. 29). In the subject work, maximum additions of Ce, La, Gd, and Nd have been 0.8 percent (wt.) and of Y, 0.50 percent (wt.); theoretically adequate to react with ~1300-1400 ppm dissolved oxygen, but believed low enough to avoid significant intermetallic formation based upon the binary Ti-RE and Zr-RE data found in Hansen (Ref. 9), Elliott (Ref. 10) and Shunk (Ref. 11). Minimum RE additions were scheduled from 1-2 orders of magnitude lower than the maximum additions, in order to better assess the true value of RE scavenging under conditions where RE intermetallics should definitely not be found.

The following table (Table 22) shows the initial alloying plan for rare-earth scavenging studies, indicating compositions of the 5.0 gm button ingots which were planned for melting and comminution testing. The six candidate braze alloys selected as alloying bases were those believed to possess the best combinations of good to excellent brazing characteristics, innate resistance to comminution, high lap-shear strengths and (in 4 cases) most favorable response to post-braze thermal treatment in prior work (i.e., representative of each alloy system; viz. Ti-Zr-Ni-Cu, Ti-Zr-Ni, and Ti-Zr-Cu). (See Table 22; also, cf. selection criteria in the section entitled "Post-Braze Thermal Treatments", Cyclic Annealing Studies, page 93.) The six base alloys were AC5-16, AC5-18 and AC1-20 (first tier) and AC5-15, AC5-21 and AC5-2 (alternates, or second tier). Braze alloys in the Ti-Zr-Cu-Mn system were omitted because of lowest potentials for comminution resistance.



NOTE:

Horizontal lines indicate free energies of formation of specific refractory oxides (oxides of candidate alloying agents for oxygen-solute scavenging). (1600°F)

Positively-sloped lines indicate the free energies of formation of Ti(O), Ti,50Zr(O) and Zr(O) liquid-metal solutions, as a function of dissolved oxygen concentration. (1600°F)

Each intercept point (marked ●) indicates the maximum dissolved oxygen concentration possible in liquid-metal solution, under the condition of thermodynamic equilibrium between liquid-metal solution and the specific refractory oxide (1600°F).

Figure 52. Free Energy of Formation of Liquid Metal (Ti-Zr)-Oxygen Solutions (1600°F); Showing Compositional Equilibria with Various Refractory Oxides

Table 22
INITIAL ALLOYING PLAN FOR RARE-EARTH SCAVENGING

Alloy System	Braze Alloy Bases (Designations)		R. E. Additions (Wt. %) - Individual Lanthanides				
			Ce-La-Nd-Gd (<u>Individual</u> Additions)				
Ti-Zr-Ni-Cu	(first tier)	AC5-16	[0.01-0.09];	0.10;	0.20;	0.40;	0.80
Ti-Zr-Ni		AC5-18	[0.01-0.09];	0.10;	0.20;	0.40;	0.80
Ti-Zr-Cu		AC1-20	[0.01-0.09];	0.10;	0.20;	0.40;	0.80
Ti-Zr-Ni-Cu	(second tier)	AC5-15	[0.01-0.09];	0.10;	0.20;	0.40;	0.80
Ti-Zr-Ni-Cu		AC5-21	[0.01-0.09];	0.10;	0.20;	0.40;	0.80
Ti-Zr-Ni-Cu		AC5-2	[0.01-0.09];	0.10;	0.20;	0.40;	0.80
			Yttrium (Y) - (<u>Individual</u> Additions)				
Ti-Zr-Ni-Cu	(first tier)	AC5-16	[0.01-0.09];	0.10;	0.30;	0.50	
Ti-Zr-Ni		AC5-18	[0.01-0.09];	0.10;	0.30;	0.50	
Ti-Zr-Cu		AC1-20	[0.01-0.09];	0.10;	0.30;	0.50	
			Yttrium (Y) - (<u>Individual</u> Additions)				
Ti-Zr-Ni-Cu	(second tier)	AC5-15	[0.01-0.09];	0.10;	0.30;	0.50	
Ti-Zr-Ni-Cu		AC5-21	[0.01-0.09];	0.10;	0.30;	0.50	
Ti-Zr-Ni-Cu		AC5-2	[0.01-0.09];	0.10;	0.30;	0.50	

Test data derived from ingot-comminution testing of 5 gm button ingots containing (high-purity) rare-earth metal additions are presented in Tables 23 through 28. Most complete studies were conducted on the first-tier base alloys. Without exception, there was no improvement noted in comminution resistance (as a measure of toughness) attributable to any rare-earth metal addition. Invariably, comminution resistances were impaired by RE additions (as-cast condition). In some instances, particularly with cerium additions over a wide range, comminution resistance for certain first-tier and second-tier braze alloys actually dropped to quite low levels; but these losses in as-cast toughness typically showed no systematic variation or correlation with the level of rare-earth addition [see Table 23 (Ce), Table 24 (La), Table 25 (Nd), and Table 27 (Gd).] Inasmuch as little or no rare-earth intermetallic formation should have been obtained with the smallest rare-earth additions programmed, rare-earth intermetallics were not prime suspects for the noted instances of embrittlement. Further, application of a "post-braze" (or "post-casting") thermal treatment to similar RE containing ingots (in many cases) restored part to nearly all of the comminution resistance, relative to levels exhibited by the respective base braze compositions (see Tables 23 through 28). In other cases,

Table 23
RESULTS OF COMMINATION STUDIES UPON CERIUM-
MODIFIED BRAZE ALLOYS

Base Braze Alloy	Experimental Alloy Designation	R. E. Admixture (% Wt.)	Ingot Commintion Rating ^(a)	
			As-Cast Cond.	"Post-Casting" Thermal Treatment ^(b)
AC5-15 (Ti-31.3Zr-15.0Ni-7.0Cu)	AC5-15; Std.	— (Baseline)	2	3
	AC5-15; Mod. A1	0.40 Ce	1	1
	AC5-15; Mod. A2	0.80 Ce	1	1
AC5-16 (Ti-27.2Zr-15.0Ni-7.0Cu)	AC5-16; Std.	— (Baseline)	3	3 (+)
	AC5-16; Mod. A3	0.10 Ce	1	2
	AC5-16; Mod. A4	0.20 Ce	2	2 (+)
	AC5-16; Mod. A1	0.40 Ce	1	2
	AC5-16; Mod. A2	0.80 Ce	1	2
AC5-2 (Ti-39.0Zr-15.0Ni-7.0Cu)	AC5-2; Std.	— (Baseline)	2	2
	AC5-2; Mod. A1	0.40 Ce	1	1
	AC5-2; Mod. A2	0.80 Ce	1	1
AC5-21 (Ti-40.0Zr-16.0Ni-4.0Cu)	AC5-21; Std.	— (Baseline)	2	3
	AC5-21; Mod. A1	0.40 Ce	1	2
	AC5-21; Mod. A2	0.80 Ce	1	2
AC5-18 (Ti-41.0Zr-18.0Ni)	AC5-18; Std.	— (Baseline)	3	3
	AC5-18; Mod. A3	0.10 Ce	1	2 (+)
	AC5-18; Mod. A4	0.20 Ce	1	2
	AC5-18; Mod. A1	0.40 Ce	1	2
	AC5-18; Mod. A2	0.80 Ce	1	2
AC1-20 (Ti-28.8Zr-28.0Cu)	AC1-20; Std.	— (Baseline)	3	3
	AC1-20; Mod. A3	0.10 Ce	2	2
	AC1-20; Mod. A4	0.20 Ce	2	2
	AC1-20; Mod. A1	0.40 Ce	2	2
	AC1-20; Mod. A2	0.80 Ce	2	2

Notes: (a) Resistance to Crushing:

- (1) Brittle; easy to crush manually.
- (2) Marginally tough; moderately resistant to manual crushing.
- (3) Tough; strongly resistant to manual crushing.
- (4) Very tough; requires initial crushing on the hydraulic press.
- (5) Very tough and ductile; cannot be crushed. Requires drilling or rolling to obtain braze forms.

(b) 1400°F, 1/2 hr., FC to 1025°F; hold 24 hrs., FC to RT
(Vac.: 1.0×10^{-4} Torr, or better)

Table 24

RESULTS OF COMMINATION STUDIES UPON LANTHANUM-MODIFIED BRAZE ALLOYS

Base Braze Alloy	Experimental Alloy Designation	R. E. Admixture (% Wt.)	Ingot Commination Rating ^(a)	
			As-Cast Cond.	"Post-Casting" Thermal Treatment ^(b)
AC5-16 (Ti-27.2Zr-15.0Ni-7.0Cu)	AC5-16; Std.	— (Baseline)	3	3 (+)
	AC5-16; Mod. C5	0.01 La	2	2 (+)
	AC5-16; Mod. C6	0.05 La	1	2 (+)
	AC5-16; Mod. C3	0.10 La	2	2
	AC5-16; Mod. C4	0.20 La	2	2 (+)
	AC5-16; Mod. C1	0.40 La	2	2 (+)
	AC5-16; Mod. C2	0.80 La	2	2 (+)
AC5-18 (Ti-41.0Zr-18.0Ni)	AC5-18; Std.	— (Baseline)	3	3
	AC5-18; Mod. C5	0.01 La	2	2
	AC5-18; Mod. C6	0.05 La	2	2 (+)
	AC5-18; Mod. C3	0.10 La	2	2 (-)
	AC5-18; Mod. C4	0.20 La	2	2
	AC5-18; Mod. C1	0.40 La	2	2 (-)
	AC5-18; Mod. C2	0.80 La	2	2 (-)
AC1-20 (Ti-28.8Zr-28.0Cu)	AC1-20; Std.	— (Baseline)	3	3
	AC1-20; Mod. C5	0.01 La	2	2
	AC1-20; Mod. C6	0.05 La	2	2
	AC1-20; Mod. C3	0.10 La	2	2
	AC1-20; Mod. C4	0.20 La	2	2
	AC1-20; Mod. C1	0.40 La	2	2
	AC1-20; Mod. C2	0.80 La	2	2
Notes: (a) Resistance to Crushing: (1) Brittle; easy to crush manually. (2) Marginally tough; moderately resistant to manual crushing. (3) Tough; strongly resistant to manual crushing. (4) Very tough; requires initial crushing on the hydraulic press. (5) Very tough and ductile; cannot be crushed. Requires drilling or rolling to obtain braze forms. (b) 1400°F, 1/2 hr., FC to 1025°F, hold 24 hrs., FC to RT (Vac.: 1.0×10^{-4} Torr, or better)				

the same thermal treatment further impaired commination resistance or resulted in no change relative to the original as-cast levels. The thermal treatment employed was that which showed most consistent promise in prior isothermal aging studies on base braze alloys (viz. 1400°F, 1/2 hr., FC to 1025°F, hold 24 hrs., FC to RT). (See section entitled "Post-Braze Thermal Treatments", page 76.)

The observed variable and apparently unsystematic influence of thermal treatment on the levels of commination resistance of rare-earth containing alloys is a further

Table 25

**RESULTS OF COMMINATION STUDIES UPON
NEODYMIUM-MODIFIED BRAZE ALLOYS**

Base Braze Alloy	Experimental Alloy Designation	R. E. Admixture (% Wt.)	Ingot Commutation Rating ^(a)	
			As-Cast Condition	"Post-Casting" Thermal Treatment ^(b)
AC5-16 (Ti-27.2Zr-15.0Ni-7.0Cu)	AC5-16; Std.	— (Baseline)	3	3 (+)
	AC5-16; Mod. B3	0.10 Nd	2	2 (+)
	AC5-16; Mod. B4	0.20 Nd	2	2 (+)
	AC5-16; Mod. B1	0.40 Nd	2	2 (+)
	AC5-16; Mod. B2	0.80 Nd	2	2 (+)
AC5-18 (Ti-41.0Zr-18.0Ni)	AC5-18; Std.	— (Baseline)	3	3
	AC5-18; Mod. B3	0.10 Nd	2	2 (+)
	AC5-18; Mod. B4	0.20 Nd	1	2 (+)
	AC5-18; Mod. B1	0.40 Nd	1	2 (+)
	AC5-18; Mod. B2	0.80 Nd	1	2 (+)
AC1-20 (Ti-28.8Zr-28.0Cu)	AC1-20; Std.	— (Baseline)	3	3
	AC1-20; Mod. B3	0.10 Nd	2 (+)	2
	AC1-20; Mod. B4	0.20 Nd	2 (+)	2
	AC1-20; Mod. B1	0.40 Nd	2 (+)	2
	AC1-20; Mod. B2	0.80 Nd	2 (+)	2
<p>Notes: (a) <u>Resistance to Crushing:</u></p> <p>(1) Brittle; easy to crush manually.</p> <p>(2) Marginally tough; moderately resistant to manual crushing.</p> <p>(3) Tough; strongly resistant to manual crushing.</p> <p>(4) Very tough; requires initial crushing on the hydraulic press.</p> <p>(5) Very tough and ductile; cannot be crushed. Requires drilling or rolling to obtain braze forms.</p> <p>(b) 1400°F, 1/2 hr., FC to 1025°F, hold 24 hours, FC to RT (Vac.: 1.0×10^{-4} Torr, or better)</p>				

indictment of (postulated) unfavorable modes of beta-matrix transformation as the probable cause of random cast-structure embrittlement. Ostensibly, the exploratory program of rare-earth alloying has aggravated, rather than resolved, the problems of matrix instability and marginal cast-structure toughness.

For the most part, experimental RE alloying of first-tier alloys adhered closely to the original alloying plan given in Table 22. Plans to fully explore RE alloying of second-tier braze alloys were cancelled (except for Ce additions) because of the poor showing with first-tier alloys. The planned evaluation of very low-level additions of rare earths (i.e., 0.01-0.09%) was de-emphasized (except for La at levels of 0.01 percent and 0.05 percent and for Gd and Y at the 0.05 percent level), because of the minimal scavenging potentials afforded and because some embrittlement

Table 26
RESULTS OF COMMINATION STUDIES UPON
YTTRIUM-MODIFIED BRAZE ALLOYS

Base Braze Alloy	Experimental Alloy Designation	R. E. Admixture (% Wt.)	Ingot Commintion Rating ^(a)	
			As-Cast Condition	"Post-Casting" Thermal Treatment ^(b)
AC5-16 (Ti-27.2Zr-15.0Ni-7.0Cu)	AC5-16; Std.	— (Baseline)	3	3 (+)
	AC5-16; Mod. D4	0.05 Y	2	2
	AC5-16; Mod. D3	0.10 Y	2	2
	AC5-16; Mod. D1	0.30 Y	2	2
	AC5-16; Mod. D2	0.50 Y	2	2
AC5-18 (Ti-41.0Zr-18.0Ni)	AC5-18; Std.	— (Baseline)	3	3
	AC5-18; Mod. D4	0.05 Y	2	2
	AC5-18; Mod. D3	0.10 Y	2	2
	AC5-18; Mod. D1	0.30 Y	2	2
	AC5-18; Mod. D2	0.50 Y	2	2
AC1-20 (Ti-28.8Zr-28.0Cu)	AC1-20; Std.	— (Baseline)	3	3
	AC1-20; Mod. D4	0.05 Y	2	1
	AC1-20; Mod. D3	0.10 Y	2	1
	AC1-20; Mod. D1	0.30 Y	2	2
	AC1-20; Mod. D2	0.50 Y	2	1
<p>Notes: (a) <u>Resistance to Crushing:</u></p> <p>(1) Brittle; easy to crush manually. (2) Marginally tough; moderately resistant to manual crushing. (3) Tough; strongly resistant to manual crushing. (4) Very tough; requires initial crushing on the hydraulic press. (5) Very tough and ductile; cannot be crushed. Requires drilling or rolling to obtain braze forms.</p> <p>(b) 1400°F, 1/2 hour, FC to 1025°F, hold 24 hours, FC to RT (Vac.: 1.0×10^{-4} Torr, or better)</p>				

was invariably noted even at the 0.10 percent RE level (Ce, Nd, La, Y, and Gd). In place of this, it was decided to evaluate the very light rare-earth-like metal, scandium (Sc). Scandium is the lowest atomic number RE, with atomic radius (1.64 Å), significantly closer to the atomic radii for both Ti and Zr base elements (1.47 Å and 1.60 Å, respectively) than the other rare-earths evaluated (range of 1.80 Å to 1.88 Å). Consequently, much greater matrix solubility was anticipated, for the case of Sc in the subject braze alloy bases, and correspondingly less probability for rare-earth intermetallic formation than with the other rare-earth additives (based upon Sc-Ti and Sc-Zr binary data in Ref. 9, 10 and 11). Because of this favorable relation, higher scavenging potentials were evaluated with scandium than in prior RE alloying work. Scandium additions over the range of 0.30 percent to 2.00 percent were programmed (Table 28); levels theoretically adequate to react with from 1600 ppm to 10,600 ppm dissolved oxygen in the liquid braze. [Considering the very high purities

Table 27
RESULTS OF COMMINATION STUDIES UPON
GADOLINIUM-MODIFIED BRAZE ALLOYS

Base Braze Alloy	Experimental Alloy Designation	R. E. Admixture (% Wt.)	Ingot Commination Rating ^(a)	
			As-Cast Condition	"Post-Casting" Thermal Treatment ^(b)
AC5-16 (Ti-27.2Zr-15.0Ni-7.0Cu)	AC5-16; Std.	— (Baseline)	3	3 (+)
	AC5-16; Mod. E4	0.05 Gd	2	2 (+)
	AC5-16; Mod. E3	0.10 Gd	2	2 (+)
	AC5-16; Mod. E1	0.40 Gd	2	2
	AC5-16; Mod. E2	0.80 Gd	2	2
AC5-18 (Ti-41.0Zr-18.0Ni)	AC5-18; Std.	— (Baseline)	3	3
	AC5-18; Mod. E4	0.05 Gd	1	2
	AC5-18; Mod. E3	0.10 Gd	2	2
	AC5-18; Mod. E1	0.40 Gd	1	1
	AC5-18; Mod. E2	0.80 Gd	1	2 (+)
AC1-20 (Ti-28.8Zr-28.0Cu)	AC1-20; Std.	— (Baseline)	3	3
	AC1-20; Mod. E4	0.05 Gd	2	2
	AC1-20; Mod. E3	0.10 Gd	2	2
	AC1-20; Mod. E1	0.40 Gd	2	2
	AC1-20; Mod. E2	0.80 Gd	2	2
<p>Notes: (a) <u>Resistance to Crushing:</u></p> <p>(1) Brittle; easy to crush manually. (2) Marginally tough; moderately resistant to manual crushing. (3) Tough; strongly resistant to manual crushing. (4) Very tough; requires initial crushing on the hydraulic press. (5) Very tough and ductile; cannot be crushed. Requires drilling or rolling to obtain braze forms.</p> <p>(b) 1400°F, 1/2 hour, FC to 1025°F, hold 24 hours, FC to RT (Vac.: 1.0×10^{-4} Torr, or better)</p>				

of elemental melting stocks used in current melting practice (typically ≤ 200 ppm oxygen) and the Ti-gettered-argon melting environment employed, actual levels of dissolved interstitial-solute contaminants are very probably much lower than 1600 ppm.]

In spite of the high scavenging potentials availed by scandium, none of the three first-tier braze alloy bases with Sc additions showed any improvement in commination resistance in the as-cast condition (Table 28). In fact, all Sc-modified alloys exhibited some degree of toughness loss (typical of the experience with other RE-containing alloys). Post-casting thermal treatment was not effective in restoration of commination resistance; in fact, partial restoration was obtained in one case; no change or further impairment in others (Table 28). In light of all the evidence collected on RE alloying, the following tentative conclusions were drawn:

Table 28

RESULTS OF COMMINATION STUDIES UPON SCANDIUM-
MODIFIED BRAZE ALLOYS

Base Braze Alloy	Experimental Alloy Designation	R. E. Admixture (% Wt.)	Ingot Commintion Rating ^(a)	
			As-Cast Cond.	"Post-Casting" Thermal Treatment ^(b)
AC5-16 (Ti-27.2Zr-15.0Ni-7.0Cu)	AC5-16; Std.	— (Baseline)	3	3 (+)
	AC5-16; Mod. G1	0.30 Sc	2 (+)	2
	AC5-16; Mod. G2	0.50 Sc	2	2
	AC5-16; Mod. G3	1.00 Sc	2	2
	AC5-16; Mod. G4	2.00 Sc	2	2
AC5-18 (Ti-41.0Zr-18.0Ni)	AC5-18; Std.	— (Baseline)	3	3
	AC5-18; Mod. G1	0.30 Sc	2	2
	AC5-18; Mod. G2	0.50 Sc	1	2 (+)
	AC5-18; Mod. G3	1.00 Sc	2	2
	AC5-18; Mod. G4	2.00 Sc	2 (+)	2 (+)
AC1-20 (Ti-28.8Zr-28.0Cu)	AC1-20; Std.	— (Baseline)	3	3
	AC1-20; Mod. G1	0.30 Sc	2 (+)	2
	AC1-20; Mod. G2	0.50 Sc	2 (+)	2 (+)
	AC1-20; Mod. G3	1.00 Sc	2 (+)	2
	AC1-20; Mod. G4	2.00 Sc	2 (+)	2
<p>Notes: (a) <u>Resistance to Crushing:</u></p> <ol style="list-style-type: none"> (1) Brittle; easy to crush manually. (2) Marginally tough; moderately resistant to manual crushing. (3) Tough; strongly resistant to manual crushing. (4) Very tough; requires initial crushing on the hydraulic press. (5) Very tough and ductile; cannot be crushed. Requires drilling or rolling to obtain braze forms. <p>(b) 1400°F, 1/2 hr., FC to 1025°F, hold 24 hrs., FC to RT (Vac.: 1.0×10^{-4} Torr, or better)</p>				

- Interstitital-element contamination is not likely a significant problem with the subject braze alloys (current processing) and probably does not contribute materially to the basic structural problem of marginal toughness/ductility (current processing).
- Rare-earth metal additions apparently contribute to matrix instability and act to aggravate problems of marginal toughness/ductility.
- Inasmuch as no benefit to commintion resistance (RT toughness) was realized through interstitial-contaminant scavenging, no further study of rare earths or other scavenging agents was indicated for this braze development program.

General Comments, End of Phase II

Braze optimization efforts to improve RT comminution resistance (as a measure of toughness) were concentrated on post-braze isothermal aging studies, post-braze cyclic annealing studies, and rare-earth-metal (interstitial-solute) scavenging studies. Cyclic annealing and interstitial-solute scavenging were found to be generally ineffective with the 12 semi-final braze candidates. However, specific isothermal aging treatments (sub-eutectoid temperatures) were found to significantly enhance RT comminution resistance of certain Ti-Zr-Ni-Cu and Ti-Zr-Ni alloys; for two candidate alloys, AC5-16 and AC5-18, up to the toughness level of the TiCuNi baseline alloy [viz. ICR 3(+)] (see Figs. 29 and 30). This trend toward improvement in toughness was believed to derive from favorable, more equilibrium modes of transformation of beta matrices. [The Ti-Zr-Cu-Mn system alloys were ultimately dismissed because of invariably marginal to submarginal ingot comminution resistances.] Because all 12 semi-final braze designs suffered some impairment in comminution resistance (toughness at high-strain-rates) following certain other isothermal aging treatments (see Figs. 27-32); the advisability of attempting control of beta-matrix transformation to develop optimum toughness appeared to be patently obvious. To implement proper post-braze thermal treatment(s), a future study of candidate-braze phase transformation(s) was indicated and recommended.

From an overall viewpoint, the following three (3) candidate alloys appeared to possess superior combined potentials for meeting toughness and other screening criteria (Phase I and Phase II) and were recommended as braze finalists for further characterization in Phase III (Fig. 1 and Table 29).

Table 29
RECOMMENDED BRAZE FINALISTS

Candidate Alloy (Finalist)	Nominal Composition	Ingot Comminution Rating (ICR)	
		As-Cast	After Preferred Isothermal Aging (1025°F)
AC5-16 (Ti-Zr-Ni-Cu)	Ti-27.2Zr-15Ni-7Cu	3	3(+)
AC5-18 (Ti-Zr-Ni)	Ti-41Zr-18Ni	3	3(+)
AC1-20 (Ti-Zr-Cu)	Ti-28.8Zr-28Cu	3	3
Note: ICR = 3, signifies "Tough, strongly resistant to manual crushing".			

BRAZE CHARACTERIZATION (PHASE III)

In this final phase of work, more stringent assessments were made than before of the candidate-braze potentials for useful, long-term RT-800°F service under applied high shear stresses and/or strong peel moments, combined with adverse environmental conditions (see Section III). In particular, machined single-lap shear specimens were tested under stress-rupture conditions at 800°F (static air), at graduated shear stresses $\geq 70\%$ of nominal (RT) shear-strength levels, for total elapsed rupture times on the order of 500 hours. Double-lap braze peel specimens were tested at a slow-strain rate (RT) to measure relative energy parameters to initiate and propagate braze-line peel cracking, and to initiate and propagate BAZ and ultimate substrate-sheet failure for each candidate-braze finalist. Peel-energy testing also served to rank braze candidates by the relative energy requirements to induce braze fracture under slow-strain-rate, for comparison with their corresponding (energy-related) rankings of ingot-comminution resistance (ICR, or cast-structure toughness), obtained in prior work at high strain rate. Finally, machined standard-size single-lap tensile-shear specimens were tested at both RT and 800°F (air), in the as-brazed + dehydrided condition (baseline) and also following 100-hour environmental conditioning (Section 3) at:

- 100°F, Aqueous salt spray
- 800°F, Moving-air oxidation
- 800°F, Hot-salt accretion in moving air

The three braze finalists recommended in the section entitled "General Comments, End of Phase III", page 113, were approved by the sponsor for Phase III studies. These braze alloys were AC5-16 (Ti-Zr-Ni-Cu system), AC5-18 (Ti-Zr-Ni system) and AC1-20 (Ti-Zr-Cu system), tested versus the baseline alloy, C2-5 (Ti-Cu-Ni system) (see Table 15). Original plans for comparison fatigue testing and flexure-beam testing were cancelled because of the inadvisability of employing conventional machining techniques (necessary for dimension control) and the related present inability to control precision braze specimen dimensions by any other technique. (Reproducible specimen dimensions and uniform braze contouring were felt to be much more critical considerations for surface-stress sensitive fatigue testing and flexure testing than for the simple lap shear tensile specimens tested in Phases I, II, and III.) (See Section III.) Very long-term (500-hour) stress-rupture test regimes were substituted in their place. At sponsor request, all Phase III tests were conducted with specimens in the as-brazed or as-brazed + dehydrided condition (Section III).

Double-Lap Peel-Energy Tests (RT)

Because of the program emphasis on relative toughness rankings, the low-strain-rate peel-energy tests were conducted first. Peel-test data for the as-brazed condition are tabulated in Table 30, and typical specimen loading versus cumulative crosshead movement plots are displayed in Figures 53-55. These curves show points of occurrence of minor braze-line peel cracks (weakly audible, but not readily visible by eye), major braze-line peel cracks (audible, and readily discernible), the stress point (A) where the braze-line peel crack invariably terminates and cracking transfers to the BAZ and substrate sheet, and point (B) where the specimen ultimately fails by tensile fracture in the substrate sheet. In all test instances, the braze-line peel cracks propagated about one-quarter the half-inch joint-overlap distance (i.e., ~0.12-0.14 in.) before the locus of cracking transferred to the substrate sheet (i.e., at Point A). The energy parameter correlatable with the mechanical energy expended to initiate and propagate fillet and braze-line peel cracking was taken as the area under each subject curve from test initiation to point (A). [(See Table 30 under column (A).] The parameter representing additional energy expended (required) to propagate BAZ and substrate-sheet cracking to the point of failure was taken as the area under each subject curve between points (A) and (B). [See Table 30 under column (B) - (A).] See Figure 4 for peel-test specimen configuration.

The peel-energy data constitutes the strongest identification and endorsement (in the program) of the innate high toughness potentials of the candidate Ti-Zr base alloys. The three braze finalists, and especially alloy AC5-16, show marked superiority in peel-energy requirements over the C2-5 baseline alloy (see Table 30 and Figs. 53-55). For example, the energy parameters for braze-line peel (Column A) are about 1.5 to 2.0 times greater for the braze-finalists versus the baseline alloy. [The same favorable ratios are valid for the total-energy parameter, Column (B).] Highest values associated with braze peel were recorded for AC5-18 (40,200 lbs. x in. x 10^{-3}), contrasted with a top parameter value of only 22,800 lbs. x in. x 10^{-3} for the C2-5 baseline. The superior metallurgical compatibility of the AC5-16 braze and its associated low-temperature braze processing (1750°F) with the Ti-6Al-4V substrate became evident when comparing the energy parameters for propagation of BAZ and substrate-sheet fracture; Column [(B) - (A)]. Here, the energy parameters for AC5-16 alloy specimens are consistently about 4.0 times greater in magnitude than those for the C2-5 baseline. This high and favorable ratio is presumably related to obvious grain coarsening and beta-embrittlement structures developed within the substrate sheet of baseline specimens by the high braze processing temperature for C2-5 (viz. 1850°F). Note the low energy parameters for C2-5 specimens (4,300 and 5,500 lbs x in. x 10^{-3}). None of the substrate sheet components comprising the three braze-finalist specimens showed any evidence of beta embrittlement or grain coarsening, again because of the lower (common) braze process temperature of 1750°F. The energies expended to propagate substrate-sheet cracking were, in all cases, substan-

Table 30
RESULTS OF DOUBLE-LAP PEEL-ENERGY TESTS (RT)

(As-Brazed Condition)		Energy Parameters(*) [Pounds x Inches x 10 ⁻³]				
Braze Alloy	Specimen Number	Load at First Audible Crack	Maximum Load (lbs)	Cumulative Crosshead Movement at Maximum Load (in. x 10 ⁻³)	Energy Expended to Point of Termination of Braze-Line Peel Fracture; Initiation of BAZ (Substrate Sheet) Fracture (A)	Energy Expended in Propagating Substrate Fracture [(B) - (A)]
C2-5 (baseline)	(-1)	200	390	42	20,000	4,300
	(-2)	190	394	75	22,800	5,500
AC5-16	(-1)	185	554	49	38,200	17,200
	(-2)	142	480	85	35,400	17,100
AC5-18	(-1)	150	420	139	40,200	7,100
	(-2)	140	419	90	37,100	14,900
AC1-20	(-1)	75	428	83	34,600	11,400
	(-2)	80	472	75	31,800	7,900
* Area under the curve of specimen loading versus cumulative crosshead movement (Ref. Fig. 53-55).						

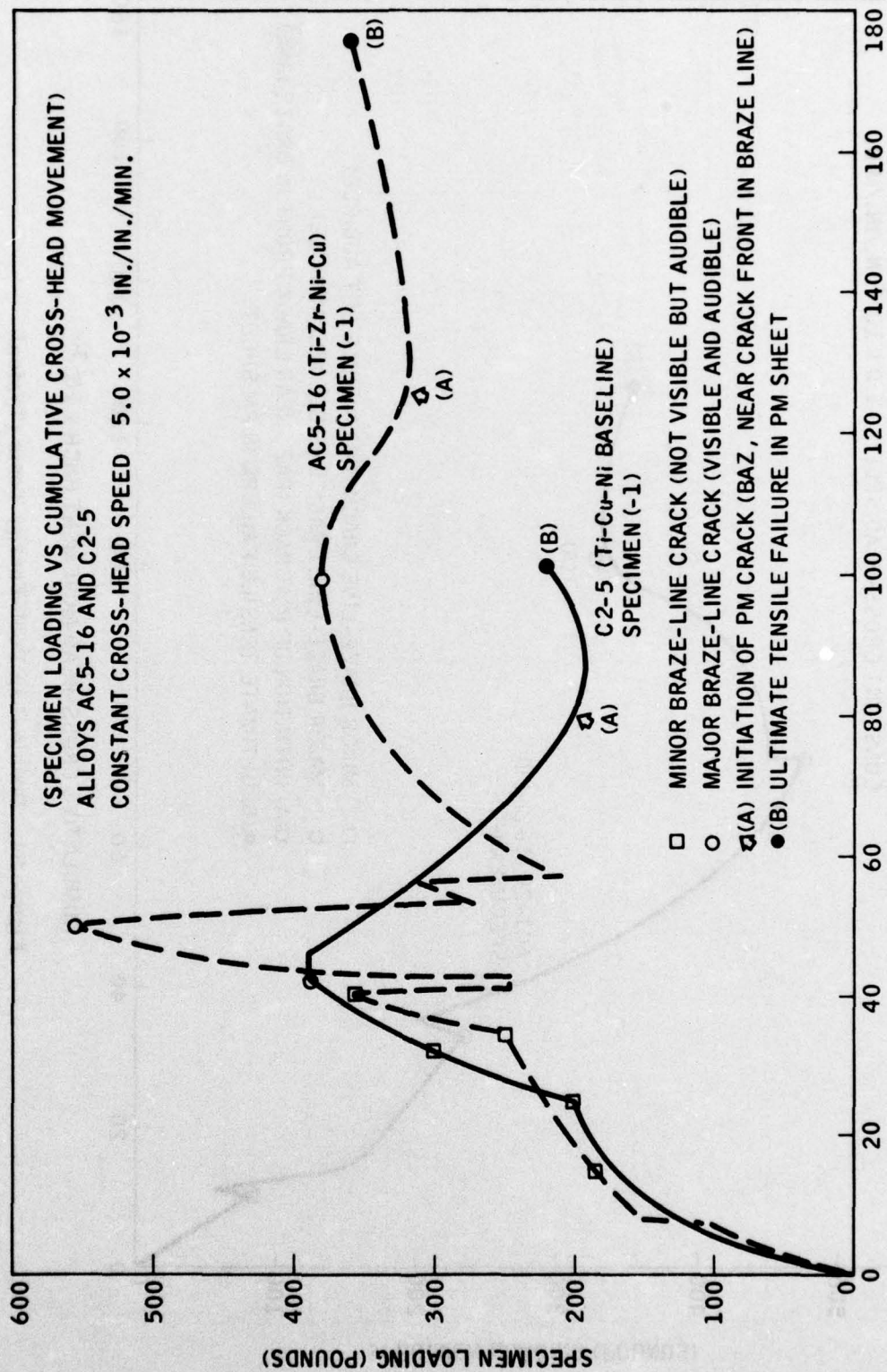


Figure 53. Double-Lap Peel-Energy Tests (Typical)

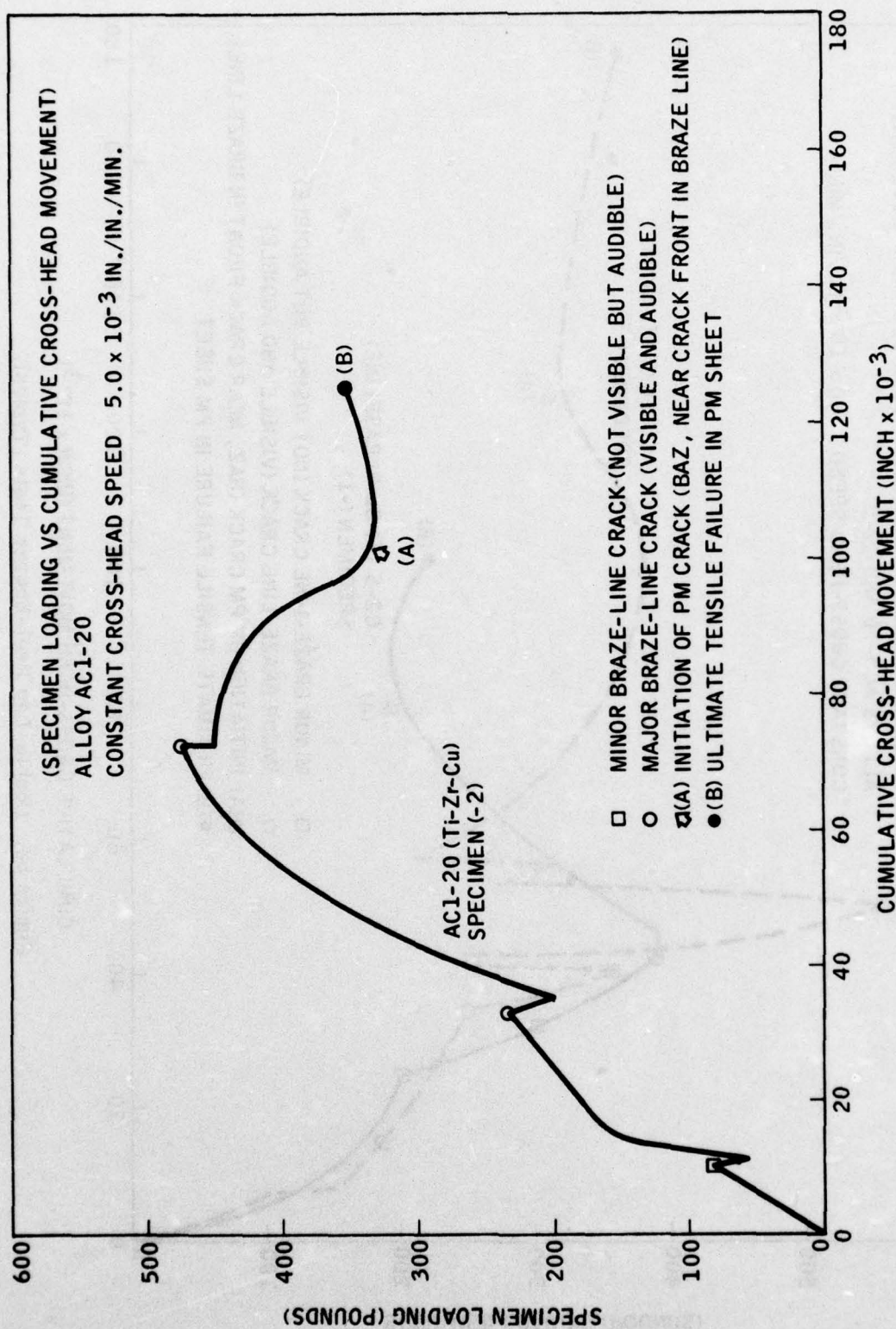


Figure 54. Double-Lap Peel-Energy Tests (Typical)

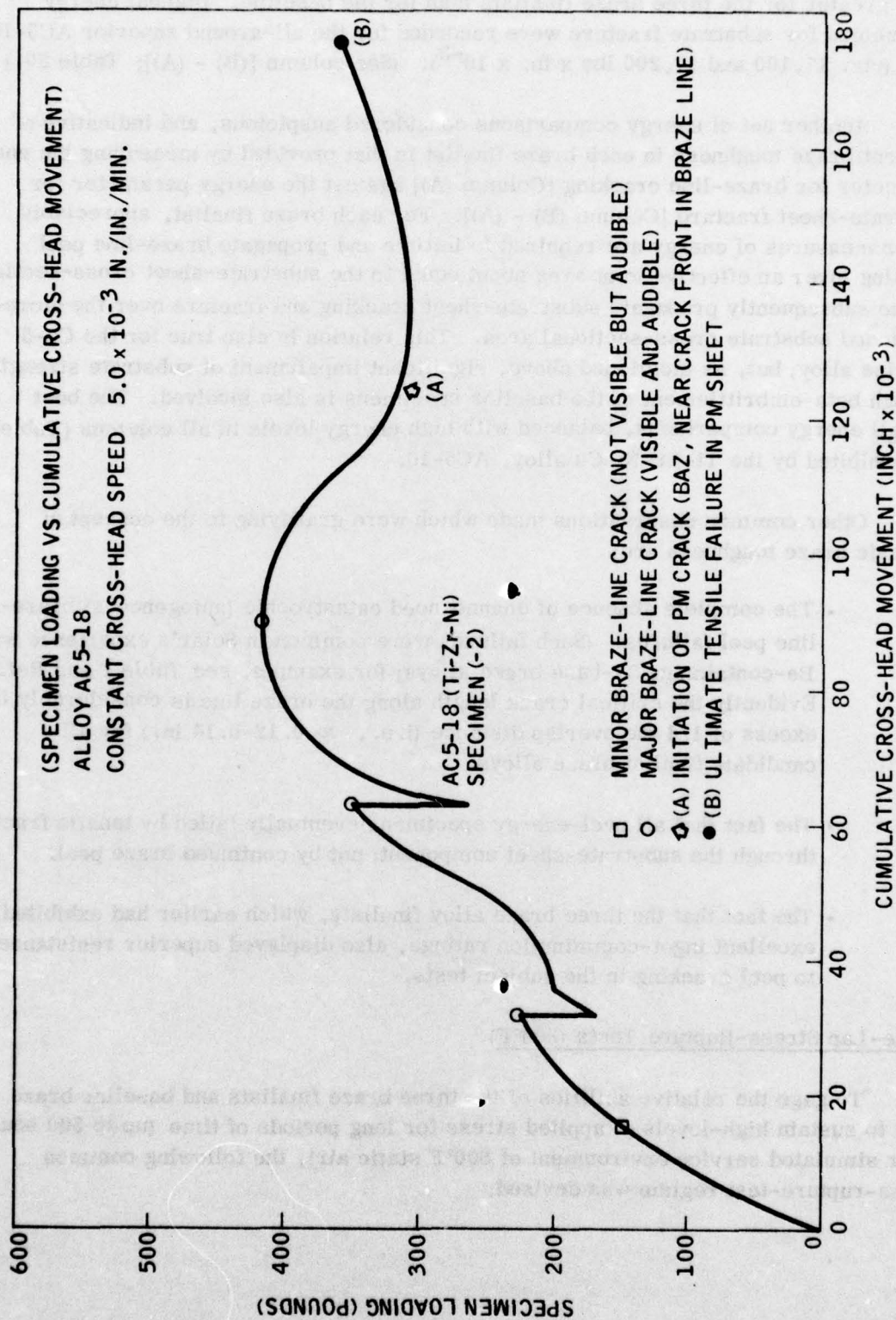


Figure 55. Double-Lap Peel-Energy Tests (Typical)

tially greater for the three braze finalists than for the baseline. Highest energy parameters for substrate fracture were recorded for the all-around superior AC5-16 alloy (viz. 17,100 and 17,200 lbs x in. x 10^{-3}). (See column [(B) - (A)]; Table 30.)

Another set of energy comparisons considered auspicious, and indicative of inherent braze toughness in each braze finalist is that provided by measuring the energy parameter for braze-line cracking [Column (A)] against the energy parameter for substrate-sheet fracture [Column (B) - (A)]. For each braze finalist, appreciably larger measures of energy are required to initiate and propagate braze-line peel cracking (over an effective joint area about equal to the substrate-sheet cross-section) than to subsequently propagate substrate-sheet cracking and fracture over the aforementioned substrate sectional area. This relation is also true for the C2-5 baseline alloy; but, as mentioned above, significant impairment of substrate strength through beta-embrittlement of the baseline specimens is also involved. The best overall energy comparisons, balanced with high energy levels in all columns (Table 30) are exhibited by the Ti-Zr-Ni-Cu alloy, AC5-16.

Other common observations made which were gratifying to the concept of intrinsic braze toughness are:

- The complete absence of unannounced catastrophic (autogeneous) braze-line peel failures. (Such failures were common in Solar's experience with Be-containing, Ti-base braze alloys; for example, see Table 1 and Ref. 1). Evidently the critical crack length along the braze line is considerably in excess of 1/4 the overlap distance (i.e., $\gg 0.12-0.14$ in.) for all candidate finalist braze alloys.
- The fact that all peel-energy specimens eventually failed by tensile fracture through the substrate-sheet component; not by continued braze peel.
- The fact that the three braze alloy finalists, which earlier had exhibited excellent ingot-comminution ratings, also displayed superior resistance to peel cracking in the subject tests.

Single-Lap Stress-Rupture Tests (800°F)

To gage the relative abilities of the three braze finalists and baseline braze alloy to sustain high-levels of applied stress for long periods of time (up to 500 hours; under simulated service environment of 800°F static air), the following common stress-rupture-test regime was devised:

Sequential Stress
Regime (800°F)

- (1) 25.0 ksi, nominal shear stress; hold 165 hours;
then increase to
- (2) 27.5 ksi, nominal shear stress; hold 165 hours;
then increase to
- (3) 30.0 ksi, nominal shear stress; hold 150 hours;
then increase to
- (4) 32.5 ksi, nominal shear stress; hold 100 hours;
then increase to
- (5) 35.0 ksi, nominal shear stress; hold 100 hours;
then increase to
- (6) 37.5 ksi, nominal shear stress; hold 100 hours;
then increase to
- (7) 40.0 ksi, nominal shear stress; hold to failure.

Full-sized tensile-shear specimens were employed, in the as-brazed plus vacuum dehydrated condition (Section III). Gage sections were machined post-braze by ECM.

It was demonstrated first that the C2-5 baseline brazements fail typically at high rupture stresses in the range of 35.0-40.0 ksi, when subjected to the above testing format (i.e., starting at a nominal shear stress of 25.0 ksi, which corresponds to about 70 percent of average short-term tensile shear strength(s) for both the baseline and candidate braze alloys). In fact, nominal tensile-shear strengths (RT-800°F) for the baseline braze also fall in the typical range 35-40 ksi. Under the above long-term rupture testing regime, then, the baseline-alloy brazements tended to fail over approximately the same range of nominal shear strengths as recorded in prior (short-term) tensile shear strength tests (RT and 800°F). With the exception of alloy AC5-18, (see Table 31) the candidate braze finalists (AC5-16 and AC1-20) also exhibited the same favorable and parallel relation between short-term (tensile) and long-term (rupture) strengths (viz. common range of 30-35 ksi); again indicating good potential for braze strength retention under stringent conditions of long-term, high-stress service at 800°F (see Section entitled "Braze Optimization Studies (Phase II), page 71). However, though the failure stresses are similar for the subject tensile-shear and rupture-shear tests, the loci of ultimate brazement fracture shifted dramatically from 100 percent braze-line fracture (i.e., interface separation; for short-term tensile shear) to 100 percent BAZ/PM fracture (for long-term stress rupture). [The single exception noted was Alloy AC5-18, which persisted in 100 percent braze-line fracture in rupture testing, and displayed extremely short rupture life at 800°F on initial loading at 25 ksi; see Table 31.] The obvious inference can be drawn from these observations that long-term isothermal holding at 800°F during rupture testing has strengthened and toughened the braze structure in the braze overlap regions to the extent that the locus of ultimate fracture is transferred from initial braze cracks to the parent metal or substrate sheet (PM). This transfer of fracture location under shear

Table 31

COMPARATIVE DATA: 800°F STRESS-RUPTURE TESTS

Environment: 800°F Air (Static)
 Specimen: Single-Lap Tensile Shear (Ti-6Al-4V; 2t Overlap)
 Stress Level: Stressed sequentially from a base level of 25.0 ksi, nominal shear stress, in stress increments of 2.5 ksi to rupture failure (see holding-time regime below)

Test Number	Braze Alloy	Nominal Shear Stress Levels (Sequentially Applied) and Corresponding Holding Times (Hours)							Locus of Rupture Failure	Cumulative Holding Time Under Rupture Stress (Hours)	Specimen Width (mils)
		25.0 ksi (hours)	27.5 ksi (hours)	30.0 ksi (hours)	32.5 ksi (hours)	35.0 ksi (hours)	37.5 ksi (hours)	40.0 ksi (hours)			
R-1	C2-5 (baseline)	165	165	150	100	6 ⁽¹⁾	---	---	BAZ/PM ⁽²⁾	586	481
R-2	C2-5 (baseline)	165	165	150	100	100	100	≤0.1 ⁽¹⁾	BAZ/PM ⁽²⁾	680	506
R-4	AC5-16	165	165	150	76 ⁽¹⁾	---	---	---	BAZ/PM ⁽²⁾	556	415
R-5	AC5-16	165	165	150	100	4 ⁽¹⁾	---	---	BAZ/PM ⁽²⁾	584	503
R-6	AC1-20	165	165	68 ⁽¹⁾	---	---	---	---	Braze (50%); then opposite BAZ/PM ⁽²⁾	398	520
R-7	AC1-20	165	165	89 ⁽¹⁾	---	---	---	---	"	419	519
R-8	AC5-18	0.4 ⁽¹⁾	---	---	---	---	---	---	Braze	0.4	518
R-9	AC5-18	0.4 ⁽¹⁾	---	---	---	---	---	---	Braze	0.4	540

(1) Brazement failure at time indicated.
 (2) Fracture initiation in braze fillet and BAZ; ultimate failure in adjacent PM.

loading occurred in every instance, even though (prior) braze-fillet cracking due to joint rotation was invariably involved; and in the case of Alloy AC1-20 test brazements, 50 percent braze-line cracking preceded the transfer (see Table 31). It can be reasonably assumed that the braze strengthening/toughening is induced by braze/substrate interdiffusion and/or more favorable braze matrix (beta) transformation in the narrow-gap (0.002 in.) overlap regions. If this assumption is valid, post-braze diffusion treatments might profitably be employed to enhance braze toughness/strength for the subject braze alloys in future development (see also section entitled "Single-Lap Tensile Shear Tests", page 123 for possible confirmation of this assumption). It should be noted that the nominal rupture stress in the parent metal or substrate sheet

is exactly double the value of nominal shear stress applied to the braze joint, because of the 2t overlap relation.

The subject long-term rupture tests performed an important function in ranking the relative capabilities of the different braze finalists for sustaining high shear loads at the maximum design service temperature of 800°F. Duplicate tests were run. As expected, the C2-5 baseline braze alloy, with maximum primary terminal solid-solution, exhibited the best stress-rupture performance; failing only after cumulative holding times of 586 and 680 hours, and at final rupture stresses of 35 ksi and 40 ksi, respectively, see Table 31. Of the braze candidate finalists, the usually superior AC5-16 braze alloy (Ti-Zr-Ni-Cu) proved again to be the best contender; failing in rupture after 556 and 584 hours, at final rupture stresses of 32.5 ksi and 35.0 ksi, respectively. The Ti-Zr-Cu alloy, AC1-20, provided a respectable second-best performance; failing in rupture after 398 and 419 hours, (both specimens) at a final rupture stress of 30 ksi. The above three braze alloys proved themselves capable of sustaining high shear stresses ($\geq 70\%$ of short-term shear strength levels) for long periods of 400 hours or more at 800°F. In contrast, the Ti-Zr-Ni alloy candidate, AC5-18, was demonstrated to be significantly weaker in stress-rupture at 800°F, (both specimens) failing in only 0.4 hour at 25 ksi (Table 31). As mentioned previously, both rupture failures propagated through the braze joints, typical of tensile shear testing. Although not apparently suited to high design levels of shear-stress, the AC5-18 alloy might still be suitable for low-stress applications to 800°F.

None of the braze alloys tested showed any visible signs of structural deterioration or other adverse reaction with the 800°F air environment, in spite of the high stresses and long holding times experienced.

Single-Lap Tensile Shear Tests (Environmental Conditioning)

The final braze characterization tests involved determination of tensile shear strengths (RT and 800°F) following long-term, harsh environmental conditioning. Full-size tensile shear specimens were employed, in the brazed plus ECM'd and vacuum dehydrided condition (similar to rupture-test specimen preparation). Vacuum dehydriding* following ECM was found to be necessary because of very evident hydrogen embrittlement of entire specimens occurring during ECM (Section III). The three different environmental conditions applied after specimen preparation were:

- 112 hours, moving-air oxidation at 800°F
- 112 hours, aqueous NaCl salt spray at 100°F (ASTM Spec. B1117)
- 112 hours, moving-air oxidation at 800°F (joint regions encrusted with with solid NaCl salt.

*Vacuum-heat treatment: 1025°F, 1 hour, FC to RT.

Details of environmental conditioning are described in Section III.

Baseline tests were conducted first without environmental conditioning using the following braze alloys: C2-5 (baseline) and the three braze candidate finalists AC5-16, AC5-18 and AC1-20 (see Table 32). As mentioned in Section III, control of gage-section width was difficult with ECM machining, yielding random widths from 0.415 in. to 0.616 in., in the subject instance. Fortunately, this variable did not appear to be significant in tensile-shear testing, with very little data scatter attributable to specimen-to-specimen width variation (see Table 32). RT shear strengths were recorded in the rather narrow range of ~34-41 ksi, typical of comparable as-brazed strength levels in prior Phase II screening work. Similarly, the effect of 2 in. versus 4 in. gage length was found to be small or nil, based upon testing in the as-brazed plus dehydrided condition (alloys AC5-16, AC5-18 and AC1-20; Table 32). Consequently, all specimens for environmental conditioning were processed with a 2 inch gage length, because of much better gage width control within each specimen. Another, and more significant processing variable, was that of hand grinding/polishing specimen gage widths after dehydriding as one method of obtaining the desired (exact) specification width (i.e., 0.500 in. \pm 0.002 in.). Careful hand grinding/polishing with 120 to 320 mesh metallographic papers had no apparent effect on the strengths of the C2-5 and AC5-16 alloys, but did drastically reduce the RT shear strengths of alloys AC5-18 and AC1-20 (levels of 10.6/14.1 ksi and 12.9/19.9 ksi, respectively; Table 32). As described in Section III, all candidate braze alloys and the baseline suffered braze damage due to mechanical machining in early Phase III work (hence the subsequent use of ECM); and the deleterious effects of even hand grinding on AC1-20 and AC5-18 may be an additional aspect of this problem. At any rate, on the basis of these findings, the C2-5 baseline braze and the AC5-16 candidate braze alloy were selected for environmental conditioning studies; and the AC1-20 and AC5-18 alloys were dismissed.

The results of environmental conditioning proved to be very encouraging, for both the C2-5 baseline and the superior candidate braze, AC5-16. As expected, the long-term salt spray exposure had no apparent visual effect on the braze specimens (original surface or fracture surface). The long-term 800°F air exposures (with and without hot-salt coating) developed a smooth black surface film and a light blue tarnish (respectively), but again no evidence of surface cracking or other structural damage. The advantages of similar-metal braze design were further supported by the RT and 800°F shear data. One can conclude (on reviewing all the data in Table 32) that the severe environmental conditions applied resulted in no significant changes in tensile shear strength levels or in normal failure modes. Shear strength levels following each of the three conditions simulating harsh service all fall within the range of ~30-38 ksi (AC5-16; RT and 800°F) and 34-42 ksi (C2-5; RT and 800°F). The C2-5 baseline braze specimens invariably fail in the substrate sheet alloy (PM), after cracking initiates in the BAZ of the sheet. This is believed due to beta-embrittlement of the sheet, occurring at the high 1850°F braze temperature. At room-temperature, the AC5-16 brazements almost always fail along the braze line; but at 800°F there is

Table 32

COMPARATIVE DATA: TENSILE SHEAR STRENGTH TESTS (RT AND 800°F)

Environment: Static Air (RT and 800°F)

Specimen: Standard size (Ti-6Al-4V; 2t overlap, 0.125 in.) (Fig. 3);
test section machined by ECM post-brazing; vacuum
dehydrating treatment applied after machining (1025°F, 1
hour, FC to RT). No gage-section hand polishing after
dehydrating except as indicated.

Brazing Temperature (°F)	Brazing Alloy	Pre-Test Conditioning	Nominal Shear Stress At Fracture (ksi) At Indicated Test Temperature		Specimen Gage Width (inch)	
			RT	800°F	RT	800°F
1850	C2-5 (baseline)	(A) As-brazed (plus ECM and dehydride)	40.0 ⁽¹⁾ 38.5 ⁽¹⁾	43.3 ⁽¹⁾ 41.4 ⁽¹⁾	0.610 0.612	0.548 0.554
		(B) As above; plus 10-20 mils hand polished from specimen width (120 and 320 mesh papers)	37.8 ⁽¹⁾ 38.1 ⁽¹⁾	--	0.499 0.499	--
1750	AC5-16	(A) As-brazed (plus ECM and dehydride)	36.7 ⁽²⁾ 34.0 ⁽²⁾ 36.6 ⁽²⁾⁽³⁾ 37.2 ⁽²⁾⁽³⁾	37.0 ⁽¹⁾ 35.6 ⁽¹⁾ -- --	0.522 0.470 0.463 0.462	0.528 0.505 -- --
		(B) As above; plus 10-20 mils hand polished from specimen width (120 and 320 mesh papers)	35.9 ⁽²⁾ 38.8 ⁽²⁾	-- --	0.498 0.502	-- --
1750	AC1-20	(A) As-brazed (plus ECM and dehydride)	36.8 ⁽²⁾ 34.7 ⁽²⁾ 38.6 ⁽²⁾⁽³⁾ 41.5 ⁽¹⁾⁽³⁾	-- -- -- --	0.601 0.605 0.464 0.464	-- -- -- --
		(B) As above; plus 10-20 mils hand polished from specimen width (120 and 320 mesh papers)	19.9 ⁽²⁾ 12.9 ⁽²⁾	-- --	0.499 0.498	-- --
1750	AC5-18	(A) As-brazed (plus ECM and dehydride)	35.8 ⁽²⁾ 35.1 ⁽²⁾ 35.9 ⁽²⁾⁽³⁾ 34.7 ⁽²⁾⁽³⁾	-- -- -- --	0.616 0.609 0.459 0.499	-- -- -- --
		(B) As above; plus 10-20 mils hand polished from specimen width (120 and 320 mesh papers)	10.6 ⁽²⁾ 14.1 ⁽²⁾	-- --	0.498 0.498	-- --
1850	C2-5 (baseline)	(A) As-brazed (plus ECM and dehydride) PLUS (C) 112 hours exposure, 800°F moving air (oxidation)	34.7 ⁽¹⁾ 34.2 ⁽¹⁾	42.4 ⁽¹⁾ 40.8 ⁽¹⁾	0.415 0.500	0.543 0.483
1750	AC5-16	(A) As-brazed (plus ECM and dehydride) PLUS (C) 112 hours exposure, 800°F moving air (oxidation)	31.2 ⁽¹⁾ 29.9 ⁽²⁾	29.8 ⁽²⁾ 30.6 ⁽²⁾	0.421 0.496	0.543 0.532
1850	C2-5 (baseline)	(A) As-brazed (plus ECM and dehydride) PLUS (D) 112 hours exposure, 100°F salt spray	38.4 ⁽¹⁾ 40.3 ⁽¹⁾	36.6 ⁽¹⁾ 36.7 ⁽¹⁾	0.506 0.461	0.469 0.498
1750	AC5-16	(A) As-brazed (plus ECM and dehydride) PLUS (D) 112 hours exposure, 100°F salt spray	37.6 ⁽²⁾ 37.2 ⁽²⁾	36.6 ⁽¹⁾ 38.3 ⁽²⁾	0.506 0.495	0.524 0.521
1850	C2-5 (baseline)	(A) As-brazed (plus ECM and dehydride) PLUS (E) 112 hours, coated with hot salt and exposed to 800°F moving air	35.4 ⁽¹⁾ 35.1 ⁽¹⁾	39.1 ⁽¹⁾ 39.3 ⁽¹⁾	0.504 0.542	0.498 0.538
1750	AC5-16	(A) As-brazed (plus ECM and dehydride) PLUS (E) 112 hours, coated with hot salt and exposed to 800°F moving air	35.5 ⁽²⁾ 36.1 ⁽²⁾	31.3 ⁽¹⁾ 33.7 ⁽¹⁾	0.505 0.417	0.422 0.521

(1) BAZ/PM fracture

(2) Braze-line fracture (joint interface)

(3) 4 inch gage length (all others; 2 inch gage length)

about a 50 percent probability of failure in the BAZ/PM. The most gratifying aspect of the 800°F shear test data noted here is the high level of 800°F strength exhibited by the AC5-16 alloy, for all environmental conditioning. (In prior Phase II work, 800°F shear strength levels were appreciably lower. See Section IV, page 69.) The difference is believed due to the 1025°F vacuum dehydriding treatment, which has apparently (though inadvertently) induced braze strengthening through substrate/braze interdiffusion and/or more favorable braze matrix (beta) transformation.

General Comments, End of Phase III

Phase III, braze characterization studies included the effects on shear strength of severe long-term service environments (simulated*), of the types well known to be life-limiting to many titanium-alloy substrate/commercial braze alloy combinations. Specifically, the environmental conditioning consisted of 100 (+) hours exposures in 100°F NaCl salt spray, or 800°F moving air or 800°F moving air with NaCl salt accretion on exposed joints. Of the three candidate braze finalists transferred from Phase II work (viz. AC5-16, AC5-18 and AC1-20), the alloys AC5-18 and AC1-20 were dismissed from this task of Phase III because of apparent extreme sensitivity to damage from hand grinding and polishing of shear specimens, preparatory to environmental conditioning. The remaining candidate braze alloy, AC5-16 (Ti-27.2Zr-15Ni-7Cu), proved to have superlative resistance to structural damage from 800°F oxidation and salt-corrosion reactions, normally associated with the subject environmental conditioning. This can be attributed to similar-metal braze design. Nominal tensile shear strengths (AC5-16) at both RT and 800°F test temperatures were maintained above 30 ksi in spite of the prior harsh conditioning. These are essentially the same shear strength levels as before environmental conditioning (Phase III, baseline), and they also compare favorably with the levels obtained for the C2-5 baseline braze. Moreover, RT shear strength data generated in Phase III with full size (ECM) machined specimens proved very similar to that from Phase I screening tests, which involved sub-size specimens with no machining after brazing (true for all alloys concerned; as-brazed or with environmental conditioning). Of greater importance, the 1025°F, 1 hour vacuum dehydriding treatment, applied to AC5-16 specimens after ECM (Phase III), served to augment 800°F shear strengths to essentially the same levels recorded for RT tests (i.e., ≥ 30 ksi). This short-term thermal treatment may have induced more nearly equilibrium transformation of beta matrix (than for the as-brazed condition); and certainly promoted a significant improvement in 800°F shear strength over the as-brazed (AC5-16) specimens tested in Phase I (see Fig. 22). Retention of higher 800°F shear strengths was excellent even after the harsh environmental conditioning.

*e.g., turbine compressor simulation; maritime or salt-desert application.

The AC5-16 lap shear brazements also exhibited superior long-term stress rupture behavior at 800°F, at high sustained shear stresses ≥ 70 percent of average nominal RT and 800°F shear-strength levels. The candidate braze, AC1-20, recorded a reasonably close second place in stress rupture performance; but AC5-18 proved very weak and wholly unsuitable for high rupture loading at 800°F.

Because of its strongly hypoeutectic cast structure, the high-melting C2-5 (Ti-15Cu-15Ni) baseline alloy exhibited typically a range of about 3 ksi to 12 ksi advantage in fracture strength over candidate alloy brazements (both in RT-800°F short-term tensile shear tests and 800°F long-term stress rupture tests, discussed above). However, the moderately hypoeutectic, lower-melting candidate braze alloys (especially AC5-16, but also AC1-20 and AC5-18) demonstrated marked advantages over C2-5 in the test area of braze-peel toughness (RT); specifically, the intrinsic energy requirements to initiate and propagate braze-line peel cracking. The input-energy requirements for slow-strain-rate, braze-line peel were about 50 percent to 100 percent greater for the three braze-candidate finalists, relative to the C2-5 baseline alloy. This favorable contrast in peel-energy requirements may also be related to the absence of grain coarsening and beta-embrittlement structure in the BAZ and general substrate associated with candidate-alloy brazing at 1750°F; as opposed to the very evident substrate grain coarsening and beta embrittlement obtained in brazing C2-5 alloy at 1850°F.

The significant improvements in 800°F tensile shear strength (Phase III) and high-strain-rate ingot-comminution ratings (ICR; Phase II) obtained through post-braze vacuum heat treatment at 1025°F (AC5-16) prompted the continued recommendation to the sponsor that constituent-phase analyses be conducted (see also "General Comments; End of Phase II"). The purpose would be to determine the different characteristic modes of beta-matrix transformation and (eventually) to select optimum post-braze thermal treatments and associated braze microstructures. ["Optimum" in this context would signify the best combination and levels of brazement strength, toughness and other pertinent design properties.] To this end, the sponsor is currently conducting constituent-phase analysis of AC5-16 braze ingot, under the direction of Dr. J. C. Williams, Department of Materials Science, Carnegie-Mellon University, Pittsburgh, PA (April 1976). Ingot chunks in different heat-treat conditions have been provided to Dr. Williams by Solar Research.

One major processing problem which was not anticipated is the inclination to braze-surface and -subsurface cracking exhibited by the baseline braze and the three candidate-braze finalists during simple machining operations, such as machine milling and grinding. Brazements of AC1-20 and AC5-18 alloys even showed similar sensitivity to finish hand grinding and polishing operations; although C2-5 and AC5-16 brazements could generally be hand ground and polished without inducing braze cracking (post ECM and dehydriding). These limitations on machining precluded the preparation and testing of fatigue and flexure-beam specimens (originally planned for Phase III); which because

of surface-stress sensitivity, require precise specimen dimensions and absence of surface and subsurface cracking to generate reproducible and meaningful data. (It is hoped that eventually, phase analysis work will evolve post-braze thermal treatment(s) which might permit conventional machining with minimal risk of braze cracking.)

From a total-program or overall viewpoint, the AC5-16 braze alloy must be considered the most outstanding similar-metal braze design for elevated-temperature service. AC5-16 also demonstrates the most promise for improvement in toughness and elevated-temperature strength through post-braze thermal treatment. The AC1-20 alloy is a close second to AC5-16, being chosen over AC5-18 primarily because of its superior long-term stress-rupture behavior (800°F).

REFERENCES

1. C. E. Smeltzer, R. K. Malik, A. N. Hammer, and W. A. Compton, "Development of Joining Processes for Titanium Foils", Technical Report AFML-TR-67-305 (Vol. I and II), Air Force Materials Laboratory, Research and Technology Division, Air Force Systems Command, Wright-Patterson Air Force Base, Ohio (Sept. 1967).
2. D. G. Howden, R. E. Monroe, "Feasibility Study of Fabricating Heat Exchangers from Titanium by Brazing", Final Report, Battelle Memorial Institute, Columbus, Ohio, Contract DAAK-02-67-C-0377 (Jan. 31, 1968).
3. M. S. Tucker and K. R. Wilson, "Attack of Ti-6Al-4V by Silver Base Brazing Alloys", Welding Research Supplement to the American Welding Journal (Dec. 1969) pp. 521-S to 527-S.
4. W. A. Compton, C. E. Smeltzer, R. K. Malik and A. N. Hammer, "Brazing Alloys for Titanium Foil Structures", Metals Engineering Quarterly, Vol. 8, No. 3 (August 1968).
5. "Recent Additions to WESGO's Line of Brazing Alloys", Company brochure dated February, 1972, Western Gold and Platinum Co., Belmont, California.
6. "AMDRY Tibeloy Brazing Alloys for Titanium, Beryllium, and Dissimilar Metal Brazing", Company brochure dated December 1971, Alloy Metals, Inc. Troy, Michigan.
7. J. R. Woodward, "Development of a Filler Metal and Joining Process for Titanium-Alloy Honeycomb Panels", Final Technical Report No. AFML-TR-73-125 on Contract F33615-71-C-1888, Air Force Materials Laboratory, Department of the Air Force, Wright-Patterson Air Force Base, Ohio (July 1973).
8. R. R. Wells, "Diffusion Bonding and Brazing", article in DMIC Memorandum #215 (Sept. 1, 1965) entitled "Titanium-1966; Lectures Given at a Norair Symposium, March 28-29, 1966".
9. "Advances in Aerospace Materials - Processing Technology; Titanium Impact Feature", Metal Progress, Vol. 105, No. 3, pp. 53-57 (March 1974).

10. R. A. Wood, "Beta Titanium Alloys", Report No. MCIC-72-11, Metals and Ceramics Information Center; Battelle Columbus Laboratories, Columbus, Ohio (Sept. 1972).
11. G. S. Hall, S. R. Seagle and H. B. Bomberger, "Development of a 900°F Titanium Alloy", Air Force Materials Laboratory, Wright-Patterson Air Force Base, Ohio, Technical Report AFML-TR-73-37 (April 1973).
12. E. W. Collings, J. C. Ho, and R. I. Jaffee, "Theory of Titanium Alloys for High-Temperature Strength", Air Force Materials Laboratory, Wright-Patterson Air Force Base, Ohio, Technical Report AFML-TR-71-228 (Oct. 1971).
13. C. J. Rosa, "Basic Mechanisms Providing Oxidation Resistance in Structural Metals at High Temperatures", Naval Air Development Center, U.S. Naval Air Systems Command, Warminster, PA., Final Report on Contract N62269-73-C-0520 (January 1974).
14. M. Hansen, "Constitution of Binary Alloys", McGraw-Hill Book Company, New York (1958).
15. R. P. Elliott, "Constitution of Binary Alloys", First Supplement, McGraw-Hill Book Company, New York (1965).
16. F. A. Shunk, "Constitution of Binary Alloys", Second Supplement, McGraw-Hill Book Company, New York (1969).
17. W. R. Young and E. S. Jones, "Alloy Systems for Brazing of Columbium and Tungsten", Directorate of Materials & Processes, Air Force Systems Command, Wright-Patterson Air Force Base, Ohio, Technical Documentary Report ASD-TR-61-592 (January 1962).
18. Ye. K. Molchanov "Atlas of Diagrams of State of Titanium Alloys", Translated from the Russian by Foreign Technology Division, Air Force Systems Command, Wright-Patterson Air Force Base, Ohio, Report FTD-MT-65-387 (August 1967).
19. "Residual Stress Measurement in Metals and Plastics", Quarterly Newsletter (No. 25, 1974), Fulmer Research Institute, Ltd., Stoke Poges, England.
20. D. J. Maykuth, et al., "Titanium Base Alloys, 6Al-4V", Processes and Properties Handbook, Defense Metals Information Center (DMIC), Battelle Memorial Institute, Columbus, Ohio (Feb. 1971).

21. A. G. Freedman, "Basic Properties of Thin-Film Diffusion-Brazed Joints in Ti-6Al-4V", Welding Research Supplement, The American Welding Journal, pp. 343-S to 356-S (August 1971).
22. M. Young, E. Levine, and H. Margolin, "The Aging Behavior of Orthorhombic Martensite in Ti-6-2-4-6", Metallurgical Transactions, Vol. 5 (August 1974).
23. Metals Handbook; Heat Treating, Cleaning and Finishing, 8th Edition, Vol. 2, American Society for Metals, Metals Park, Ohio (1964).
24. C. E. Smeltzer, R. K. Malik, A. N. Hammer and W. A. Compton, "Development of Joining Processes for Titanium Foils", Air Force Materials Laboratory, Wright-Patterson Air Force Base, Ohio, Technical Report AFML-TR-67-305, Vols. I and II (Sept. 1967).
25. L. Kaufmann and H. Nesor, "Computer Analysis of Alloy Systems", Technical Report No. AFML-TR-73-56, Air Force Materials Laboratory, Air Force Systems Command, Wright-Patterson Air Force Base, Ohio (March 1973).
26. W. M. Latimer and J. H. Hildebrand, Reference Book of Inorganic Chemistry, McMillan Co., (New York, Third Edition, 1952) pp. 451-461.
27. K. A. Gschneider, N. Kppenhan, and D. McMasters, "Thermochemistry of the Rare Earths; Part 1. Rare Earth Oxides", Report No. IS-RIC-6, Rare Earth Information Center, Institute for Atomic Research, Iowa State University, Ames, Iowa (Aug. 1973).
28. K. A. Gschneider and N. Kippenhan, "Thermochemistry of the Rare Earth Carbides, Nitrides and Sulfides for Steelmaking", Report No. IS-RIC-5; Rare Earth Information Center, Institute for Atomic Research, Iowa State University, Ames, Iowa (Aug. 1971).
29. K. A. Gschneider, Rare Earth Alloys, D. Van Nostrand Co., Princeton, NJ (1961).

APPENDIX

COMPILATION OF PRINCIPAL EXPERIMENTAL BRAZE ALLOYS (PHASE I)

Designation	Composition (% Wt.)						Fusion Temperatures		ICR ⁽²⁾
	Ti	Zr	Co	Cr	Cb	Ta	Solidus (°F)	Liquidus ⁽¹⁾ (°F)	
A10-1	45.0	45.0	10.0				2100	2280	-
A10-2	42.5	42.5	15.0				1900	1950	-
A10-3	40.0	40.0	20.0				1730	1800	-
A10-4	37.5	37.5	25.0				1750	1770	-
A11-1	45.0	45.0	6.0	4.0			1850	>2200	-
A11-2	42.5	42.5	9.0	6.0			1850	2060	-
A11-3	40.0	40.0	12.0	8.0			1750	1840	-
A11-4	37.5	37.5	15.0	10.0			1770	1870	-
A12-1	45.0	45.0	7.9		2.1		1870	>2330	-
A12-2	42.5	42.5	11.8		3.2		1870	>2250	-
A12-3	40.0	40.0	15.8		4.2		1770	1880	-
A12-4	37.5	37.5	19.6		5.4		1790	1840	-
A14-1	45.0	45.0	6.8			3.2	1970	>2300	-
A14-2	42.5	42.5	10.2			4.8	1930	>2320	-
A14-3	40.0	40.0	13.6			6.4	1860	2030	-
A14-4	37.5	37.5	17.0			8.0	1780	1850	-
			V						
E1	16.0	56.0	28.0				2070	2090	4/5
E17	19.0	55.0	26.0				2150	2230	4/5
E7	45.0	35.0	20.0				>2550	--	4/5
E18	40.0	40.0	20.0				2550	>2600	4/5
E9	35.0	45.0	20.0				2450	2490	4/5
E19	30.0	50.0	20.0				2410	2460	4/5
E10	25.0	55.0	20.0				2350	2480	4/5
E20	45.0	40.0	15.0				>2500	--	4/5
E21	40.0	45.0	15.0				>2550	--	4/5
E22	35.0	50.0	15.0				>2600	--	4/5
E23	30.0	55.0	15.0				2450	>2500	4/5
E24	45.0	30.0	25.0				2565	--	4/5
E25	40.0	35.0	25.0				2495	--	4/5
E26	35.0	40.0	25.0				2470	2520	4/5
E27	30.0	45.0	25.0				2350	2440	4/5
E28	25.0	50.0	25.0				2350	2390	4/5

(1) Outstanding braze characteristics (T-joint configuration)

(2) Resistance to Crushing:

- (1) Brittle; easy to crush manually.
- (2) Marginally tough; moderately resistant to manual crushing.
- (3) Tough; strongly resistant to manual crushing.
- (4) Very tough; requires initial crushing on the hydraulic press.
- (5) Very tough and ductile; cannot be crushed. Requires drilling or rolling to obtain braze forms.

Designation	Composition (% Wt.)									Fusion Temperatures		ICR ⁽²⁾
	Ti	Zr	V	Ni	Co	Fe	Be	Cu	Mn	Solidus (°F)	Liquidus ⁽¹⁾ (°F)	
E16	45.0	25.0	30.0							>2500	--	4/5
E8	25.0	45.0	30.0							2240	2310	4/5
E6	35.0	35.0	30.0							2400	2450	4/5
E29	30.0	40.0	30.0							2480	2560	4/5
E30	40.0	30.0	30.0							2520	2590	4/5
E31	20.0	50.0	30.0							2220	2280	4/5
E32	25.0	40.0	35.0							2350	2460	4/5
E33	20.0	45.0	35.0							2250	2280	4/5
E34	15.0	50.0	35.0							2230	2260	4/5
E35	20.0	47.5	32.5							2210	2230	4/5
E36	15.0	52.5	32.5							2200	2220	3+/4
E37	15.0	60.0	25.0							2260	2280	4/5
E38	20.0	57.5	22.5							2270	2310	4/5
E39	15.0	62.5	22.5							2190	2280	4/5
E40	20.0	60.0	20.0							2330	2380	4/5
E41	15.0	65.0	20.0							2270	2340	4/5
E42		70.0	30.0							2275	2275	3+/4
E43	15.0	45.0	40.0							2230	2270	4/5
E44	10.0	60.0	30.0							2180	2210	3+/4
E45	10.0	55.0	35.0							2170	2270	4/5
E46	10.0	65.0	25.0							2220	2280	3+/4
E47	10.0	50.0	40.0							2170	2280	4/5
E48	10.0	70.0	20.0							2220	2380	3+/4
E49	20.0	40.0	40.0							2220	2440	4/5
E50	10.0	45.0	45.0							2200	2280	4/5
E51	5.0	50.0	45.0							2200	2250	4/5
E52	17.5	50.0	32.5							2220	2240	4/5
E53	20.0	52.5	27.5							2230	2240	4/5
E54	5.0	45.0	50.0							2190	2250	4/5
E55	10.0	42.5	47.5							2240	2310	4/5
E56	15.0	41.0	44.0							2200	2410	4/5
E31-1	19.6	49.0	29.4	2.0						2090	>2200	3
E31-2	19.2	48.0	28.8	4.0						2090	>2200	3
E31-3	18.8	47.0	28.2	6.0						2070	2200	2
E31-4	19.6	49.0	29.4		2.0					2050	2170	3
E31-5	19.2	48.0	28.8		4.0					2030	2100	3
E31-6	18.8	47.0	28.2		6.0					2025	2090	2
E31-7	19.6	49.0	29.4			2.0				2100	2150	3
E31-8	19.2	48.0	28.8			4.0				2150	2200	2
E31-9	18.8	47.0	28.2			6.0				2190	2200	1(+)
E31-10	19.6	49.0	29.4				2.0			1800	1975	3
E31-11	19.2	48.0	28.8				4.0			1750	1800	2
E31-12	18.8	47.0	28.2				6.0			1750	1780	2
E31-13	18.0	45.0	27.0	10.0						2100	2190	1
E31-14	17.0	42.5	25.5	15.0						2050	2130	1
E31-15	16.0	40.0	24.0	20.0						2020	2090	1
E31-16	18.0	45.0	27.0					5.0	5.0	2000	2090	2
E31-17	16.0	40.0	24.0					10.0	10.0	2000	2025 (1)	1
E31-18	14.0	35.0	21.0					15.0	15.0	1930	2025 (1)	1

Designation	Composition (% Wt.)									Fusion Temperatures		ICR ⁽²⁾
	Ti	Zr	V	Cu	Mn	Pd	Ni	Cr	Sn	Solidus	Liquidus ⁽¹⁾	
										(°F)	(°F)	
E31-16	18.0	45.0	27.0	5.0	5.0					2000	2090	2
E31-17	16.0	40.0	24.0	10.0	10.0					2000	2025 (1)	1
E31-18	14.0	35.0	21.0	15.0	15.0					1930	2025 (1)	1
E31-19	18.0	45.0	27.0			5.0	5.0			2070	2080 (1)	2
E31-20	16.0	40.0	24.0			10.0	10.0			2080	2170	1(+)
E31-21	14.0	35.0	21.0			15.0	15.0			2080	2180	1
E31-22	18.0	45.0	27.0				5.0	5.0		2000	2140	1
E31-23	16.0	40.0	24.0				10.0	10.0		2000	2140	1
E31-24	14.0	35.0	21.0				15.0	15.0		2170	2240	1
E31-25	19.6	49.0	29.4	2.0						2170	>2300	3
E31-26	19.2	48.0	28.8	4.0						2050	2120	3
E31-27	18.8	47.0	28.2	6.0						2000	2040	3
E31-28	19.6	49.0	29.4		2.0					2150	2170	2
E31-29	19.2	48.0	28.8		4.0					2165	2180	2
E31-30	18.8	47.0	28.2		6.0					2120	2140	1(+)
E31-31	19.6	49.0	29.4						2.0	2230	2250	4
E31-32	19.2	48.0	28.8						4.0	2230	2270	4
E31-33	18.8	47.0	28.2						6.0	2230	2250	4
				Al	Cb		Ga					
E31-34	19.6	49.0	29.4	2.0						2200	2220	3
E31-35	19.2	48.0	28.8	4.0						2200	2250	2
E31-36	18.8	47.0	28.2	6.0						>2300	--	1(+)
E31-37	18.0	45.0	27.0		10.0					>2300	--	4
E31-38	17.0	42.5	25.5		15.0					>2300	--	4
E31-39	16.0	40.0	24.0		20.0					>2300	--	4
E31-40	18.0	45.0	27.0			10.0				>2300	--	2
E31-41	17.0	42.5	25.5			15.0				2200	2225	1(+)
E31-42	16.0	40.0	24.0			20.0				2220	2280	1(+)
E31-43	18.0	45.0	27.0						10.0	2270	>2290	3(+)
E31-44	17.0	42.5	25.5						15.0	2250	>2280	3
E31-45	16.0	40.0	24.0						20.0	2225	>2300	3
E31-46	19.6	49.0	29.4				2.0			2160	2200	2
E31-47	19.2	48.0	28.8				4.0			2160	2175	2
E31-48	18.8	47.0	28.2				6.0			--	--	1(+)
				Si	Ge	Cu						
E31-49	19.6	49.0	29.4	2.0						>2300	--	3
E31-50	19.2	48.0	28.8	4.0						2200	>2300	2
E31-51	18.8	47.0	28.2	6.0						2200	>2300	2
E31-52	19.6	49.0	29.4		2.0					2150	2170	3(+)
E31-53	19.2	48.0	28.8		4.0					2150	2180	3
E31-54	18.8	47.0	28.2		6.0					2160	2190	3
E31-55	16.0	40.0	24.0			20.0				1910	>2000	2
E31-56	14.0	35.0	21.0			30.0				1860	2000	1(+)
E31-57	12.0	30.0	18.0			40.0				1845	2020	1(+)
E31-58	10.0	25.0	15.0			50.0				--	--	1(+)
E31-59	18.0	45.0	27.0			10.0				1860	>2110	2
E31-60	17.0	42.5	25.5			15.0				1780	>2150	2

Designation	Composition (Wt. %)						Fusion Temperatures		ICR ⁽²⁾
	Ti	Zr	Cu	Ni	V	Cr	Solidus (°F)	Liquidus ⁽¹⁾ (°F)	
E31-61	19.6	49.0			29.4	2.0	--	--	4
E31-62	19.2	48.0			28.8	4.0	>2020	--	3
E31-63	18.8	47.0			28.2	6.0	2145	2160	3
E31-64	18.0	45.0			27.0	10.0	2220	>2250	2
E21-65	17.0	42.5			25.5	15.0	--	--	1
A2-5	35.0	35.0	15.0	15.0			1620	1675(1)	2/2(-)
B2-5	49.0		15.0	15.0	21.0		1950	>2070	3
C2-5	70.0		15.0	15.0	(Baseline)		1750	>1900	3
D2-5		70.0	15.0	15.0			1650	1690	2
A2-1	45.0	45.0	10.0				1960	>2250	3
A2-2	42.5	42.5	15.0				1950	>2250	3
A2-3	40.0	40.0	20.0				1880	2020	3
A2-4	35.0	35.0	30.0				1635	1650(1)	2
A2-6	30.0	30.0	40.0				1660	1680	1
A2-7	25.0	25.0	50.0				--	--	1
B2-1	63.0		10.0		27.0		>2250	--	4
B2-2	59.5		15.0		25.5		>2250	--	4
B2-3	56.0		20.0		24.0		>2200	--	4
B2-4	49.0		30.0		21.0		2020	>2200	3
B2-6	42.0		40.0		18.0		1830	~1975	3
B2-7	35.0		50.0		15.0		1850	~2075	2
C2-1	90.0		10.0				--	--	5
C2-2	85.0		15.0				--	--	5
C2-3	80.0		20.0				2050	2080	5
C2-4	70.0		30.0				1860	1880	5
C2-6	60.0		40.0				1835	1885	3
C2-7	50.0		50.0				1875	2000	2
D2-1		90.0	10.0				--	--	5
D2-2		85.0	15.0				--	--	4(+)
D2-3		80.0	20.0				1880	1940	3
D2-4		70.0	30.0				1750	1860	3
D2-6		60.0	40.0				1675	1685	3
D2-7		50.0	50.0				--	--	1
A2-8	40.0	40.0	10.0	10.0			1725	>1880	2
C2-8	80.0		10.0	10.0			1760	>1900	4
D2-8		80.0	10.0	10.0			1700	1730	1
AC1-1	42.0	28.0	30.0				1650	1690(1)	2
AC1-2	49.0	21.0	30.0				1650	1760	3
AC1-3	56.0	14.0	30.0				1650	1850	3
AD1-1	28.0	42.0	30.0				--	--	1
AD1-2	21.0	49.0	30.0				--	--	1
AD1-3	14.0	56.0	30.0				--	--	1
					Sn	Ge			
C3-1	71.4		20.0		8.6		1650	>2060	4
C3-2	57.1		30.0		12.9		1650	>2040	3
C3-3	42.8		40.0		17.2		1660	>2020	2
C4-1	72.6		20.0			7.4	1840	>2000	4
C4-2	58.9		30.0			11.1	1835	>1980	3
C4-3	45.2		40.0			14.8	1850	>2010	3

Designation	Composition (% Wt.)						Fusion Temperatures		ICR ⁽²⁾
	Ti	Zr	Cu	Ni	Mn	Si	Solidus (°F)	Liquidus ⁽¹⁾ (°F)	
C5-1	73.3		20.0		6.7		1880	>2010	4
C5-2	60.0		30.0		10.0		1840	1880	3
C5-3	46.6		40.0		13.4		1770	1840	2
C6-1	78.0		20.0			2.0	1900	>2050	4
C6-2	67.0		30.0			3.0	1900	1940	4
C6-3	56.0		40.0			4.0	1850	≥1950	3/3(+)
AC1-4	37.5	37.5	25.0				1640	1770	3
AC1-5	45.0	30.0	25.0				1660	≥1860	3
AC1-6	52.5	22.5	25.0				1725	≥1950	3
AC1-7	52.5	20.0	27.5				1710	≥1950	3
AC2-1	71.5			28.5			1850	1900	2/2(-)
AC2-2	42.0	42.0		16.0			1750	1910	2(+)/3
AC2-3	40.0	40.0		20.0			1700	1720	2(+)/3
AC3-1	33.8	33.7			32.5		>1900	--	1
AC3-2	37.5	37.5			25.0		>1850	--	1(+)
AC3-3	36.5	36.5		7.0	20.0		>1850	--	1
AC3-4	37.5	37.5		10.0	15.0		>1850	--	1
AC3-5	39.0	39.0		12.0	10.0		>1850	--	1
AC3-6	40.0	40.0		15.0	5.0		>1850	--	1
AC3-7	40.0	40.0		9.0	12.0		1800	>1900	2(+)
AC3-8	40.0	40.0		10.0	10.0		1780	1880	2
AC3-9	35.0	35.0		12.0	18.0		>1850	--	1
AC3-10	35.0	35.0		15.0	15.0		>1850	--	1
AC3-11	45.0	45.0			10.0		>1850	--	3
AC3-12	41.3	41.2			17.5		>1850	--	2
AC1-8	46.0	25.0	29.0				1650	1760	2
AC1-9	45.0	25.0	30.0				1670	1760(1)	2
AC1-10	43.5	25.0	31.5				1670	1700(1)	2
AC1-11	47.5	22.5	30.0				1650	1780(1)	2
AC1-12	46.0	22.5	31.5				1700	1740	2
AC1-13	47.5	20.0	32.5				1700	1750(1)	2
AC1-14	49.5	19.0	31.5				1700	1820	2
AC1-15	50.0	17.5	32.5				1740	1775(1)	2
AC5-1	37.5	37.5	10.0	15.0			1625	1670	2
AC5-2	39.0	39.0	7.0	15.0			1600	1650(1)	2/2(-)
AC5-3	40.0	40.0	5.0	15.0			1600	1650(1)	2/2(-)
AC5-4	41.0	41.0	5.0	13.0			1625	1750	2
AC5-5	40.0	40.0	7.5	12.5			1690	1740	2
AC5-6	42.5	42.5	5.0	10.0			1610	≥1920	2
AC5-7	37.5	37.5	12.5	12.5			1610	1640(1)	2/2(-)
AC6-1	32.5	32.5	30.0		5.0		--	--	1
AC6-2	30.0	30.0	30.0		10.0		--	--	1
AC6-3	35.0	35.0	25.0		5.0		--	--	1
AC6-4	32.5	32.5	25.0		10.0		--	--	1
AC6-5	30.0	30.0	25.0		15.0		--	--	1
AC6-6	37.5	37.5	20.0		5.0		--	--	1(+)
AC6-7	35.0	35.0	20.0		10.0		--	--	1(+)
AC6-8	32.5	32.5	20.0		15.0		--	--	1(+)
AC6-9	30.0	30.0	20.0		20.0		--	--	1
AC1-16	37.0	37.0	26.0				1680	1750	3
AC1-17	36.5	36.5	27.0				1640	1725(1)	2
AC1-18	36.0	36.0	28.0				1620	1695(1)	2
AC1-19	43.8	29.2	27.0				1625	≥1680	2
AC1-20	43.2	28.8	28.0				1630	1740(1)	3
AC1-21	42.6	28.4	28.0				1620	1730(1)	3
AC1-22	49.7	21.3	29.0				1610	1830	2(+)/3
AC1-23	49.0	21.0	30.0				1720	1780	2(+)/3
AC1-24	48.3	20.7	31.0				1650	1740(1)	3

Designation	Composition (% Wt.)						Fusion Temperatures		ICR ⁽²⁾
	Ti	Zr	Cu	Ni	V	Fe	Solidus (°F)	Liquidus ⁽¹⁾ (°F)	
AC5-8	2.5	2.5	47.5	47.5	(Very erosive)		1670	>1820	5
AC5-9	5.0	5.0	45.0	45.0	(Very erosive)		1650	1780	4(+)
AC5-10	7.5	7.5	42.5	42.5	(Very erosive)		1670	1750	4
AC5-11	10.0	10.0	40.0	40.0	(Very erosive)		1686	1790	4(+)
AC5-13	38.8	38.8	11.2	11.2			1650	1740	2
AC5-14	42.9	35.1	7.0	15.0			1650	1710	2
AC5-15	46.7	31.3	7.0	15.0			1640	1730(1)	2
AC5-16	50.8	27.2	7.0	15.0			1630	1730(1)	3
AC5-17	54.7	23.3	7.0	15.0			1650	1775	3
AC5-18	41.0	41.0		18.0			1650	1730(1)	3
AC5-19	40.0	40.0	2.0	18.0			1640	1680	2
AC5-20	41.0	41.0	2.0	16.0			1675	1750	2
AC5-21	40.0	40.0	4.0	16.0			1640	1700(1)	2/2(+)
AC5-22	40.5	40.5	2.0	17.0			1640	1750(1)	2
AC5-23	40.0	40.0	3.0	17.0			1640	1700	1
AC5-24	39.5	39.5	4.0	17.0			--	--	1
AC5-25	39.5	39.5	3.0	18.0			--	--	1
AC5-26	39.0	39.0	4.0	18.0			--	--	1
AC5-27	39.5	39.5	2.0	19.0			--	--	1
AC5-28	39.0	39.0	2.0	20.0			--	--	1
AC5-29	36.0	36.0	24.0	4.0			--	--	1
AC5-30	36.5	36.5	25.0	2.0			--	--	1
E9-1	26.2	33.8	25.0		15.0		1780	≥1900	2
E9-2	24.5	31.5	30.0		14.0		1790	≥1900	2
E9-3	29.8	38.2		15.0	17.0		1860	≥2000	2
E9-4	28.0	36.0		20.0	16.0		1770	1970(1)	2
E27-1	22.5	33.7	25.0		18.8		1810	>2000	2
E27-2	21.0	31.5	30.0		17.5		1800	>1960	2
E27-3	25.5	38.2		15.0	21.3		1780	1980	1
E27-4	24.0	36.0		20.0	20.0		1670	>2000	1
AB-1	59.5			15.0	25.5		>2010		4
AB-2	56.0			20.0	24.0		1890	>2015	4
AB-3	49.0			30.0	21.0		1870	1900	4
AB-4	42.0			40.0	18.0		1850	1940	4(+)
AB-5	52.4			25.0	22.6		1870	>2010	4
AB-6	56.0				24.0	20.0	>2000	--	2
AB-7	49.0				21.0	30.0	>2010	--	2
AB-8	50.0	15.0		20.0	15.0		--	--	1
AB-9	47.5	12.5		25.0	15.0		--	--	1
AB-10	45.0	10.0		30.0	15.0		--	--	1
AB-11	47.0	5.0		30.0	18.0		--	--	1
AB-12	48.0	20.0		20.0	12.0		--	--	1
AB-13	45.5	17.5		25.0	12.0		--	--	1
AB-14	46.0	25.0		20.0	9.0		--	--	1
AB-15	44.5	23.5		23.0	9.0		--	--	1
AB-16	49.5	7.5		25.0	18.0		--	--	1
						Mn			
AC6-15	42.0	18.0	30.0			10.0	1680	1710(1)	2/2(-)
AC6-16	48.0	12.0	30.0			10.0	1660	1750(1)	2/2(-)
AC6-17	33.4	33.3	25.0			8.3	1680	1730	1
AC6-18	46.7	30.0	25.0			8.3	1675	1750(1)	2/2(-)
AC6-19	53.4	13.3	25.0			8.3	1730	1900	2
AC6-20	40.7	22.0	28.0			9.3	1670	1700(1)	1
AC6-21	41.7	25.0	25.0			8.3	1680	1710(1)	2/2(-)
AC6-22	40.0	20.0	30.0			10.0	1700	1740	1
AC6-23	37.7	25.0	28.0			9.3	1680	1730	1